The Relationship between Equivalent Fall Height and Ground Reaction Force in Freestyle Ski Jumping

Master's thesis

J.R. van der Schot

TU Delft

Cover photo: © F-Tech Snowparks (used with permission)

The Relationship between Equivalent Fall Height and Ground Reaction Force in Freestyle Ski Jumping

by

J.R. van der Schot

to obtain the degree of Master of Science
at the Delft University of Technology,
to be defended publicly on Monday August 28, 2023 at 15:00 PM.

Student number:	4595955	
Project duration:	August 1, 2022 – August 28, 2023	
Thesis committee:	Dr. J.K. Moore,	TU Delft, supervisor
	Prof. Dr. M. Hubbard,	UC Davis, supervisor
	D. Röck,	Prinoth AG, supervisor
	Prof. Dr. F.C.T. van der Helm	TU Delft

TU Delft

Statement on the Utilization of ChatGPT

For this thesis, I used ChatGPT as a tool to improve my English writing skills. This AI provided recommendations for improving spelling, grammar, and paragraph and sentence structure. I carefully evaluated these suggestions and independently chose which ones to integrate into my text. It is important to note that the AI did not write any complete sentences, nor did I copy entire sections of text. The application of this tool improved my efficiency but did not yield a thesis that I otherwise could not have written.

Preface

Thank you for taking the time to read my thesis about freestyle skiing. Over the past year, I have put a lot of time and effort into this project, which will, hopefully, contribute to snow parks being safer and enjoyable for a larger public. Unfortunately, when I was in Italy, to conduct the experiments described in this research, I was faced with the dangers of snow sports myself. A bone in four pieces and a surgery in an Italian hospital later, the importance of my project was more evident to me than ever. Luckily, with the unconditional support of my friends, family, and girlfriend, I was able to get back home, recover, and eventually finish my project. I would like to express my great gratitude towards them, because, without them, this would not have been possible. I would also like to thank my supervisors, Jason Moore, Mont Hubbard, and Daniel Röck, for their guidance and support during the project. Our meetings were always pleasant, educational, and cooperative. Finally, I would like to thank all members of the Bicycle Lab. Being part of this research group has made me feel as if I was not working alone and our VrijMiBo's were an enjoyable way to let off some steam after a week of hard work. To the reader: I hope you enjoy reading this thesis.

J.R. van der Schot
Delft, August 2023

Contents

The Relationship between Equivalent Fall Height and Ground Reaction Force in Freestyle Ski Jumping

J.R. van der Schot

Abstract

This study investigated the relationship between Equivalent Fall Height (EFH) and peak Ground Reaction Force (GRF) in freestyle ski jumping. An experiment was conducted in which a semi-professional freestyle skier was instrumented with Inertial Measurement Units (IMUs) and a position sensor. The skier performed jumps off 'kickers' in snow parks in four different ski resorts in Northern Italy. The gathered sensor data was utilized to calculate the EFH and GRF of every jump. The data reveals convincing evidence that a positive correlation between these two parameters exists. However, the coefficient of determination, R^2, indicates only a moderate correlation. The results suggest that alternating landing strategies might have affected the measured GRF as well. This indicates that a higher correlation between EFH and GRF might exist than shown in this research. Further research should focus on how individual parameters, such as EFH and landing strategy, affect the GRF. This should develop a more comprehensive understanding of how to enhance the safety and enjoyment of freestyle ski jumps for a broader audience.

Keywords: freestyle, ski, impact, safety

1 Introduction

Freestyle skiing is often considered an exhilarating pursuit by both athletes and spectators. The sport involves performing jumps and tricks on various features such as kickers, half-pipes, rails, boxes, and many more. However, especially features that include large jumps are associated with severe injuries and there are few guidelines on how these features can be built in the safest manner [1–4] . Besides the negative impact on the injured individual, injuries can cause a burden on public health care and treatment can be costly.

The focus of this research is on a feature that involves large jumps: kicker-lines. A kicker is a take-off ramp off which freestyle athletes jump. These kickers are often placed in sequence to create a 'line' (Fig. 1). The area in front of a kicker is called the inrun, while the area behind it is called the landing area. Between the kicker and the landing area lies a knuckle, which is a point where the inclination of the slope changes rapidly.

After a jump, a skier needs to dissipate all his kinetic energy directed perpendicular to the slope. This is achieved through the Ground Reaction Force (GRF), which generates an impulse equal to the skier's change in momentum during landing, in accordance with Newton's second law. Since the momentum normal to the slope is brought to zero, the change in momentum is equal to the total momentum the skier has, in this same direction, before landing, $mv_\perp$ (Eq. 1). The location on the slope where the total impulse while landing is the smallest is called the 'sweet spot'. It is located right after the knuckle and it is the point where athletes intend to touch down after a jump, because it facilitates the smoothest landing.

$$mv_\perp = \int GRF \ \ dt \tag{1}$$

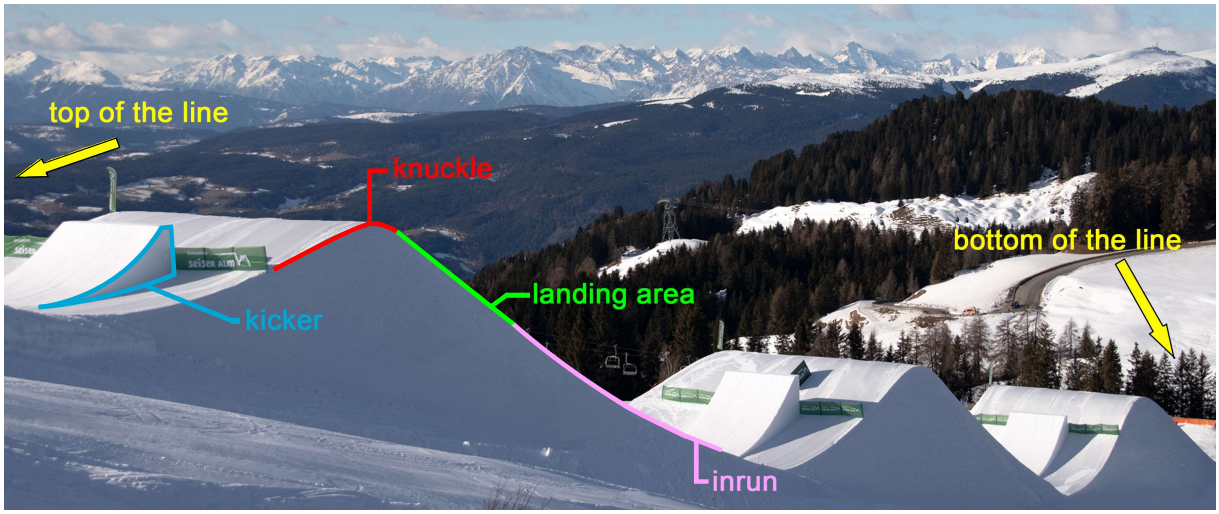

Fig. 1 A kicker line in Seiser Alm, Italy. The different segments of the kicker line are highlighted. © F-tech Snowparks (used with permission).

The commonly used method for designing kicker-lines is through trial and error instead of an engineered approach, which may pose significant risks [5]. A poorly constructed kicker-line could substantially heighten the likelihood of injury because the placement of the landing area is important. Depending on rider behaviour, and snow-, and weather conditions, a skier can have different flight trajectories and the design of the kicker line should facilitate smooth landings for most, if not all, of these trajectories. In the past, negligent kicker-line design and construction have caused multiple severe injuries [6]. In these examples, the skiers' speeds normal to the landing surface, $v_\perp$, were very high.

It has been proposed that kicker-lines can be designed in such a way that $v_\perp$ is small for every possible flight curve [7–9]. The shape of the landing area, together with the flight trajectory of the skier, influences $v_\perp$. As can be observed in Fig. 2, the difference between the angle formed by the skier's trajectory with the horizontal, φ_{skier}, and the inclination angle of the landing surface, φ_{slope}, determines the component of velocity directed perpendicular to the slope.

$$v_\perp = |\bar{v}| \sin\left(\varphi_{skier} - \varphi_{slope}\right) \tag{2}$$

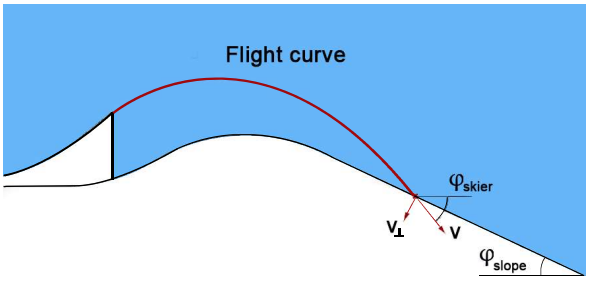

Fig. 2 An arbitrary kicker line displaying the flight curve, the landing slope angle (φ_{slope}), skier angle (φ_{skier}), and the normal landing velocity ($v_\perp$).

While $v_\perp$ serves as an appropriate measure for assessing landing impact, understanding what a comfortable and safe range for this parameter is can be challenging. Intuitively, individuals have a better understanding on how to assess the safety of a certain height from which they fall, rather than the speed at which they will land. Therefore, researchers have put forward a metric that quantifies $v_\perp$ as a height from which one would need to fall vertically, starting from a stationary position, to achieve this same velocity upon landing: the equivalent Fall Height (EFH) [7–9].

$$EFH = \frac{v_\perp^2}{2g} = \frac{|v|^2 \sin^2(\varphi_{skier} - \varphi_{slope})}{2g} \tag{3}$$

By combining Eq. 1 and Eq. 3, the relationship between total impulse and EFH can be described.

$$m\sqrt{2gEFH} = \int GRF \ \ dt \tag{4}$$

The suggestion that a jump with a low EFH is safe, is based on the assumption that the total impulse generated by the GRF during landing determines the safety of the athlete. However, the peak value of the GRF might be a better indication of this, since high forces can break bones. Therefore, the aim of this research was to find a relationship between EFH and peak GRF. If a positive correlation exists, and if peak GRF is deemed an appropriate measure of safety, then EFH can also be interpreted as such.

To test this hypothesis, an experiment was designed where a skier performed freestyle ski jumps while being equipped with sensors to allow the calculation of both the EFH and the GRF. The sensors measured the position, acceleration, and angular velocity of the skier. The position data was differentiated with respect to time to obtain the skier's velocity. The acceleration of the skier normal to the slope was considered to represent the GRF divided by his mass. The data was used to calculate the EFH, the momentum before landing, and the impulse during landing. Consequently, an analysis was done to see if there is a correlation between EFH and peak GRF. Additionally, the validity of the gathered data was tested by comparing the momentum before landing and impulse after landing, which should be equal (Eq. 1).

2 Methodology

2.1 Experimental setup

The experiment took place on four separate days, each in a different ski resort in Italy and was conducted in collaboration with the company 'Prinoth'. Each ski resort had one kicker-line, except for Madonna di Campiglio. This resort had two lines, one with medium-sized kickers, and one with large kickers. In total, 13 different kickers were used and a total of 50 trials were performed. The skier jumped 121 times and 104 of these jumps are used for the analysis (Table 1). The 17 jumps were omitted because during these specific jumps, the RTK correction signal from the position sensor was lost. Therefore, the position data of the skier was not accurate enough for the analysis. In Appendix A, an overview is given of the different ski resorts and jumps that were used for the analysis.

Table 1 Overview of the different ski resorts, how many kickers were present, and how many trials and jumps the skier performed in the resort.

Ski resort	# Kickers	# Trials	# Jumps
Kronplatz	3	10	30
Obereggen	2	11	22
Seiser Alm	2	18	36
Madonna di Campiglio	6	11	33
M-line	3	6	18
L-line	3	5	15
All	**13**	**50**	**121**

The focus of this experiment lies on the relationship between EFH and GRF. Therefore, we attempted to keep all other parameters constant. Consequently, we only recruited one single semi-professional freestyle skier, based on his availability throughout the duration of the experiment. This was important because every skier behaves differently while performing a jump. Especially the landing strategy could be different throughout athletes. Some might land on the tail of their ski's and flex their knees and hips a lot, while others might apply a much stiffer technique. This could have a large effect on the peak GRF because, while the total impulse stays the same, the duration of the landing increases.

Because we wanted to minimize the variety of landing strategies throughout the experiment, the skier was instructed to execute each jump in a uniform manner, adhering to the same take-off and landing strategy. He was asked to refrain from any aerial maneuvers that cause rotations or body configuration changes other than the ones he needed to land safely. The skier jumped up and down three times before going down the slope, did some turns to control his take-off speed, jumped of the kicker, and landed flat on his ski's. The three jumps at the start of the trial were later used to time synchronize the signals. The

skier did change his body configuration a little bit in the air in order to "create air awareness".

The participant was thoroughly informed about the nature, purpose, and procedures of the experiment before providing written consent through a consent form. The participant had the opportunity to ask questions and seek clarification regarding any concerns he had before signing the consent form. The experiment was approved by the Human Research Ethics Committee (HREC) of Delft, University of Technology.

Each testing day began with surveying the landing surface with an RTK position sensor; the Leica iCON gps 70 (Leica Geosystems, Heerbrugg, Switzerland). We dragged a pole, on which the sensor was mounted, over the surface on both sides of the slope and parallel to the traveling direction of the skier. Surface points were recorded every 0.5 meter. These points were later used to create a mesh of points that represent the entire landing surface. A more detailed explanation on how the landing surface is surveyed can be found in Appendix B.

In the meantime, the skier engaged in some warm-up laps and was afterwards equipped with the required sensors. A second RTK position sensor, the Leica GS18 (Leica Geosystems, Heerbrugg, Switzerland), was carried by the skier on a backpack (Fig. 3). It recorded the position of the sensor with a sampling frequency of 20Hz. Both the position data and the surface points are recorded in a global reference frame in which the x-, y-, and z-axes point east, north, and upwards respectively. The accuracy of both sensors when stationary is approximately 2 cm.

Two Shimmer3 IMUs (Shimmer, Dublin, Ireland) were mounted on the skier's chest and upper back by making use of a GoPro harness (Fig. 4). The Inertial Measurement Units recorded acceleration and angular velocity at a sampling frequency of 504Hz.

For each trial, the measurements were initiated at the top of the line and completed at the bottom of the line (Fig. 1). Before the start of the next trial, a brief questionnaire was administered to record the skier's perceived level of control

Fig. 3 The skier wore a backpack on which the position sensor was mounted. The sensor attached to a small aluminium plate which was secured to the backpack using straps.

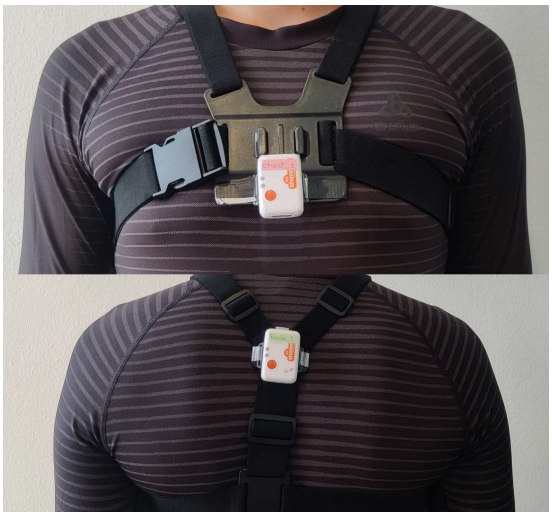

Fig. 4 Placement and attachment of the IMU on the chest (top) and the IMU on the back (bottom).

and impact experienced during the previous jump, rated on a scale ranging from 1 to 10. Finally, any anomalies experienced during the preceding trial were noted. Video recordings of some jumps were made for analysis.

2.2 Time synchronization

The signals from the Leica GS18 and both IMUs were time synchronized. We first differentiated the position data gathered by the GS18 with respect to time using the forward difference approach to obtain the velocity of the sensor: $\bar{v} = \begin{bmatrix} v_x & v_y & v_z \end{bmatrix}^T$.

Then, we differentiated a second time, now using the backward difference approach to get the acceleration of the sensor: $\bar{a} = \begin{bmatrix} a_x & a_y & a_z \end{bmatrix}^T$. After that, we cross correlated this absolute acceleration with the absolute acceleration measured by each separate accelerometer. In this process, one signal is shifted in time with respect to the other one. The time shift at which the highest correlation between the two signals occurred was considered the time delay between the sensors. Consequently, the IMU signals were shifted in time to achieve synchronization between all three sensors. However, it was noticed that the signals still did not align sufficiently. To be able to cross correlate the signals, the accelerometer data had to be resampled to match the sampling frequency of the position data. Therefore, the time delay that we found was always a multiple of 0.05 seconds, corresponding to the sampling frequency of the position sensor, 20 Hz. This meant that the exact time delay between the signals could not be found by this method. By carefully evaluating the signals, we shifted them in time manually to synchronize them.

2.3 Calculating EFH

To calculate the EFH of the skier, his speed, v, and the two angles, φ_{skier}, and φ_{slope} at the time of landing needed to be extracted from the measured data. The time of landing is defined as the moment the total acceleration measured by the accelerometer on the chest is equal to g for the first time after airtime. The accelerometer does not measure the gravitational acceleration and therefore gives readings close to zero when it is in the air. If the total acceleration equals g, it indicates that the skier is supporting only his own body weight.

A typical curve of the speed of the skier during a jump is shown in Fig. 5. The take-off and landing point are characterized by small spikes in the velocity curves. At the take-off, this can be explained by the fact that jumping off the kicker results in some additional speed. At landing, it can be a result of the skier slowing down normal to the slope faster than that he is accelerating along the snow surface due to gravity. This causes a decrease in velocity after which the skiers starts gaining speed again.

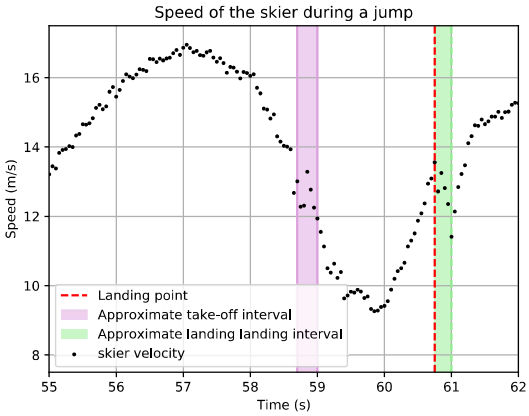

Fig. 5 The black dots represent the speed of the skier during a jump. The pink area is the approximate moment of takeoff. The red-dotted line is the exact moment of landing, and the green area is time of the landing which is approximately 0.25 s.

To calculate φ_{skier}, the velocity vector of the position sensor, as described in Section 2.2, at the time of landing was utilized.

$$\varphi_{skier} = \arcsin\left(\frac{-v_z}{|\bar{v}|}\right) \tag{5}$$

By evaluating the surveyed snow surface around the landing point, φ_{slope} was determined. We found the surface points that were closest to the position sensor right before and after landing and used these points to calculate the inclination of the slope (Fig. 6). Plots for all jumps are attached in Appendix G.

Although we assume the entire experiment to be planar, all three coordinates are needed for this calculation since the kicker lines are not aligned with one of the axes of the global reference frame.

$$\varphi_{slope} = \arcsin\left(\frac{z_1 - z_2}{\sqrt{(x_1 - x_2)^2 + (y_1 - y_2)^2 + (z_1 - z_2)^2}}\right) \tag{6}$$

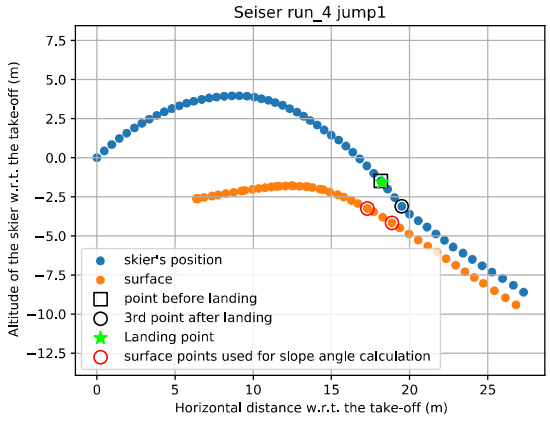

Fig. 6 Flight curve of an arbitrary jump with the take-off point set at the origin. The landing point is shown as a green star. The point before the landing point and the 3^{rd} point after the landing point are highlighted with a black square and a black circle, respectively. The points on the surface that are closest to these points are encircled in red and used for the calculation of the slope angle (φ_{slope}, Eq. 6).

2.4 Calculating GRF

The accelerometers were used to estimate the GRF of the skier at impact. Since the exact weight of the skier is not known, the GRF is expressed in terms of the skier's body weight.

$$\begin{aligned} GRF &= ma_{\perp} \\ \frac{GRF}{mg} &= \frac{a_{\perp}}{g} \end{aligned} \tag{7}$$

First, a Butterworth low-pass filter with a cut-off frequency of 15 Hz was applied. The duration of a jump landing can be as short as 0.1 seconds, which corresponds to a frequency of 10 Hz. We did not want to lose valuable information about the characteristics of the landing, so the cutoff frequency was chosen with margin. The accelerometer gives readings in an upper body fixed frame with the x-, y- and z- axes in the medial, superior, and anterior direction of the body, respectively. This data needed to be converted into the global reference frame. To do so, the orientation of the IMU ,θ, needed to be determined (Fig. 7). Both the accelerometer and the gyroscope can estimate the orientation of the sensor, θ_a and θ_g respectively. The accelerometer does this by evaluating

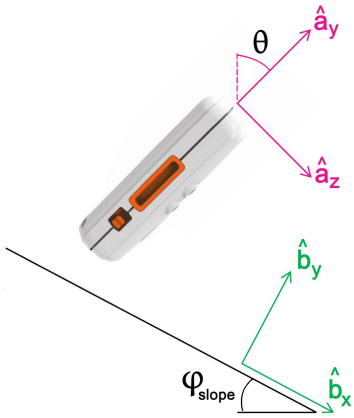

Fig. 7 The reference frame of the IMU in pink and the reference frame of the slope in green; the orientation of the IMU, θ and the slope angle, φ_{slope}.

how much of the gravitation acceleration is picked up by its individual axes (Eq. 8). The angular velocity measured by the gyroscope can be integrated over time to estimate the same orientation (Eq. 9).

$$\theta_a = arctan(\frac{-a_z}{a_y}) \tag{8}$$

$$\theta_{g_{n+1}} = \theta_{g_n} + \omega_n(t_{n+1} - t_n) \tag{9}$$

Both methods have limitations. The accelerometer is sensitive to dynamical movement and noise in the gyroscope data could lead to gyro drift when integrating over a longer period of time. To achieve a reliable orientation estimate, a complementary filter was designed to combine data from both sensors. This filtering method relies on a weight factor, denoted as α, to dictate the level of confidence placed in the orientation estimates provided by both sensors.

$$\theta_n = \alpha\theta_{a_n} + (1-\alpha)(\theta_{n-1} + \omega_{x_n}\Delta t) \tag{10}$$

where:

θ_n : Orientation estimate at time step n,
α : Weight coefficient, $0 \leq \alpha \leq 1$,
θ_{a_n} : Accelerometer's orientation estimate,
ω_{x_n} : Angular velocity of the gyroscope,
Δt : $t_n - t_{n-1}$

This sensor fusion technique capitalizes on the accelerometer's accuracy at low frequencies and the gyroscope's accuracy at high frequencies. The weight factor, α, is chosen to be 0.05, which means that the gyroscope is the predominant sensor for estimating the orientation of the IMU. This is done because the IMU operates in a very dynamic environment and high frequency movements occur. The complementary filter is tested in an experimental setup prior to doing the experiments. A detailed description of the complementary filter and this procedure is given in Appendix D.

In Fig. 7, the relevant reference frames are shown. The component of acceleration normal to the landing surface $(\bar{a} \cdot \hat{b}_y)$ is described by Eq. 11.

$$\bar{a} \cdot \hat{b}_y = cos(\varphi_{slope} - \theta)a_y + sin(\varphi_{slope} - \theta)a_z \quad (11)$$

In Fig. 8, an acceleration plot of a representative jump landing is presented. The predominant component of the total acceleration is the normal acceleration. This is as expected, and therefore an indication that the orientation estimation is correct.

Around the landing point, the normal acceleration is evaluated to determine its peak value. This number is divided by g in order to obtain the peak GRF in terms of the skier's body weight, in accordance with Eq. 7. Plots for all jumps are provided in Appendix H.

The impulse, divided by the skier's mass, was calculated by integrating the normal acceleration over the time of landing. We chose a time period that started at the time of touchdown and had a duration of 0.25 seconds. We chose this specific duration by looking at all acceleration plots in Appendix H. All landings should have been completed in this time period to get a reliable estimate of the impulse that is generated by the GRF. This number is reinforced by a similar experiment done by Petrone et al. [10].

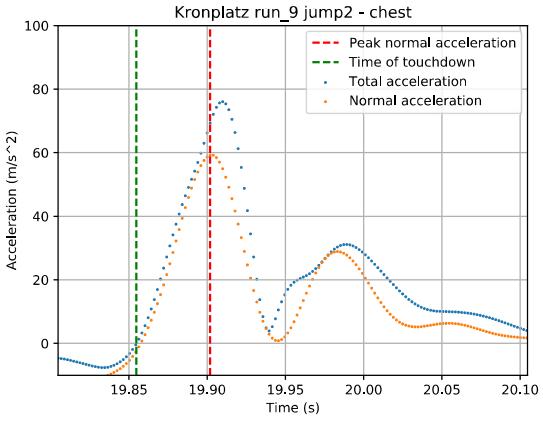

Fig. 8 Acceleration plot of a representative jump landing; including the total and normal acceleration at landing. The dashed green line is the moment the skier touches down and the dashed red line shows the time where the largest normal acceleration occurs.

3 Results

In Fig. 9, the normal acceleration, integrated over the landing time vs. $v_\perp$ is shown. During landing, $v_\perp$ is brought to zero, and therefore these two parameters should be equal. Two data sets are shown, for both IMUs that we used to estimate the GRF.

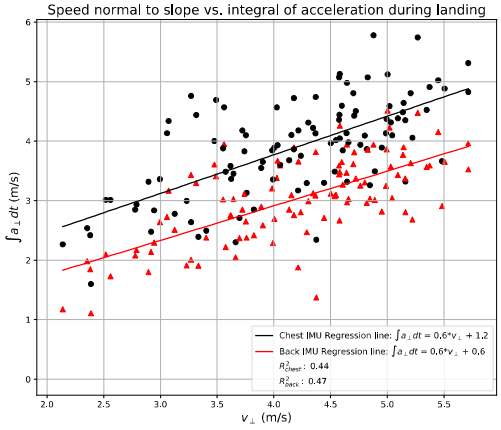

Fig. 9 The normal acceleration integrated over the time of landing plotted against the speed of the skier normal to the slope, right before landing. Red triangles for the normal acceleration of the IMU on the back; black dots for the normal acceleration of the IMU on the chest.

Through both data sets, a linear regression line was fitted and the coefficient of determination (R^2) is calculated. This coefficient was a measure of how well the data fits the regression line. An R^2-value of 0 means no correlation , while an R^2-value of 1 means a perfect fit. We expected to see a regression line of the form $y = x$, because this would mean that the calculated parameters comply with Newton's second law. Even though the data shows a positive linear correlation, the slopes of the regression lines are smaller than 1.

In Fig. 10, the peak GRF is plotted against EFH. Also here, two data sets are shown, one for each IMU. Linear regression lines are fitted through the data and the R^2-values are calculated. Additionally, we did an hypothesis test with a null hypothesis that states that there is no correlation between the two parameters. The p-values of this hypothesis test and the R^2-coefficients are provided in Table 2.

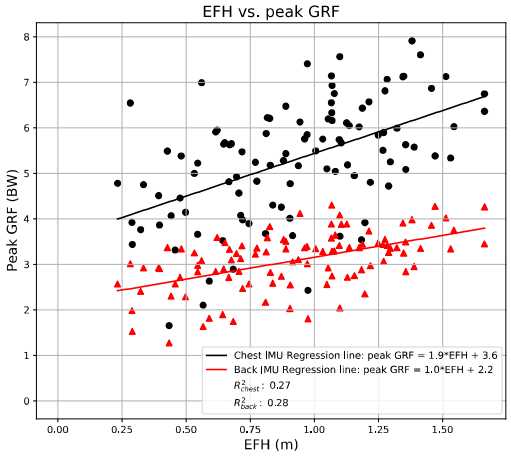

Fig. 10 EFH plotted against peak GRF for each IMU and every jump. The regression line in drawn through the scattered data and the mathematical expression is given in the legend. The calculated R^2 values are added to the legend.

It can be observed that there is evidence that there is a positive relationship between EFH and peak GRF, hence the very small p-values of 6.2e-9 and 2.1e-8. The moderate R^2-values of 0.27 and 0.28 for the IMUs on the chest and the back respectively, suggest that peak GRF is dependent on EFH but that there might be other factors present. It is noteworthy that there are significant differences in R^2- and p-values when examining separate ski resorts. These differences do not only exist between ski resorts, but also between IMUs; for example in Obereggen, where the IMU on the back suggests a much higher correlation than the one on the chest (Table 2).

Table 2 R^2 and p-values for both the back IMU and the chest IMU in every ski resort.

Line	R^2_{back}	R^2_{chest}	p_{back}	p_{chest}
Kronplatz	0.52	0.55	1.47e-5	6.1e-6
Madonna_M	0.54	0.40	7.3e-4	6.4e-3
Madonna_L	0.25	0.23	9.5e-2	0.11
Obereggen	0.36	0.16	0.03	0.17
Seiser Alm	0.17	0.04	1.6e-2	0.28
All	**0.28**	**0.27**	**6.2e-9**	**2.1e-8**

In Appendix E, a table is provided with the relevant parameters of all jumps. EFH vs. peak GRF plots for different ski areas are provided in Appendix F.

4 Discussion

4.1 Landing point

Right before landing, the speed of the skier is increasing rapidly and it is therefore important to obtain the exact time of landing. Time synchronizing the signals of the three sensors was an important step in this process. However, the method used to accomplish this is not very accurate. As described in Section 2.2, time synchronizing the signals was done manually. A better method to obtain EFH might be to calculate EFH as a continuous signal and evaluate what its peak value around the time of landing is.

4.2 Estimation of the GRF by using IMUs

During this experiment, the GRF is estimated separately by two IMUs. The results show that these estimates for the same jump are often far apart. In this section, limitations of the experiment are discussed that can explain these differences.

4.2.1 IMU placement

The IMUs are not placed at the center of mass (CoM). This means that besides a translational component of velocity, they also have an angular velocity due to the rotation of the skier's upper body. Because of this angular velocity, additional acceleration components are present. Because both IMUs are fixed on distinct positions on the body, these additional components are different for each IMU. The difference in total acceleration measured, compared to the acceleration of the center of mass, can be calculated by using the acceleration two-point theorem (Eq. 12) [11].

$$\bar{a}_{IMU2} - \bar{a}_{CoM} = \bar{\alpha} \times \bar{r} + \bar{\omega} \times (\bar{\omega} \times \bar{r}) \qquad (12)$$

where:

$\bar{a}_{IMU1}$: The total acceleration of the first IMU,
$\bar{a}_{CoM}$: The total acceleration of the CoM,
$\bar{\alpha}$: The angular acceleration of the upper back,
$\bar{\omega_x}$: The angular velocity of the upper back,
$\bar{r}$: The position vector of the IMU with, respect to the CoM

An estimation can be made on how much the angular velocity of the skier ω_x) affects the accelerometer readings since it is measured. The maximum ω_x during landing is found to be between 2.4 and 10 rad/s, for different jumps. If α is considered to be 0 and r is approximated to be $\begin{bmatrix}0 & 0.3 & 0\end{bmatrix}^T$ m, this would result in a difference in total acceleration of 1.7-30 m/s^2, between the IMU and the CoM. This additional acceleration could therefore be significant and the reason for that the GRFs estimated by the IMUs on the chest and the back are different.

4.2.2 IMU attachment

If the exact movement of the skier's body needs to be measured using an IMU, it is important that the IMU is fixed on the body properly. If the IMU can move with respect to skier's body, it does not exactly mimic the movement of the skier which means that measured accelerations and angular velocities do not represent those of the skier's upper body. Therefore, this could lead to inaccurate GRF calculations and differences between IMUs. This limitation even exists when the IMU is glued to a person's body because the skin can move with respect to underlying body parts [12]. This effect is amplified when more layers, for example clothes, are worn between the IMU and the body. In this experiment, the IMUs were worn on top of the clothes of the skier. This is done because the IMUs needed to be turned on and off every run and needed to be easily accessible. Since the experiment took place in a cold area, the skier was wearing multiple layers of clothing. On sunny days, the skier was asked if he felt warm enough to take off his top layer of clothing. Even though the harness that held the IMUs was tightened around the skier's body as much as possible, it still had some freedom of movement. Especially when high frequency movement occurred, this likely affected the readings of the IMUs.

Gluing the IMUs to the body can be a solution to the limitation described above. One would have to think of a way to access the IMUs during the experiment without the skier having to undress in the freezing cold. A solution could be to record the entire session as one measurement, instead of turning the IMUs on and off, before and after each run.

4.2.3 IMU orientation estimation

For this experiment, a complementary filter was designed to calculate the orientation of the IMUs. Imprecision in this orientation estimate leads to an inaccurate GRF calculation. Even though the filter is tested extensively in a lab environment, the different circumstances of the experiment could have influenced the validity of the filter. The orientation of the IMU is only relevant at the landing point. The accuracy of the complementary filter at that specific moment in time is affected by the fact that during the flight phase, only the gyroscope is used to estimate this orientation. This means that gyro drift could have occurred which affected the orientation estimate at landing. Nevertheless, the observation that the normal component of acceleration is dominant in the total acceleration, as discussed in Section 2.4, suggests that the complementary filter performs effectively.

4.3 Slope angle calculation

The position sensor that is used to survey the landing area is very accurate. However, only surveying the sides of the slope could have affected the reliability of the calculated φ_{slope}. Bumps and holes in the landing area may have affected the GRF. However, it is not accounted for in the EFH calculation.

4.4 Relationship between EFH and GRF

The hypothesis of this research was that there exists a positive correlation between EFH and GRF. However, it is important to note that EFH is not the sole parameter influencing the GRF. The skier's landing strategy also plays a significant role. When the skier lands on the tail of his skis, the skis absorb more energy, leading to a softer landing [13]. Similarly, GRF can be reduced by flexing the hips and knees more during impact . Puddle et al. showed that a stiffer landing strategy during vertical jump landings, result in a significantly higher peak GRF; 5.2 compared to 3.2 times the jumpers body weight [14]. Additionally, snow properties have an effect on GRF. Softer snow acts as a dampening factor, whereas icy snow does not provide the same cushioning effect. The presence of these additional parameters suggests that there might be a higher correlation between EFH and GRF than what is observed in the results of this study. This relationship could be obscured by the influence of these parameters.

4.5 Recommendations

If the experiment would be repeated, a better method to estimate the GRF is needed. Different sensors could be used that directly measure force instead of acceleration. For example, appropriate load cells or pressure sensors could be mounted between the skis and bindings. If this is not possible, the accelerometers could be used in a more reliable manner. Placing them closer to the approximate center of mass of the skier could reduce the effect of angular velocity and acceleration. Even better might be to place additional IMUs on the thighs, shanks, and skis of the skier. Then, the position of the center of mass of the skier could be estimated and differences in landing strategy could be observed and analyzed.

The data we gathered in this experiment could be further analyzed. A more elaborate investigation into the effect of the angular velocity and acceleration might improve the results significantly. The angular acceleration could be derived by differentiating the angular velocity with respect to time, and, together with a more precise estimation of the location of the center of mass, the total acceleration of the center of mass of the skier could be calculated. This would result in a more reliable estimation of the GRF.

Furthermore, it could be investigated how other individual, independent variables such as the slope angle, absolute landing velocity, and placement of an IMU affect the results. This might lead to new insights in which of these parameters influence the peak GRF.

5 Conclusion

The objective of this research was to find a relationship between EFH and peak GRF of a skier performing a freestyle ski jump. An experiment was conducted to collect the necessary data for calculating these parameters. The results convincingly demonstrate a positive relationship between the two variables. The null-hypothesis that there is no correlation between EFH and GRF was rejected. Even though the coefficient of determination (R^2) does not suggest a very strong correlation, a stronger linear correlation between the two parameters could still exist. Other factors not examined in this research, such as landing strategy and snow conditions, also influence the GRF and as a result, the expected effect of EFH on the GRF might not be fully recognizable in the results of this study. Further research should focus on developing a more detailed model that incorporates the skier's landing strategy to gain deeper insights into the relationship between EFH and peak GRF.

References

[1] H. Ogawa, H. Sumi, Y. Sumi, and K. Shimizu, "Pelvic fractures resulting from snowboarding," *The American Journal of Sports Medicine*, vol. 38, no. 3, pp. 538–542, 2010.

[2] K. Russell, W. H. Meeuwisse, A. Nettel-Aguirre, C. A. Emery, J. Wishart, N. T. Romanow, B. H. Rowe, C. Goulet, and B. E. Hagel, "Feature-specific terrain park-injury rates and risk factors in snowboarders: a case–control study," *British journal of sports medicine*, vol. 48, no. 1, pp. 23–28, 2014.

[3] F. Tarazi, M. F. Dvorak, and P. C. Wing, "Spinal injuries in skiers and snowboarders," *The American Journal of Sports Medicine*, vol. 27, no. 2, pp. 177–180, 1999.

[4] K. Wakahara, K. Matsumoto, H. Sumi, Y. Sumi, and K. Shimizu, "Traumatic spinal cord injuries from snowboarding," *The American Journal of Sports Medicine*, vol. 34, no. 10, pp. 1670–1674, 2006.

[5] M. Hubbard and A. Swedberg, "Design of terrain park jump landing surfaces for constant equivalent fall height is robust to "uncontrollable" factors," in *Skiing trauma and safety: 19th volume*, ASTM International, 2012.

[6] J. Moore, B. Cloud, M. Hubbard, and C. A. Brown, "Safety-conscious design of terrain park jumps: Ethical issues and online software,"

[7] M. Hubbard, J. McNeil, N. Petrone, and M. Cognolato, "Impact performance of standard tabletop and constant equivalent fall height snow park jumps," in *Skiing trauma and safety: 20th volume*, ASTM International, 2015.

[8] J. A. McNeil, M. Hubbard, and A. D. Swedberg, "Designing tomorrow's snow park jump," *Sports Engineering*, vol. 15, no. 1, pp. 1–20, 2012.

[9] D. Levy, M. Hubbard, J. A. McNeil, and A. Swedberg, "A design rationale for safer terrain park jumps that limit equivalent fall height," *Sports Engineering*, vol. 18, no. 4, pp. 227–239, 2015.

[10] N. Petrone, M. Cognolato, J. A. McNeil, and M. Hubbard, "Designing, building, measuring, and testing a constant equivalent fall height terrain park jump," *Sports Engineering*, vol. 20, pp. 283–292, 2017.

[11] J. K. Moore, *Learn Multibody Dynamics*. 2022.

[12] B. J. Bastiaansen, E. Wilmes, M. S. Brink, C. J. de Ruiter, G. J. Savelsbergh, A. Steijlen, K. M. Jansen, F. C. van der Helm, E. A. Goedhart, D. van der Laan, *et al.*, "An inertial measurement unit based method to estimate hip and knee joint kinematics in team sport athletes on the field," *JoVE (Journal of Visualized Experiments)*, no. 159, p. e60857, 2020.

[13] N. Kurpiers, P. McAlpine, and U. G. Kersting, "Predictors of falls in recreational snowboard jumping: An observational study," *Injury*, vol. 48, no. 11, pp. 2457–2460, 2017.

[14] D. L. Puddle and P. S. Maulder, "Ground reaction forces and loading rates associated with parkour and traditional drop landing techniques," *Journal of sports science & medicine*, vol. 12, no. 1, p. 122, 2013.

A

Ski resorts

The experiment took place in 4 different ski resort in northern Italy on 4 days scattered over a period of 2 weeks. The ski resorts were: Seiser Alm, Obereggen, Kronplatz, and Madonna di Campiglio.In total, 121 are jump are performed on 13 distinctive kickers. Throughout all testing days, the duration of the experiment was limited to within a 2-hour timeframe. This decision was primarily motivated by the desire to maintain consistent conditions. The skiers' physical condition and fatigue level was also taken into account. Of the 121 jumps, 17 jumps were omitted because during these specific jumps, the RTK correction signal was lost. Therefore, it was not certain that the position data of the skier was still accurate enough for the analysis. In table A.1, an overview of all jumps is given where the omitted jumps are marked with a ×. Below, a short description of the snowparks is given and an overview is given of the number of jumps performed.

A.1. Seiser Alm

Seiser Alm is ski resort in the Italian dolomites. The snow park where the experiment took place, consists of one single line with two very large kickers. During this day, a skidoo was available to tow the skier back from the bottom of the run to the start of the run. This saved a lot of time because it is a lot faster than the ski lift. Because of this, in a short amount of time, 18 runs are performed. This adds up to 36 jumps on two distinctive kickers.

A.2. Obereggen

The snow park in Obereggen also consists of a line with 2 consecutive kickers. The run starts right on top of the lift station, so this day the ski lift is used to get back at the start of the run. This resulted in fewer runs: 11, adding up top 22 jumps on two distinctive kickers

A.3. Kronplatz

Kronplatz is a ski resort which has multiple kicker lines in its snow park. The largest one with the longest jumps is chosen for the experiment to get a good variability in the types of kickers throughout the whole experiment. This line consists of 3 consecutive kickers. Again, the ski lift is used to get back to the start of the run. A total of 10 runs are performed, meaning a total of 30 jumps on 3 consecutive kickers.

A.4. Madonna di Campiglio

The snow park in Madonna di Campiglio has two different lines, an medium sized one and a large one, both consisting of three consecutive kickers. On this day, again a skidoo was available to tow the skier back to the start of the run. This time advantage made it possible to perform the experiment on both runs. On the M-line and the L-line, 5 and 6 runs are performed, respectively. This resulted in a total of 33 jumps performed on 6 distinctive kickers.

Table A.1: All the jumps that were performed. Jumps used for the analysis are highlighted with a ✓, omitted jumps are marked with a ×, and '-' indicates that there wasn't a 3^{rd} jump in the park.

		Jump 1	Jump 2	Jump 3
Seiser Alm	Run 1	✓	✓	-
	Run 2	✓	✓	-
	Run 3	✓	✓	-
	Run 4	✓	✓	-
	Run 5	✓	✓	-
	Run 6	×	×	-
	Run 7	✓	✓	-
	Run 8	✓	✓	-
	Run 9	✓	✓	-
	Run 10	✓	✓	-
	Run 11	✓	✓	-
	Run 12	✓	✓	-
	Run 13	✓	✓	-
	Run 14	✓	✓	-
	Run 15	✓	✓	-
	Run 16	✓	✓	-
	Run 17	✓	✓	-
	Run 18	✓	✓	-
Obereggen	Run 1	×	×	-
	Run 2	×	✓	-
	Run 3	✓	×	-
	Run 4	✓	×	-
	Run 5	✓	×	-
	Run 6	✓	✓	-
	Run 7	✓	✓	-
	Run 8	✓	×	-
	Run 9	✓	×	-
	Run 10	✓	×	-
	Run 11	✓	✓	-
Kronplatz	Run 1	✓	✓	✓
	Run 2	✓	✓	✓
	Run 3	✓	✓	✓
	Run 4	✓	✓	✓
	Run 5	✓	✓	✓
	Run 6	✓	✓	✓
	Run 7	✓	×	×
	Run 8	✓	✓	✓
	Run 9	✓	✓	✓
	Run 10	✓	✓	✓

		Jump 1	Jump 2	Jump 3
Madonna di Campiglio	Run 1	✓	✓	✓
	Run 2	✓	✓	✓
	Run 3	✓	✓	×
	Run 4	✓	✓	✓
	Run 5	✓	✓	✓
	Run 6	✓	✓	✓
	Run 7	✓	✓	✓
	Run 8	✓	×	×
	Run 9	✓	✓	✓
	Run 10	✓	✓	✓
	Run 11	✓	×	✓

B

Sensors

This appendix gives an overview of the sensors that were used and what they were used for during the experiment. Two different types of sensors were used: two Inertial Measurement Units (IMUs) and two, very similar, position sensors that use Real-Time Kinematic positioning (RTK).

B.1. IMUs

The IMUs measured the acceleration and the angular velocity of the skier. They are from the brand Shimmer (Figure B.1a). They have their own local coordinate system, which can be calibrated as desired. The coordinate system that was chosen for this experiment is shown in Figure B.1b. For this experiment, the problem was considered as two-dimensional. The IMUs are equipped with a low-noise accelerometer, a wide-range accelerometer, a gyroscope, and a magnetometer. The low-noise accelerometer can capture accelerations up to ± 2g while the wide-range accelerometer captures accelerations up to ± 16g. The sample rate of the IMUs is set to 504Hz in order to capture the landing period with enough data points.

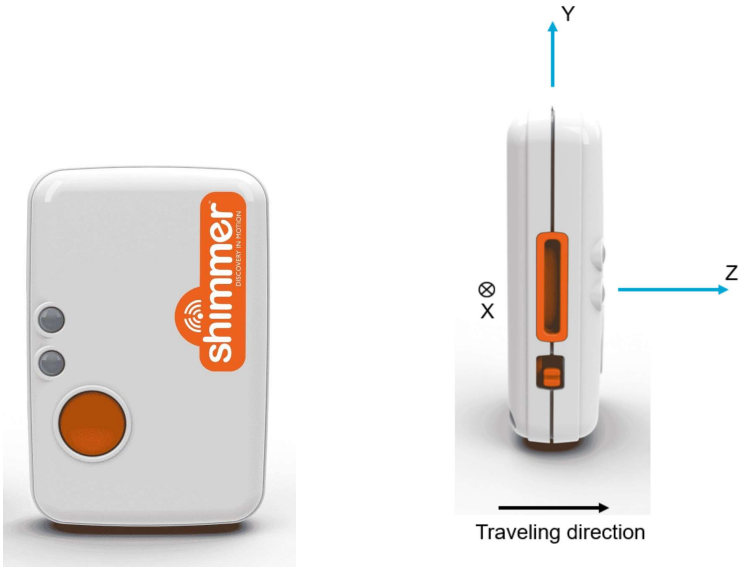

(a) (b)

Figure B.1: Front view (a) and side view with the chosen coordinate system (b) of the Shimmer3 IMU. Image: ©https://shimmersensing.com/product/shimmer3-imu-unit

B.1.1. Placement and attachment

The IMUs were attached to the skier's body with clips that came with the sensors. These clips are taped to a harness that can be strapped around the upper body of the skier. This harness is normally used to attach a GoPro camera and consists of two elastic straps that go around the chest and two elastics straps going over the shoulders (Figure **??**). The harness is worn on top of the skier's clothes. The straps are tightened as much as possible to prevent moment of the IMUs with respect to the skier's body. The placement of the IMUs was determined experimentally, as described in Appendix D.2.1

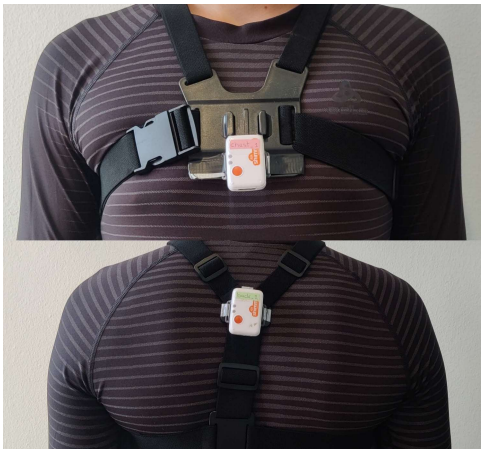

Figure B.2: Attachment of the IMU clips

B.2. Position sensors

For the experiment, two position sensors are used. One for measuring the position of the skier and one for surveying the landing surface. The sensors are identical, except for the fact that the sensor used for measuring the skier's position can record at a higher sampling frequency, 20 Hz, compared to the other position sensor, 2 Hz. This higher sampling frequency is needed to accurately track the skier when he is traveling down the slope and flying in the air. Airtime on jumps during the experiments varied between ~1-3 seconds. On the smallest jumps, the 2Hz sensor would only capture one or two data points in the air, which is considered not enough.

The position sensors used are the Leica iCON GPS 70 (Figure B.3a) and the Leica GS18 (Figure B.3b). These are Global Navigation Satellite Systems (GNSS) sensors that use Real-Time Kinematic positioning (RTK) to determine the sensors positions very accurately. The sensors, called rovers, communicate with a reference station that is positioned somewhere in the mountains (Figure B.4). The coordinates of this station are known and therefore the signal propagation errors caused by atmospheric disturbances can be calculated. Consequently, the reference station sends correction data to the rover, which then refines its own position estimate. Hence, this technique results in a higher accuracy than normal GNSS does, which typically operates within a range of several meters. By employing RTK, the rovers, when stationary, can be as accurate as 1-2 centimeters.

(a) The Leica iCON GPS 70 sensor (©image: https://www.sccssurvey.co.uk/leica-icon-gps-70-series.html)

(b) The Leica GS18 sensor (©image: https://ecnk.ru/catalog/41569/)

Figure B.3: The GNSS RTK sensors used during the experiment

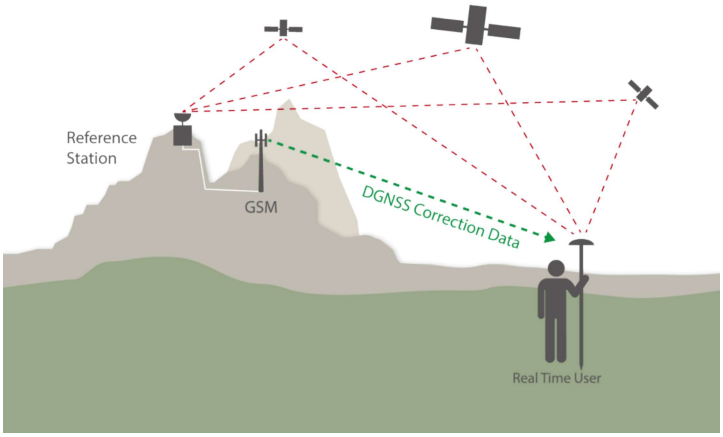

Figure B.4: Visual representation on how RTK sensors work. Correction data is received from a base station of which the positions in known. Incorporating this correction data is the position signal received from the satellites leads in an accurate position estimate. (©image: https://www.swisstopo.admin.ch/en/knowledge-facts/surveying-geodesy/observation-procedures/satellite-observations/gps-observation.html)

B.2.1. Surveying the landing area

In each snow park, the landing area is surveyed using the Leica iCON GPS 70. The sensor is mounted on a pole which is dragged over the snow surface on both sides of the kicker-line. The sensor compensates for the length and tilting of the pole, and therefore recorded the coordinates of the bottom of the pole. The recorded points are 0.5 meters apart and a visual representation of them is given in Figure B.5. To be able to calculate the slope angle at a specific landing point, a detailed profile of the landing surface was needed. Therefore, a mesh of points was created which is considered to represent the entire slope. This was done by first adding 10 additional points in between the recorded points for each side of the slope, through linear interpolation, as shown in Figure B.6. To finish the mesh of points, the two sides of the slopes were connected by adding points every 0.1 m (Figure B.7)

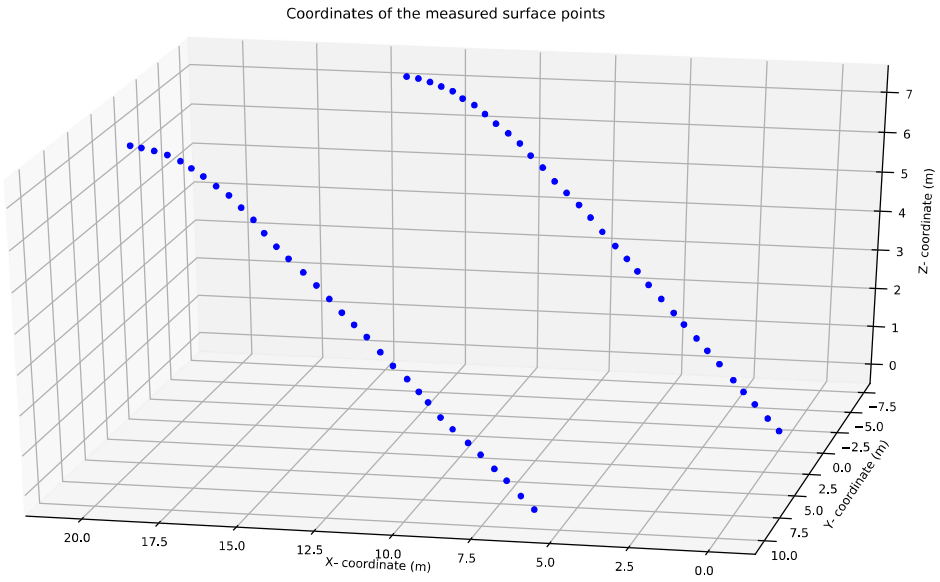

Figure B.5: Landing area data points recorded by the Leica iCON 70 in Madonna di Campiglio on the 1^{st} jump.

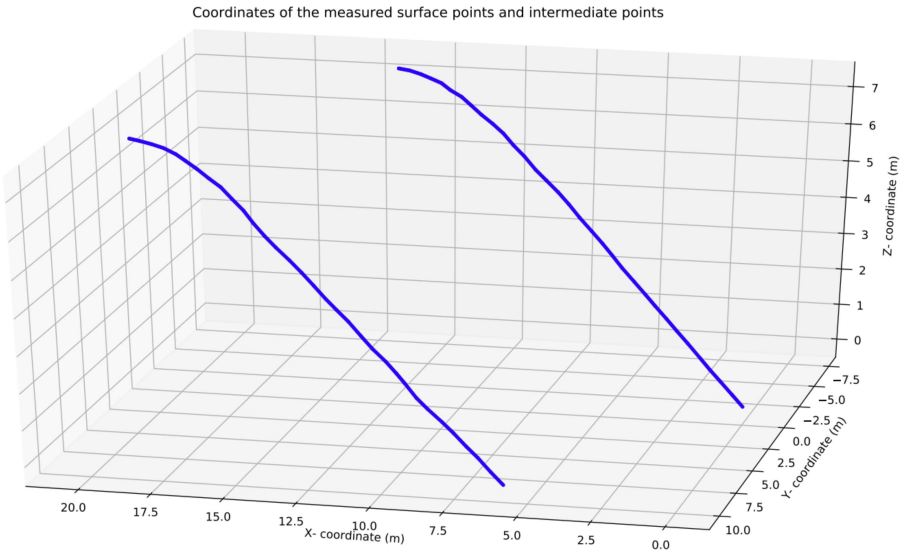

Figure B.6: Coordinates of the measured surface points and intermediate points

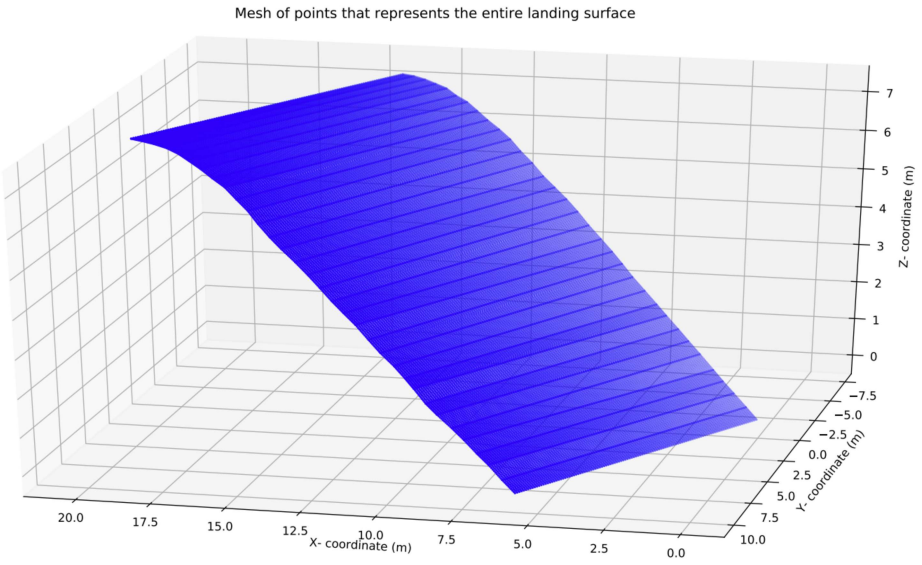

Figure B.7: Mesh of points that represents the entire landing surface

B.2.2. Measuring skier's flight trajectory

The Leica GS18 is used to measure the trajectory of the skier. It records its position at a sampling frequency of 20 Hz. The sensor is attached to a backpack which was carried by the skier (figure B.8). It was important that the sensor was on the outside of the backpack because the signal it has to receive is easily blocked by other objects and materials. This is done by mounting the sensor on an L-shaped plate that can be attached to the backpack using simple straps. The backpack had a waistband and a chest band that are strapped tightly to minimize amount of possible movement of the sensor with respect to the skier's body. The skier claimed not to be affected by the extra weight on his back.

Figure B.8: Leica GS18 sensor attached to the backpack

C

Equivalent Fall Height

This appendix gives a detailed explanation of how EFH is calculated with the data that is gathered during the experiment. In order to calculate the EFH, the following parameters need to be extracted from the data gathered by the position sensor:

- Landing point (t_l)
- Velocity of the skier at the landing point (v_l)
- Angle the skier's trajectory makes wit the horizontal at the landing point (φ_{skier})
- Inclination of the slope at the landing point ($\varphi_{landing}$)

C.1. Landing point

The landing point is defined as the moment where the total acceleration, measured by the low-noise accelerometer on the chest, is equal to g for the first time after time in the air. Since the data is discrete, the total acceleration measured is never exactly equal to g. Therefore, the last point where the total acceleration is still lower than g, and the consecutive point were found. By using linear interpolation, the exact time of landing (t_l) is determined (C.3)

$$t_l = t_0 + \frac{(g - a_1) * (t_1 - t_0)}{a_1 - a_0} \tag{C.1}$$

where:

t_l : Exact landing time,
t_0 : Last point after airtime where $a_{tot} < g$,
t_1 : First point after airtime where $a_{tot} > g$,
a_0 : Total acceleration at t_0,
a_1 : Total acceleration at t_1.

In order to also find this exact moment in time in the position data, the two sensors are time synchronized. Data from both sensors have a timestamp. The IMUs record unixtime, while the position sensors allocate each data point an 'point-ID'. These point-ID's are constructed as $XXXXMMDDhhmmsspp$, in which:

MM : Month
DD : Day
hh : Hour
mm : Minute
ss : Second
pp : $1/100$ of a second

The point-ID's were converted to unixtime.

C.2. Landing velocity

The velocity of the skier at any point in time was determined by differentiating the position data with respect to time. The data contains the x, y, and z coordinates of the sensor in a global reference frame. These signals are differentiated individually, after which the absolute velocity was calculated (C.2).

Let $\mathbf{r} = [x, y, z]$

$$\text{for } i \text{ in } \mathbf{r} : v_i = \frac{i_{n+1} - i_n}{t_{n+1} - t_n}$$

$$|\mathbf{v}| = \sqrt{v_x^2 + v_y^2 + v_z^2} \tag{C.2}$$

Because the time of landing is known, the velocity at that point could be found. This is also done by linear interpolation, since the data points are scattered around this time of landing (C.3)

$$v_l = v_0 + \frac{(t_l - t_0) * (v_1 - v_0)}{t_1 - t_0} \tag{C.3}$$

where:

v_l : Landing velocity,
t_l : Landing time,
t_0 : Time at last data point before t_l,
t_1 : Time at first data point after t_l,
v_0 : Velocity at t_0,
v_1 : Velocity at t_1.

C.3. Skier angle

To find the skier angle at time step n, the velocity vector calculated in the previous section is used (C.4)

$$\varphi_{skier} = \arcsin\left(\frac{-v_z}{|\bar{v}|}\right) \tag{C.4}$$

Again, linear interpolation is used to find the skier angle at the exact time of landing (C.5)

$$\varphi_{skier_{t_l}} = \varphi_{skier_0} + \frac{(t_l - t_0) * (\varphi_{skier_1} - \varphi_{skier_0})}{t_1 - t_0} \tag{C.5}$$

where:

$\varphi_{skier_{t_l}}$: Skier angle at time of landing,
t_l : Landing time,
t_0 : Time at last data point before t_l,
t_1 : Time at first data point after t_l,
φ_{skier_0} : Skier angle at t_0,
φ_{skier_1} : Skier angle at t_1.

C.4. Slope angle

As described in appendix B.2.1, a mesh of point is created to be able to calculate the inclination of the slope at the landing point. To find the slope angle at the landing point (φ_{slope}), two points of the landing surface mesh are picked that are close to the landing point, and inline with the skiers' trajectory. This was done by finding the position data point of the skier right before landing, and the one a little after landing. Consequently, the distance between these points and all points in the landing surface mesh were calculated. The points in the mesh that are closest to the two position data points were used to calculate the slope angle. A visual representation of this is given in figure C.1. The coordinates of the surface points were used to calculate the inclination of the slope (C.6)

$$\varphi_{slope} = \arcsin\left(\frac{z_1 - z_2}{\sqrt{(x_1 - x_2)^2 + (y_1 - y_2)^2 + (z_1 - z_2)^2}}\right) \tag{C.6}$$

where:

x_1 : X-coordinate of the first point on the surface
x_2 : X-coordinate of the second point on the surface
y_1 : Y-coordinate of the first point on the surface
y_2 : Y-coordinate of the second point on the surface
z_1 : Z-coordinate of the first point on the surface
z_2 : Z-coordinate of the second point on the surface

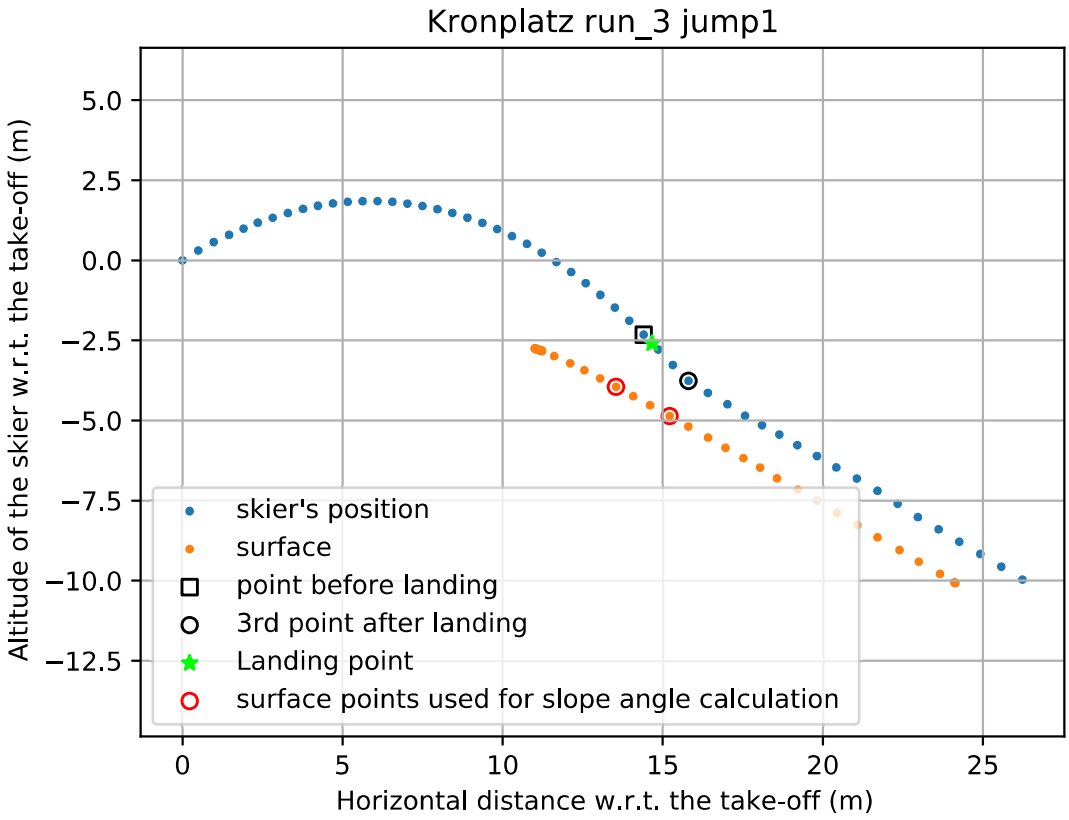

Figure C.1: Flight curve of an arbitrary jump with the take-off point set as the origin. The landing point is shown as a green star. The point before the landing point and the 3rd point after the landing point are highlighted with black shapes. The points on the surface that are closest to these points are encircled in red and used for the calculation of the slope angle ($\varphi_{landing}$).

D

Peak GRF

The peak Ground Reaction Force (GRF) is the maximum force that the skier experiences normal to the snow surface he is landing on. IMUs were used to estimate the GRF, since they are equipped with an accelerometer. The GRF is expressed in terms of the skier's body weight (BW). Therefore, the peak GRF can also be represented by the peak normal acceleration at impact divided by g (D.1).

$$GRF = m * a_{?}$$
$$\frac{GRF}{m * g} = \frac{a_{?}}{g} \tag{D.1}$$

The acceleration of the skier is known in the local coordinate system of the IMUs. In order to determine the component of acceleration normal to the landing surface, the orientation of the IMU and the inclination angle of the slope at the moment of impact were calculated.

D.1. IMU orientation

In order to calculate the normal component of acceleration at impact, the orientation of the IMU has to be known. The IMU has three sensors, which all have some information about its orientation: the accelerometer, the gyroscope, the magnetometer. In early stages of the experimental setup, it is concluded that a combination of the accelerometer and the gyroscope can be used to find the orientation of the IMU.

D.1.1. Accelerometer

The accelerometer can be helpful to calculate the orientation of the IMU, especially when it is at rest. Since the direction of gravity is known, the orientation of the IMU can be determined by looking at how much of the this acceleration vector is picked up by the the individual components of the accelerometer. This is displayed in figure D.1. The orientation of the IMU is then a function of the accelerometer data (D.2)

$$\theta = arctan(\frac{-a_z}{a_y}) \tag{D.2}$$

The accelerometer's estimation of the orientation is stable and reliable over a longer period of time. The downside of this method is that accelerometers are sensitive

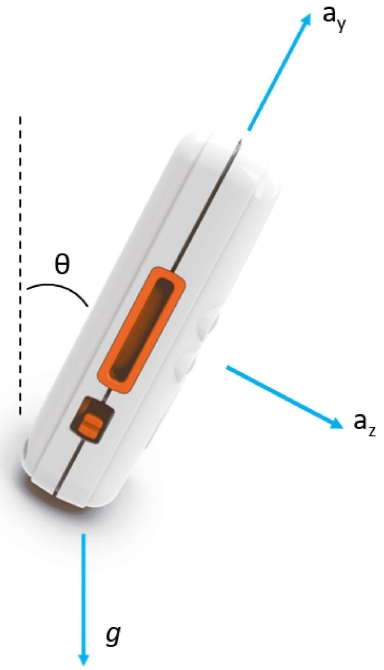

Figure D.1: IMU orientation

to dynamic motion, which results in inaccuracies during high-frequency movements. Therefore, the low-noise accelerometer of the IMU was used. To filter out the high-frequency components of the signal, an aggressive moving average filter with a Gaussian kernel is used.

D.1.2. Gyroscope

Another way to determine the orientation of the IMU is by integrating the data gathered by the gyroscope. If the initial orientation of the IMU is known (θ_i), the orientation after a certain amount of time can be calculated (D.3)

$$\theta_t = \theta_i + \int_0^t \omega_z \, dt \tag{D.3}$$

The gyroscope accurately captures short-term changes in orientation. However, it suffers from integration drift over time, causing orientation errors to accumulate.

D.1.3. Sensor fusion

By using sensor fusion, the benefits of both sensors can be capitalized and the effect of their limitations can be minimized. As said earlier, the accelerometer is accurate for low-frequency movements, while the gyroscope is accurate for high-frequency dynamics.

The sensor fusion technique used in this study is referred to as a complementary filter. This filtering method relies on a weight factor, denoted as α, to dictate the level of confidence placed in the orientation estimates provided by the respective sensors. Choosing a small α, means that the gyroscope's estimation of the orientation is considered more accurate during each discrete time step, especially when high-frequency movement occurs. The inclusion of the accelerometer's orientation estimates in this process significantly impacts the final orientation estimation, effectively minimizing the gyroscope's inherent drift over time. In the end, this results in a robust and accurate orientation estimation over the entire course of the experiment. The mathematical description of this complementary filter is given in equation D.4

$$\theta_n = \alpha * \theta_{a_n} + (1 - \alpha) * (\theta_{n-1} + \omega_{x_n} * \Delta t) \tag{D.4}$$

where:

θ_n : Orientation estimate at time step n,
α : Weight coefficient, $0 < \alpha < 1$,
θ_{a_n} : Accelerometer's orientation estimate
ω_{x_n} : Angular velocity of the gyroscope
Δt : $t_n - t_{n-1}$

The weight factor α, is chosen to be 0.05. The number is small because the experiment took place in an environment where a lot of high frequency movement can disturb the orientation estimation done by the accelerometer. An exception is made when the skier is in the air. Since the accelerometer does not measure the gravitational acceleration when it is not on the ground, the orientation estimate it provides is not accurate. Therefore, during that time, the orientation of the IMU is solely determined by the gyroscope's estimate. Also during the first 0.5 seconds of impact, the accelerometer is not considered, because very high frequency movements occur.

D.1.4. Complementary filter validation

The complementary filter described above is validated prior to the experiment. This was done by sticking an IMU on a large wooden stick on which two large red dots are drawn. A video is made of a person jumping up and down while rotating the stick in an arbitrary way. The orientation of the stick could be derived from the location of the two red dots on the end (Figure D.2). After comparing the

results with the orientation output of the complementary filter it is concluded that the filter worked as expected and that it is a robust way to determine the orientation of the IMU while attached to a skier performing freestyle jumps.

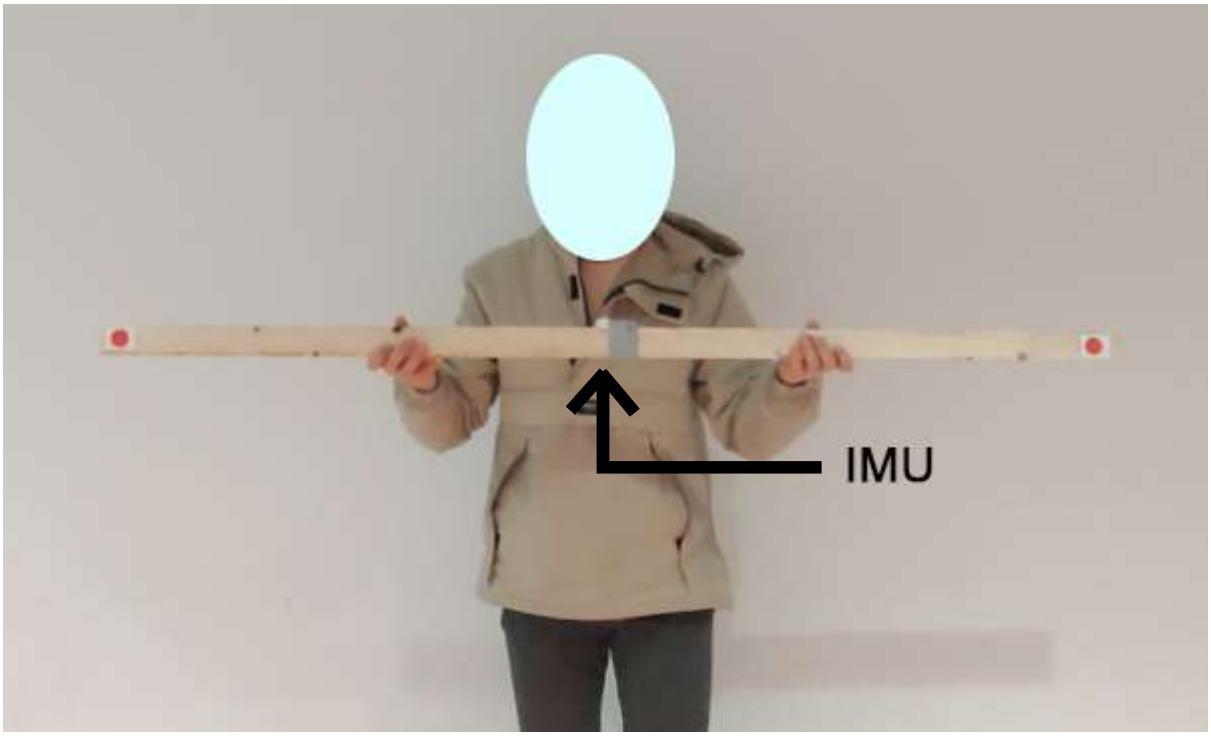

Figure D.2: The stick that was used to validate the orientation estimation of the IMUs.

D.2. Peak normal acceleration

With the orientation of the IMUs known, the component of acceleration normal to the landing surface can be calculated. In Figure D.3, an overview of the relevant coordinate systems is given. Equation D.5 describes the relation between these coordinate systems.

$$\begin{bmatrix} c_x \\ c_y \\ c_z \end{bmatrix} = \begin{bmatrix} 1 & 0 & 0 \\ 0 & cos(\varphi_l - \theta) & sin(\varphi_l - \theta) \\ 0 & -sin(\varphi_l - \theta) & cos(\varphi_l - \theta) \end{bmatrix} \begin{bmatrix} b_x \\ b_y \\ b_z \end{bmatrix} \tag{D.5}$$

So the normal component of acceleration in terms of the local accelerations measured by the IMUs van be written as:

$$^{C}a_y = cos(\varphi_l - \theta) * {}^{B}a_y + sin(\varphi_l - \theta) * {}^{B}a_z \tag{D.6}$$

To find the peak normal acceleration, a period of ~0.5 seconds after the flight phase is evaluated to find the highest value of the normal acceleration. Consequently, this number is divided by g, which results in the peak GRF in terms of the skiers body weight.

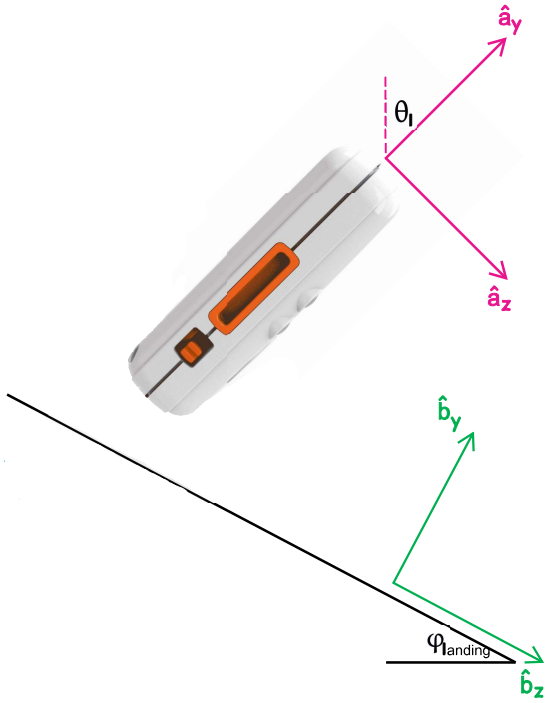

Figure D.3: The reference frame of the IMU in pink and the reference frame of the slope in green; the orientation of the IMU, θ and the slope angle, $\varphi_{landing}$.

D.2.1. Validation test

Prior to the experiment, a test is conducted to see if the method described above yields realistic values for the peak GRF. Two load cells are mounted on a plate (Figure D.4). Heavy, known weights are put on them to find the weight-voltage curve. This 'force plate' was then used to perform a series of jumps while wearing the IMUs on four different positions on the body: the chest, the upper back, and on both the front and backside of the waist. The GRF was calculated by the method described above and compared to the readings of the force plate. Results of this test were that the chest and upper back are appropriate locations to place the IMUs because, although not perfect, the results were comparable with the force plate readings.

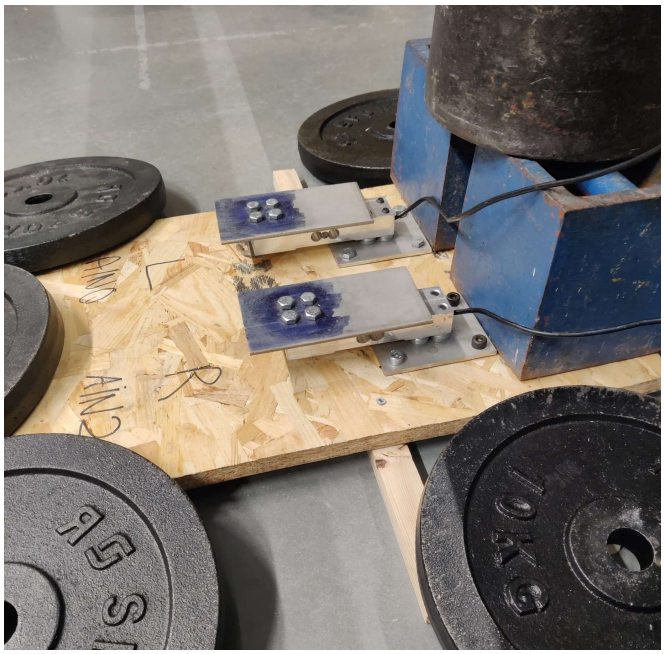

Figure D.4: The force plate that was created to validate the methodology of estimating the GRF by using IMUs. Two load cells are mounted on a wooden plate, which is kept at its place by heavy weights.

E

Relevant parameters table

In the table below an overview of all jumps with their relevant metrics is given. These metrics are EFH, landing velocity (v_l), skier angle (ϕ_{skier}), slope angle (ϕ_{slope}), GRF_{chest}, and GRF_{back}.

line	run	jump	v_l	φ_{skier}	φ_{slope}	EFH	GRF_{chest}	GRF_{back}
Kronplatz	run_1	jump1	13.72	0.89	0.51	1.30	5.25	3.35
Kronplatz	run_1	jump2	16.43	0.93	0.58	1.66	6.75	4.26
Kronplatz	run_1	jump3	12.66	0.71	0.40	0.75	3.90	2.57
Kronplatz	run_2	jump1	13.59	0.82	0.51	0.87	4.26	2.73
Kronplatz	run_2	jump2	15.92	0.91	0.57	1.46	6.87	3.86
Kronplatz	run_2	jump3	12.65	0.69	0.42	0.59	2.63	1.81
Kronplatz	run_3	jump1	13.14	0.81	0.50	0.81	3.67	2.17
Kronplatz	run_3	jump2	15.69	0.86	0.57	1.08	5.04	3.64
Kronplatz	run_3	jump3	13.98	0.79	0.50	0.84	4.30	2.59
Kronplatz	run_4	jump1	14.69	0.80	0.51	0.88	5.28	3.54
Kronplatz	run_4	jump2	16.84	0.92	0.59	1.54	6.02	3.75
Kronplatz	run_4	jump3	13.88	0.78	0.50	0.77	5.24	3.23
Kronplatz	run_5	jump1	13.50	0.80	0.50	0.82	6.22	3.59
Kronplatz	run_5	jump2	15.68	0.89	0.57	1.28	7.06	3.41
Kronplatz	run_5	jump3	13.12	0.75	0.47	0.68	2.89	1.74
Kronplatz	run_6	jump1	14.13	0.85	0.51	1.11	5.67	3.88
Kronplatz	run_6	jump2	15.91	0.90	0.57	1.39	5.57	2.95
Kronplatz	run_6	jump3	14.39	0.78	0.50	0.83	5.18	2.82
Kronplatz	run_7	jump1	13.89	0.81	0.50	0.90	4.01	2.03
Kronplatz	run_8	jump1	12.32	0.83	0.47	0.97	5.85	3.39
Kronplatz	run_8	jump2	15.84	0.90	0.57	1.36	5.63	3.49
Kronplatz	run_8	jump3	15.95	0.84	0.52	1.28	6.81	3.55
Kronplatz	run_9	jump1	13.68	0.82	0.50	0.96	5.75	3.37
Kronplatz	run_9	jump2	15.89	0.87	0.57	1.14	6.05	3.37
Kronplatz	run_9	jump3	14.79	0.85	0.50	1.32	5.99	3.36
Kronplatz	run_10	jump1	14.71	0.80	0.52	0.81	5.87	3.27
Kronplatz	run_10	jump2	17.38	0.90	0.58	1.51	7.13	4.02
Kronplatz	run_10	jump3	14.94	0.81	0.50	1.03	5.75	3.28

line	run	jump	v_l	φ_{skier}	φ_{slope}	EFH	GRF_{chest}	GRF_{back}
Madonna_M	run_1	jump1	11.71	0.71	0.48	0.33	4.75	2.92
Madonna_M	run_1	jump2	13.64	0.77	0.50	0.72	5.47	3.41
Madonna_M	run_1	jump3	13.65	0.78	0.51	0.71	4.57	2.84
Madonna_M	run_2	jump1	11.92	0.79	0.49	0.65	5.67	3.48
Madonna_M	run_2	jump2	13.08	0.81	0.48	0.89	5.43	3.50
Madonna_M	run_2	jump3	13.34	0.79	0.51	0.71	4.07	3.12
Madonna_M	run_3	jump1	11.40	0.77	0.48	0.53	5.00	3.25
Madonna_M	run_3	jump2	13.79	0.83	0.49	1.07	7.14	3.89
Madonna_M	run_4	jump1	12.20	0.82	0.50	0.78	4.82	3.36
Madonna_M	run_4	jump2	13.51	0.85	0.50	1.13	6.11	3.89
Madonna_M	run_4	jump3	13.14	0.71	0.49	0.40	3.86	2.91
Madonna_M	run_5	jump1	11.33	0.74	0.48	0.43	5.49	3.37
Madonna_M	run_5	jump2	12.06	0.68	0.47	0.32	3.76	2.40
Madonna_M	run_5	jump3	15.18	0.82	0.50	1.19	6.43	3.44
Madonna_M	run_6	jump1	10.61	0.70	0.44	0.39	4.51	2.92
Madonna_M	run_6	jump2	12.85	0.71	0.48	0.46	3.31	2.57
Madonna_M	run_6	jump3	13.68	0.81	0.50	0.92	3.63	3.05
Madonna_L	run_7	jump1	13.12	0.90	0.55	1.07	6.33	4.30
Madonna_L	run_7	jump2	13.92	0.74	0.48	0.70	4.92	3.24
Madonna_L	run_7	jump3	14.69	0.77	0.47	0.98	2.43	1.80
Madonna_L	run_8	jump1	13.52	0.93	0.55	1.25	5.84	3.47
Madonna_L	run_9	jump1	14.26	0.90	0.55	1.21	6.57	3.73
Madonna_L	run_9	jump2	14.92	0.86	0.57	0.94	6.13	4.12
Madonna_L	run_9	jump3	17.06	0.78	0.58	0.62	5.95	3.59
Madonna_L	run_10	jump1	13.49	0.80	0.55	0.55	5.22	2.98
Madonna_L	run_10	jump2	14.13	0.75	0.53	0.48	4.46	2.71
Madonna_L	run_10	jump3	14.92	0.74	0.54	0.43	1.65	1.27
Madonna_L	run_11	jump1	12.94	0.79	0.55	0.48	5.38	3.34
Madonna_L	run_11	jump3	14.39	0.75	0.52	0.57	2.10	1.63
Obereggen	run_2	jump2	12.98	0.83	0.45	1.17	6.02	3.37
Obereggen	run_3	jump1	10.61	0.73	0.45	0.44	4.07	2.30
Obereggen	run_4	jump1	11.90	0.80	0.49	0.67	5.62	3.33
Obereggen	run_5	jump1	11.06	0.77	0.47	0.55	3.66	2.84
Obereggen	run_6	jump1	10.37	0.68	0.45	0.28	6.54	3.01
Obereggen	run_6	jump2	12.36	0.76	0.46	0.68	5.65	3.10
Obereggen	run_7	jump1	10.32	0.66	0.46	0.23	4.78	2.57
Obereggen	run_7	jump2	13.75	0.82	0.51	0.91	4.77	2.55
Obereggen	run_8	jump1	11.36	0.79	0.48	0.62	5.91	2.84
Obereggen	run_9	jump1	10.78	0.77	0.48	0.50	4.14	2.28
Obereggen	run_10	jump1	10.12	0.63	0.39	0.29	3.92	1.98
Obereggen	run_10	jump2	13.47	0.78	0.51	0.65	5.64	2.90
Obereggen	run_11	jump1	9.41	0.57	0.31	0.29	3.44	1.52

line	run	jump	v_l	φ_{skier}	φ_{slope}	EFH	GRF_{chest}	GRF_{back}
Seiser	run_1	jump1	15.14	0.85	0.58	0.83	6.21	3.83
Seiser	run_1	jump2	16.81	0.90	0.58	1.41	7.60	3.35
Seiser	run_2	jump1	13.76	0.86	0.52	1.07	6.16	3.29
Seiser	run_2	jump2	15.35	0.96	0.58	1.66	6.36	3.45
Seiser	run_3	jump1	12.84	0.89	0.45	1.53	5.33	3.34
Seiser	run_3	jump2	15.07	0.81	0.57	0.64	3.52	1.90
Seiser	run_4	jump1	13.65	0.89	0.53	1.18	3.54	2.88
Seiser	run_4	jump2	15.58	0.87	0.57	1.10	5.74	3.41
Seiser	run_5	jump1	13.80	0.84	0.51	1.05	6.19	2.92
Seiser	run_5	jump2	14.93	0.85	0.56	0.89	6.47	3.34
Seiser	run_7	jump1	12.91	0.86	0.47	1.22	4.80	2.97
Seiser	run_7	jump2	14.91	0.90	0.56	1.27	5.50	3.44
Seiser	run_8	jump1	13.88	0.86	0.52	1.07	6.55	3.58
Seiser	run_8	jump2	13.71	0.75	0.39	1.20	3.92	2.35
Seiser	run_9	jump1	12.83	0.87	0.46	1.36	5.08	2.84
Seiser	run_9	jump2	15.50	0.92	0.58	1.35	7.13	3.25
Seiser	run_10	jump1	13.71	0.87	0.51	1.16	4.95	2.75
Seiser	run_10	jump2	14.08	0.81	0.47	1.10	3.62	2.04
Seiser	run_11	jump1	13.28	0.85	0.50	1.05	5.10	2.56
Seiser	run_11	jump2	14.91	0.87	0.56	1.07	6.93	2.74
Seiser	run_12	jump1	13.85	0.90	0.53	1.29	4.72	3.26
Seiser	run_12	jump2	14.93	0.89	0.57	1.13	5.19	2.72
Seiser	run_13	jump1	13.71	0.89	0.52	1.27	5.90	3.07
Seiser	run_13	jump2	14.29	0.83	0.52	1.01	5.49	3.34
Seiser	run_14	jump1	14.65	0.87	0.57	0.97	7.41	3.01
Seiser	run_14	jump2	15.68	0.88	0.57	1.10	7.56	4.08
Seiser	run_15	jump1	13.92	0.89	0.51	1.38	7.91	3.98
Seiser	run_15	jump2	15.55	0.91	0.57	1.35	7.12	3.90
Seiser	run_16	jump1	13.83	0.80	0.53	0.72	3.98	2.47
Seiser	run_16	jump2	15.70	0.79	0.57	0.56	6.99	3.08
Seiser	run_17	jump1	14.39	0.79	0.54	0.67	4.81	2.71
Seiser	run_17	jump2	15.72	0.87	0.58	1.08	6.75	3.30
Seiser	run_18	jump1	13.91	0.83	0.52	0.94	5.17	3.10
Seiser	run_18	jump2	16.72	0.91	0.58	1.47	5.38	4.27

EFH vs. peak GRF plots

In this appendix, the peak GRF vs. EFH plots are provided. First the plot for all jumps. Then, the plots for different ski resorts.

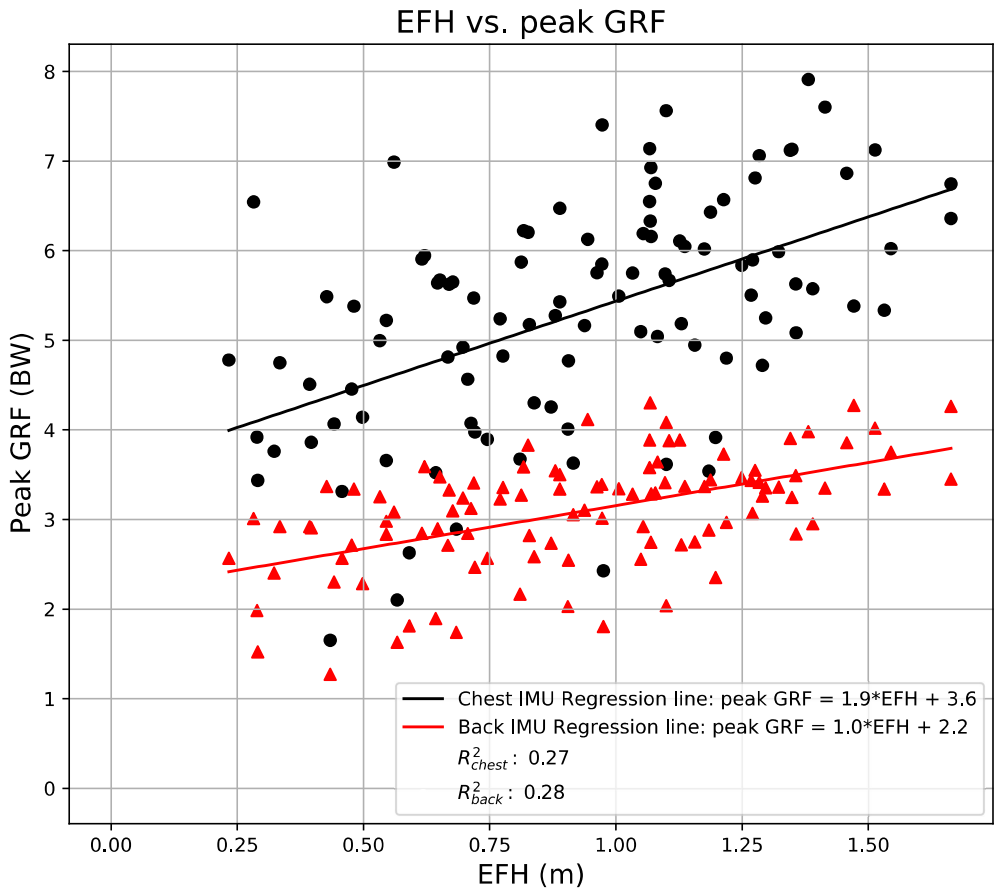

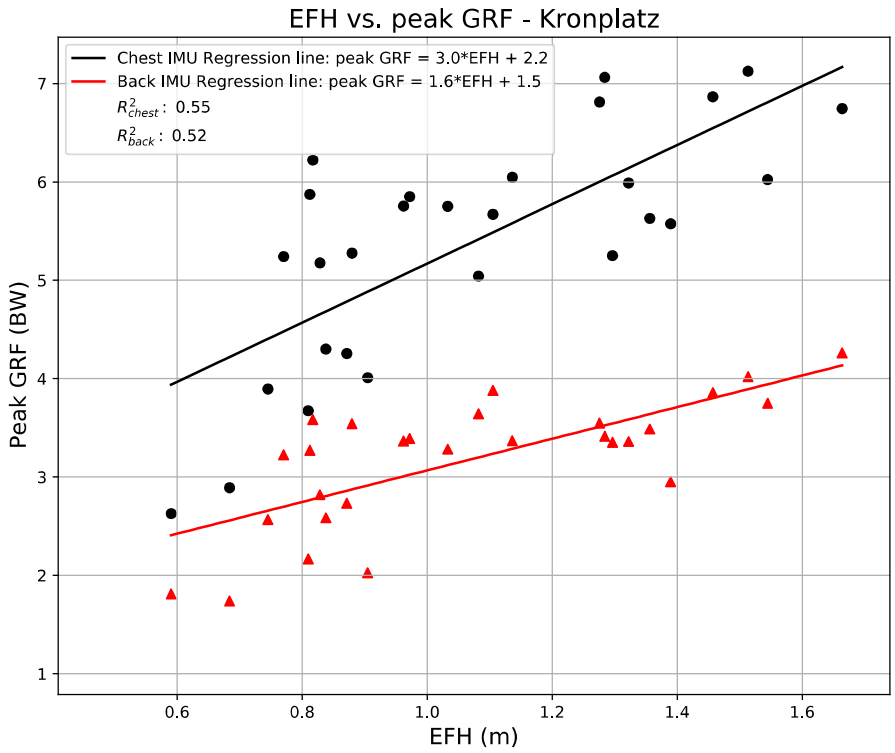
EFH vs. peak GRF - Kronplatz
Chest IMU Regression line: peak GRF = 3.0*EFH + 2.2
Back IMU Regression line: peak GRF = 1.6*EFH + 1.5
R^2_{chest}: 0.55
R^2_{back}: 0.52
Peak GRF (BW)
EFH (m)

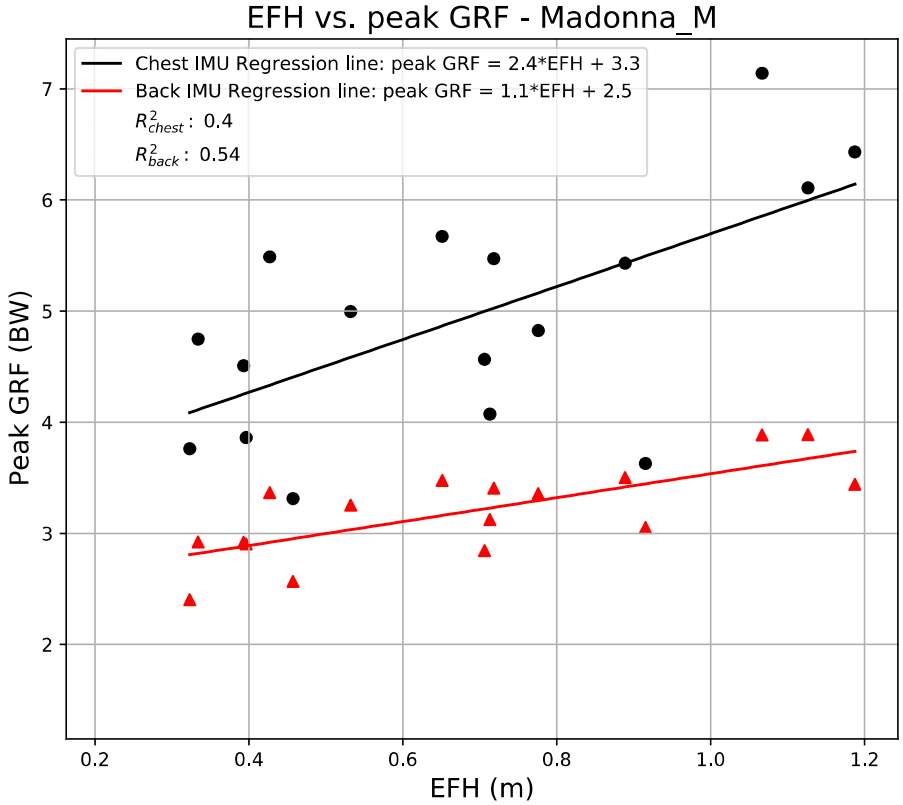
EFH vs. peak GRF - Madonna_M
Chest IMU Regression line: peak GRF = 2.4*EFH + 3.3
Back IMU Regression line: peak GRF = 1.1*EFH + 2.5
R^2_{chest}: 0.4
R^2_{back}: 0.54
Peak GRF (BW)
EFH (m)

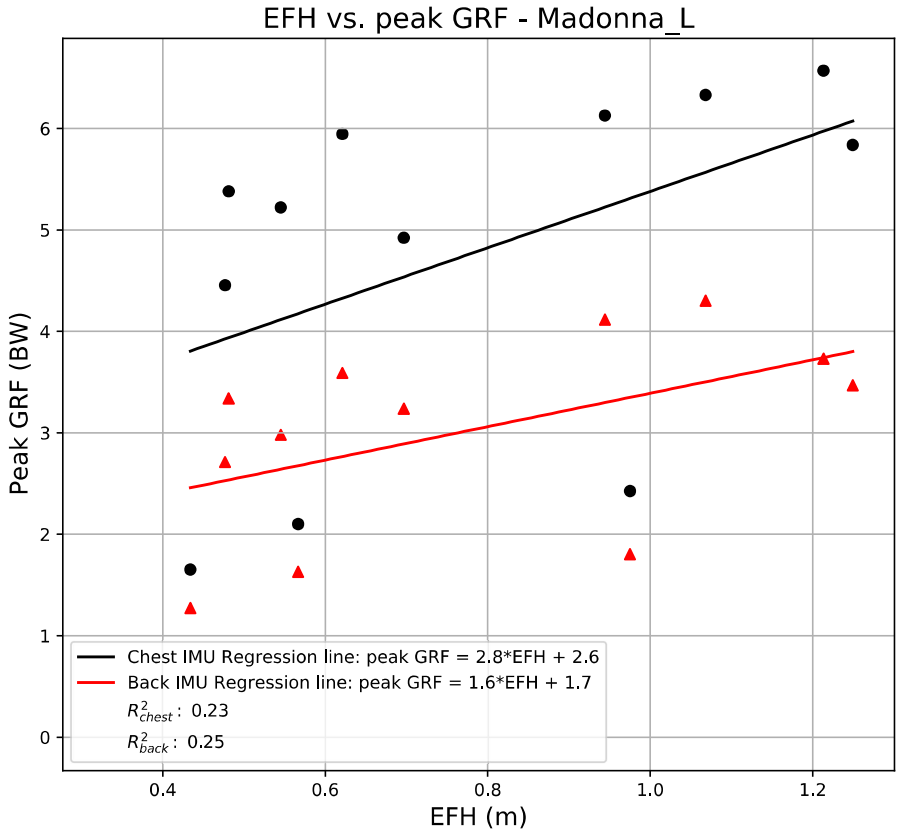
EFH vs. peak GRF - Madonna_L
Peak GRF (BW)
EFH (m)
Chest IMU Regression line: peak GRF = 2.8*EFH + 2.6
Back IMU Regression line: peak GRF = 1.6*EFH + 1.7
R^2_{chest}: 0.23
R^2_{back}: 0.25

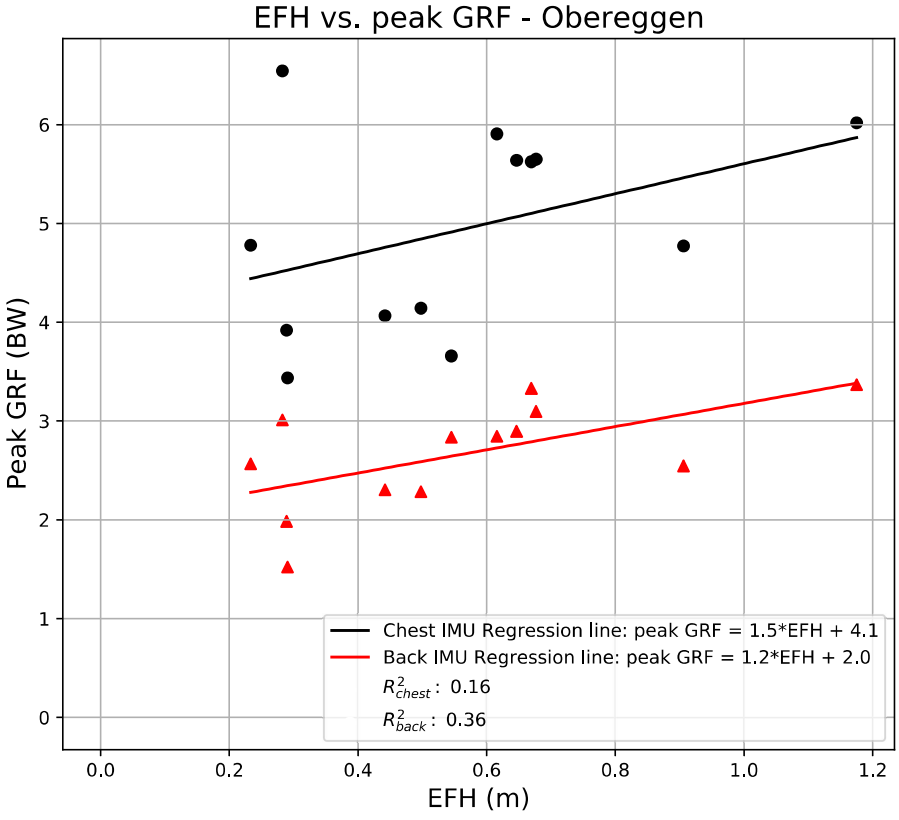
EFH vs. peak GRF - Obereggen
Peak GRF (BW)
EFH (m)
Chest IMU Regression line: peak GRF = 1.5*EFH + 4.1
Back IMU Regression line: peak GRF = 1.2*EFH + 2.0
R^2_{chest}: 0.16
R^2_{back}: 0.36

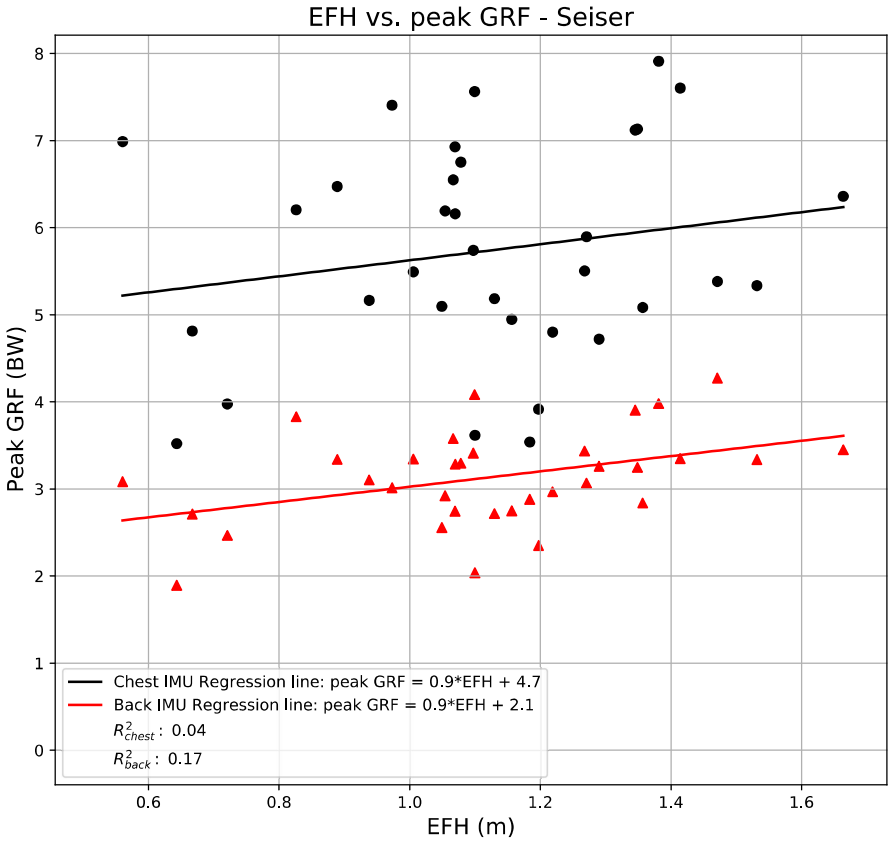
EFH vs. peak GRF - Seiser
Peak GRF (BW)
EFH (m)
0
1
2
3
4
5
6
7
8
0.6
0.8
1.0
1.2
1.4
1.6
Chest IMU Regression line: peak GRF = 0.9*EFH + 4.7
Back IMU Regression line: peak GRF = 0.9*EFH + 2.1
R^2_{chest}: 0.04
R^2_{back}: 0.17

G

Flight curves

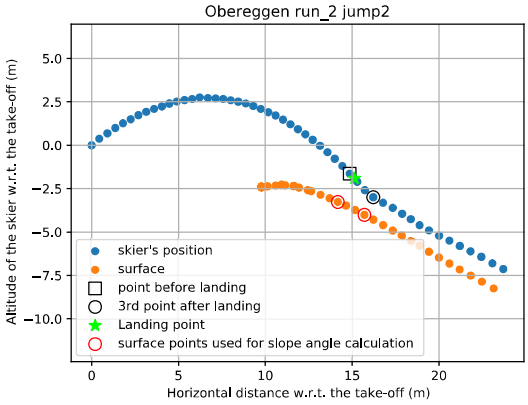

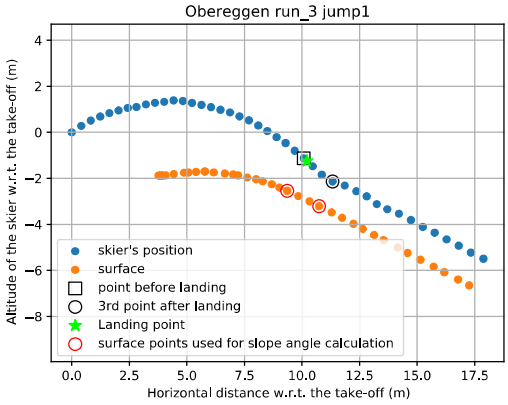

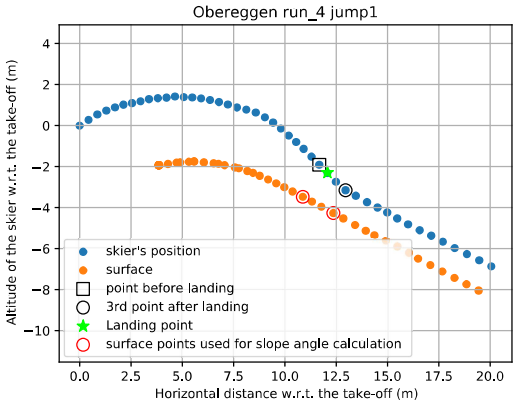

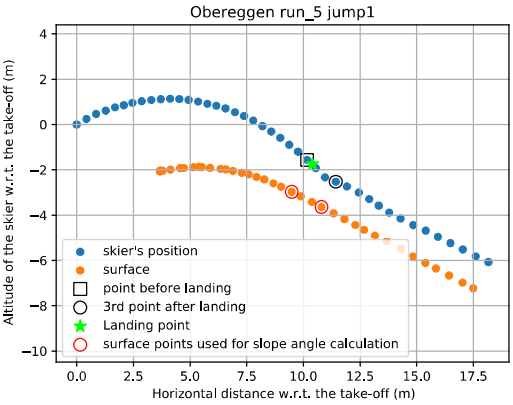

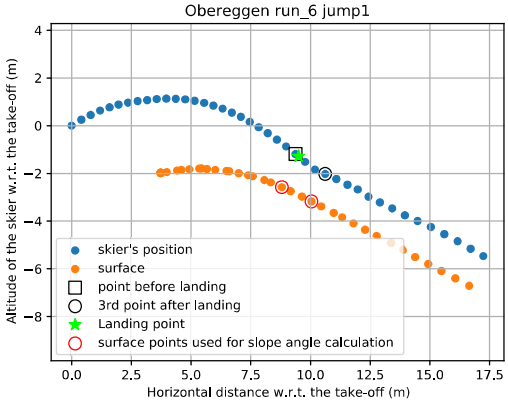

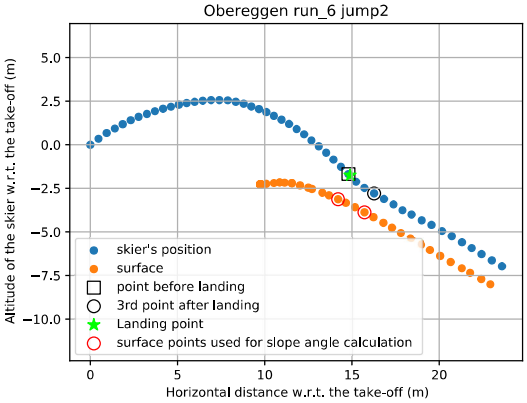

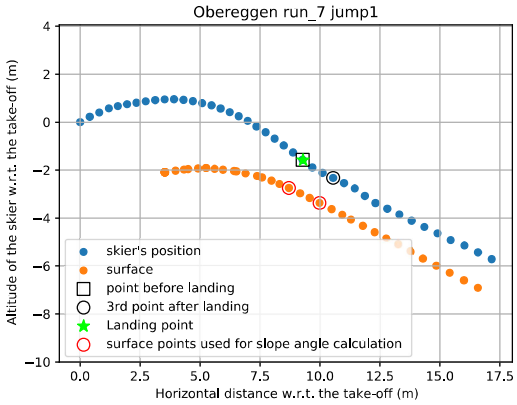
Obereggen run_7 jump1
Altitude of the skier w.r.t. the take-off (m)
Horizontal distance w.r.t. the take-off (m)
skier's position
surface
point before landing
3rd point after landing
Landing point
surface points used for slope angle calculation

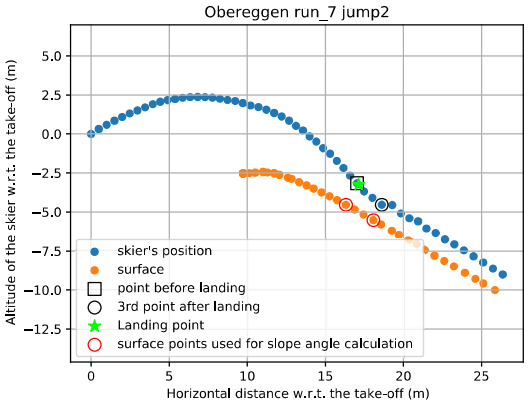
Obereggen run_7 jump2
Altitude of the skier w.r.t. the take-off (m)
Horizontal distance w.r.t. the take-off (m)
skier's position
surface
point before landing
3rd point after landing
Landing point
surface points used for slope angle calculation

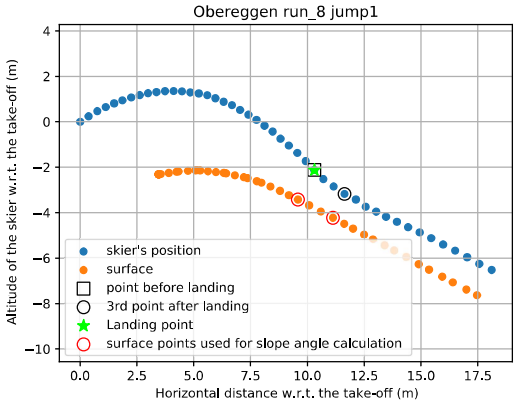
Obereggen run_8 jump1
Altitude of the skier w.r.t. the take-off (m)
Horizontal distance w.r.t. the take-off (m)
skier's position
surface
point before landing
3rd point after landing
Landing point
surface points used for slope angle calculation

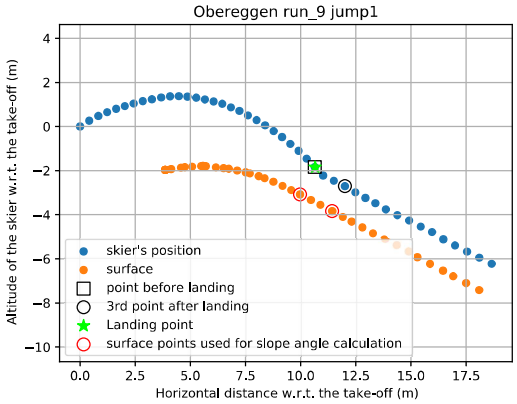
Obereggen run_9 jump1
Altitude of the skier w.r.t. the take-off (m)
Horizontal distance w.r.t. the take-off (m)
skier's position
surface
point before landing
3rd point after landing
Landing point
surface points used for slope angle calculation

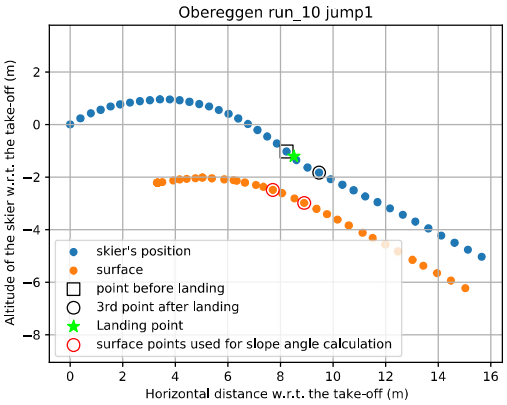
Obereggen run_10 jump1
Altitude of the skier w.r.t. the take-off (m)
Horizontal distance w.r.t. the take-off (m)
skier's position
surface
point before landing
3rd point after landing
Landing point
surface points used for slope angle calculation

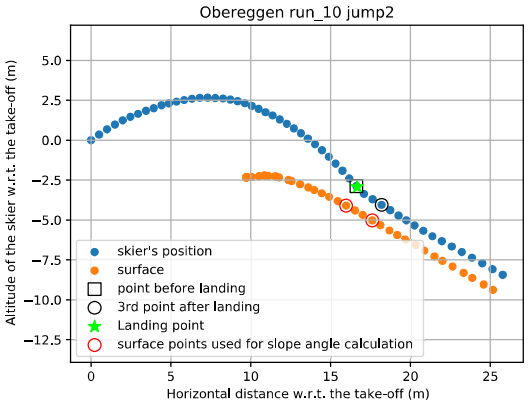
Obereggen run_10 jump2
Altitude of the skier w.r.t. the take-off (m)
Horizontal distance w.r.t. the take-off (m)
skier's position
surface
point before landing
3rd point after landing
Landing point
surface points used for slope angle calculation

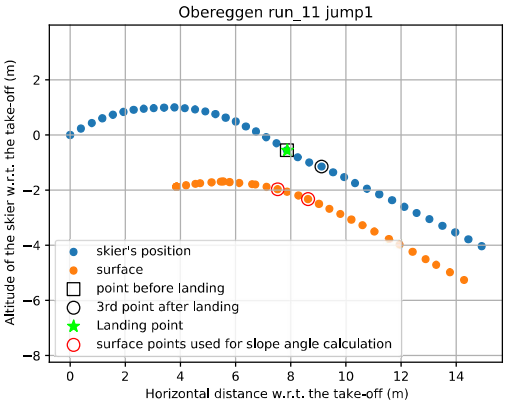
Obereggen run_11 jump1
Altitude of the skier w.r.t. the take-off (m)
Horizontal distance w.r.t. the take-off (m)
skier's position
surface
point before landing
3rd point after landing
Landing point
surface points used for slope angle calculation

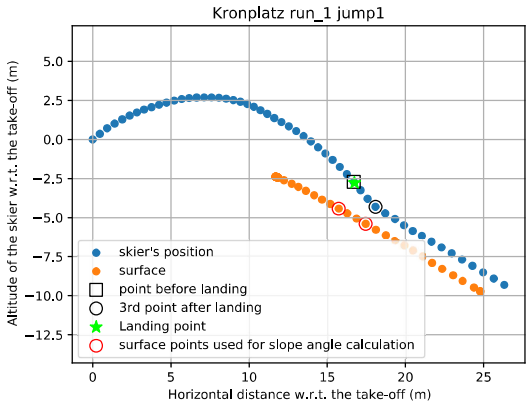
Kronplatz run_1 jump1
Altitude of the skier w.r.t. the take-off (m)
Horizontal distance w.r.t. the take-off (m)
skier's position
surface
point before landing
3rd point after landing
Landing point
surface points used for slope angle calculation

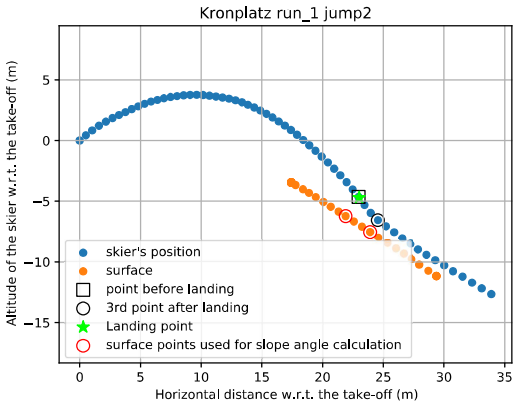
Kronplatz run_1 jump2
Altitude of the skier w.r.t. the take-off (m)
Horizontal distance w.r.t. the take-off (m)
skier's position
surface
point before landing
3rd point after landing
Landing point
surface points used for slope angle calculation

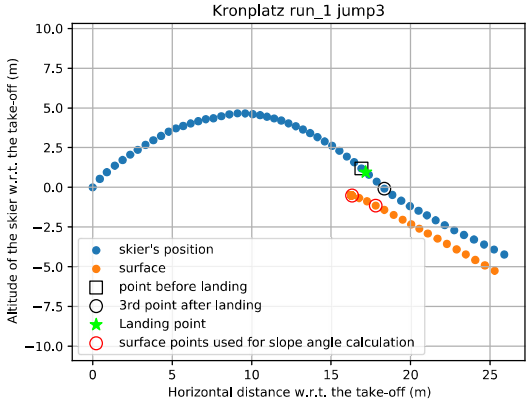
Kronplatz run_1 jump3
Altitude of the skier w.r.t. the take-off (m)
Horizontal distance w.r.t. the take-off (m)
skier's position
surface
point before landing
3rd point after landing
Landing point
surface points used for slope angle calculation

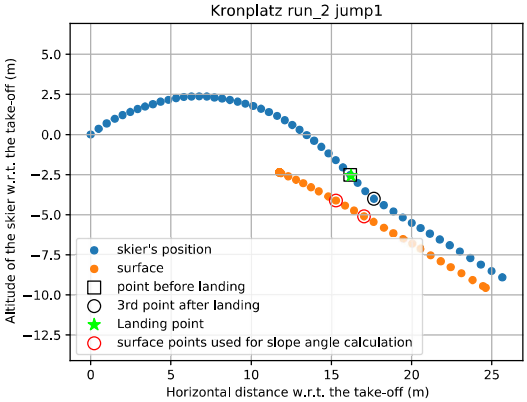
Kronplatz run_2 jump1
Altitude of the skier w.r.t. the take-off (m)
Horizontal distance w.r.t. the take-off (m)
skier's position
surface
point before landing
3rd point after landing
Landing point
surface points used for slope angle calculation

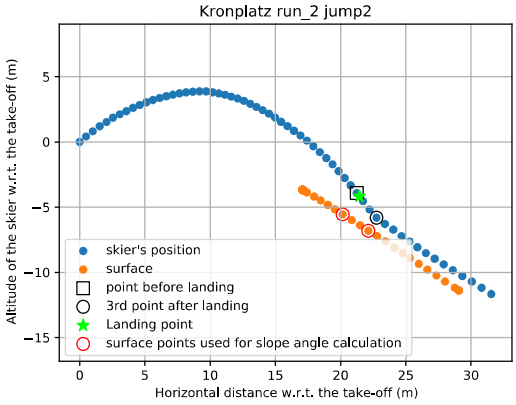
Kronplatz run_2 jump2
Altitude of the skier w.r.t. the take-off (m)
Horizontal distance w.r.t. the take-off (m)
skier's position
surface
point before landing
3rd point after landing
Landing point
surface points used for slope angle calculation

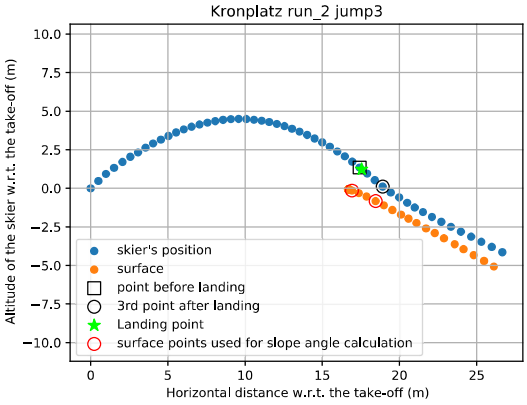
Kronplatz run_2 jump3
Altitude of the skier w.r.t. the take-off (m)
Horizontal distance w.r.t. the take-off (m)
skier's position
surface
point before landing
3rd point after landing
Landing point
surface points used for slope angle calculation

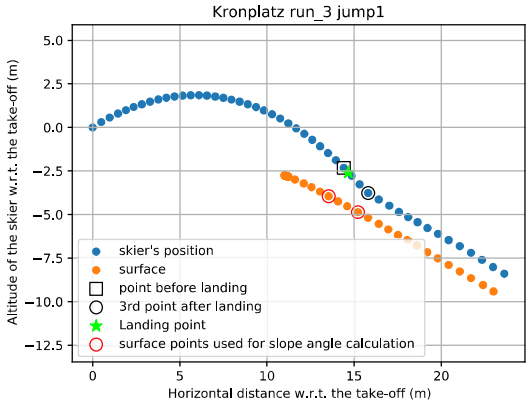
Kronplatz run_3 jump1
Altitude of the skier w.r.t. the take-off (m)
Horizontal distance w.r.t. the take-off (m)
skier's position
surface
point before landing
3rd point after landing
Landing point
surface points used for slope angle calculation

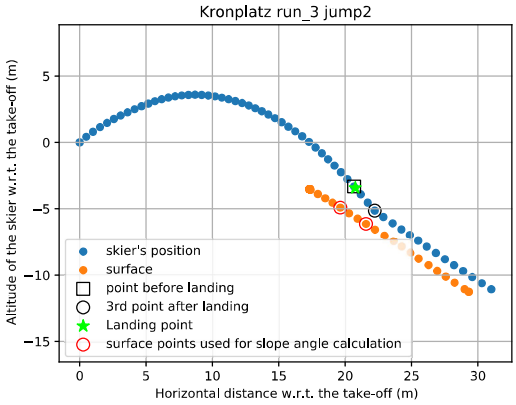
Kronplatz run_3 jump2
Altitude of the skier w.r.t. the take-off (m)
Horizontal distance w.r.t. the take-off (m)
skier's position
surface
point before landing
3rd point after landing
Landing point
surface points used for slope angle calculation

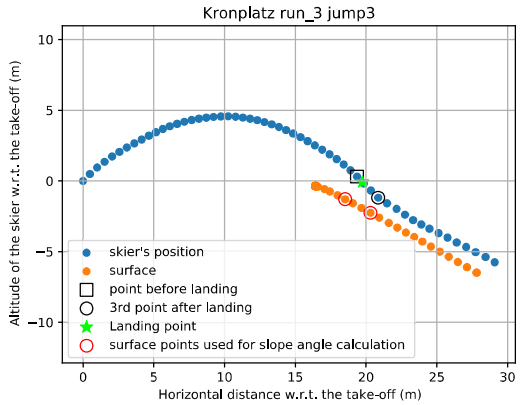
Kronplatz run_3 jump3
Altitude of the skier w.r.t. the take-off (m)
Horizontal distance w.r.t. the take-off (m)
skier's position
surface
point before landing
3rd point after landing
Landing point
surface points used for slope angle calculation

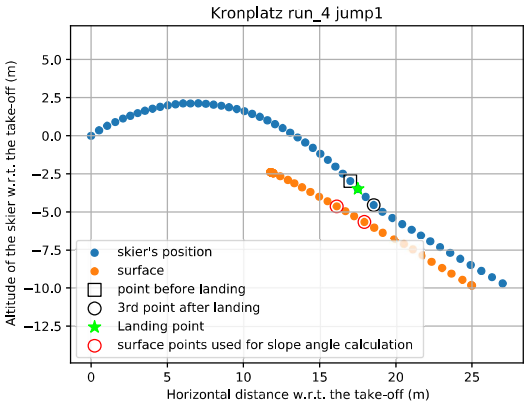
Kronplatz run_4 jump1
Altitude of the skier w.r.t. the take-off (m)
Horizontal distance w.r.t. the take-off (m)
skier's position
surface
point before landing
3rd point after landing
Landing point
surface points used for slope angle calculation

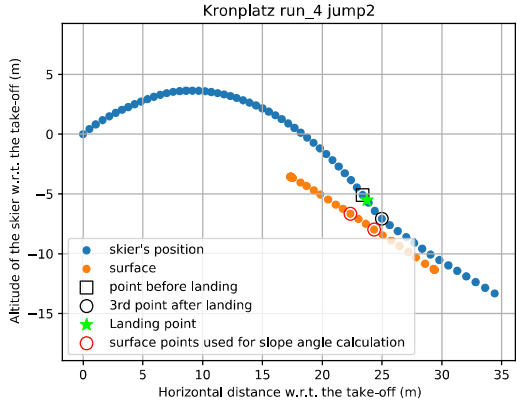
Kronplatz run_4 jump2
Altitude of the skier w.r.t. the take-off (m)
Horizontal distance w.r.t. the take-off (m)
skier's position
surface
point before landing
3rd point after landing
Landing point
surface points used for slope angle calculation

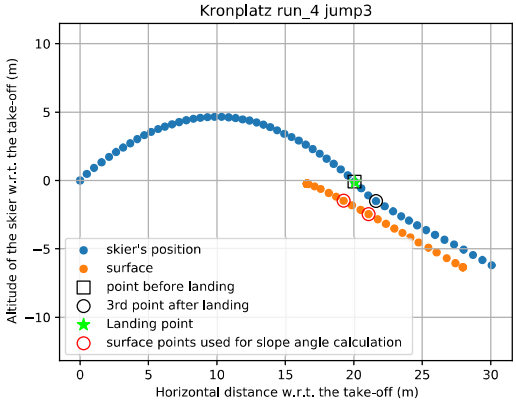
Kronplatz run_4 jump3
Altitude of the skier w.r.t. the take-off (m)
Horizontal distance w.r.t. the take-off (m)
skier's position
surface
point before landing
3rd point after landing
Landing point
surface points used for slope angle calculation

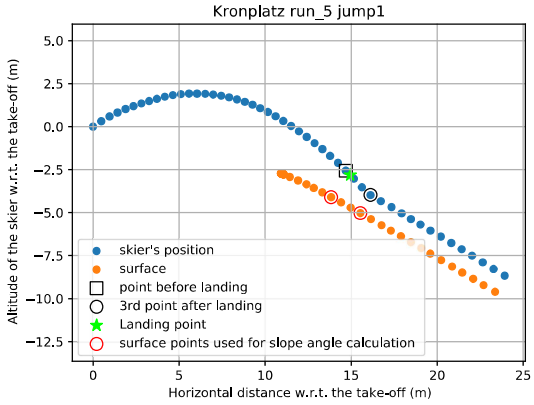
Kronplatz run_5 jump1
Altitude of the skier w.r.t. the take-off (m)
Horizontal distance w.r.t. the take-off (m)
skier's position
surface
point before landing
3rd point after landing
Landing point
surface points used for slope angle calculation

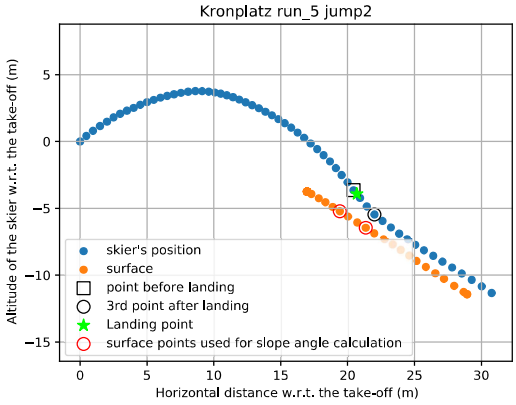
Kronplatz run_5 jump2
Altitude of the skier w.r.t. the take-off (m)
Horizontal distance w.r.t. the take-off (m)
skier's position
surface
point before landing
3rd point after landing
Landing point
surface points used for slope angle calculation

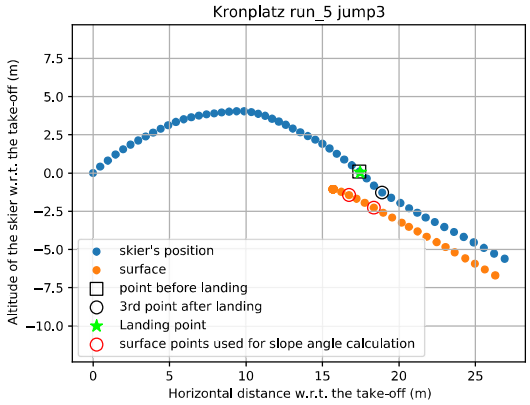
Kronplatz run_5 jump3
Altitude of the skier w.r.t. the take-off (m)
Horizontal distance w.r.t. the take-off (m)
skier's position
surface
point before landing
3rd point after landing
Landing point
surface points used for slope angle calculation

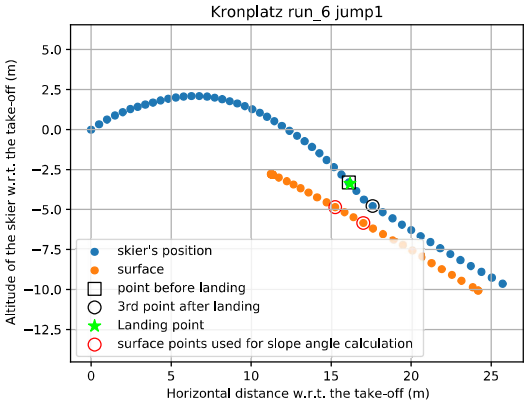
Kronplatz run_6 jump1
Altitude of the skier w.r.t. the take-off (m)
Horizontal distance w.r.t. the take-off (m)
skier's position
surface
point before landing
3rd point after landing
Landing point
surface points used for slope angle calculation

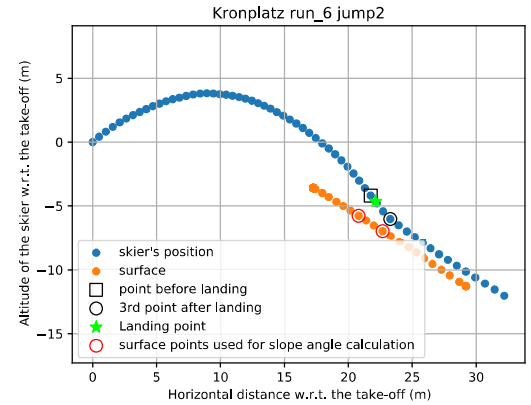
Kronplatz run_6 jump2
Altitude of the skier w.r.t. the take-off (m)
Horizontal distance w.r.t. the take-off (m)
skier's position
surface
point before landing
3rd point after landing
Landing point
surface points used for slope angle calculation

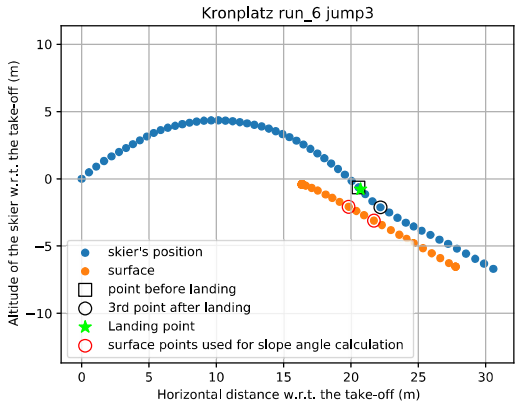
Kronplatz run_6 jump3
Altitude of the skier w.r.t. the take-off (m)
Horizontal distance w.r.t. the take-off (m)
skier's position
surface
point before landing
3rd point after landing
Landing point
surface points used for slope angle calculation

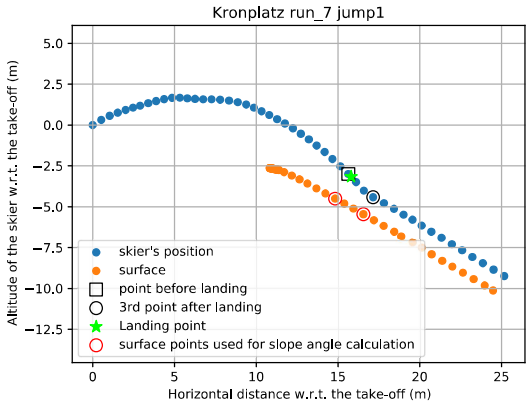
Kronplatz run_7 jump1
Altitude of the skier w.r.t. the take-off (m)
Horizontal distance w.r.t. the take-off (m)
skier's position
surface
point before landing
3rd point after landing
Landing point
surface points used for slope angle calculation

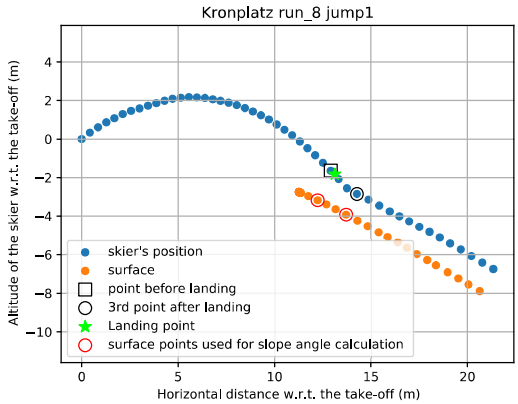
Kronplatz run_8 jump1
Altitude of the skier w.r.t. the take-off (m)
Horizontal distance w.r.t. the take-off (m)
skier's position
surface
point before landing
3rd point after landing
Landing point
surface points used for slope angle calculation

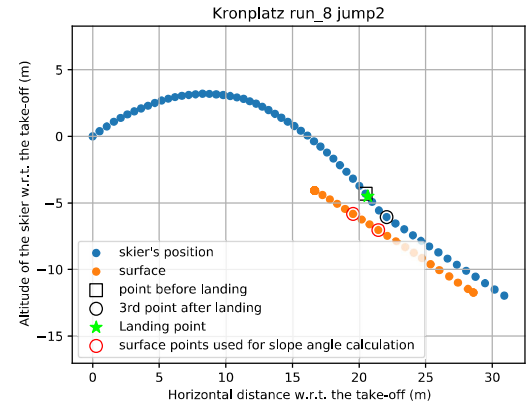
Kronplatz run_8 jump2
Altitude of the skier w.r.t. the take-off (m)
Horizontal distance w.r.t. the take-off (m)
skier's position
surface
point before landing
3rd point after landing
Landing point
surface points used for slope angle calculation

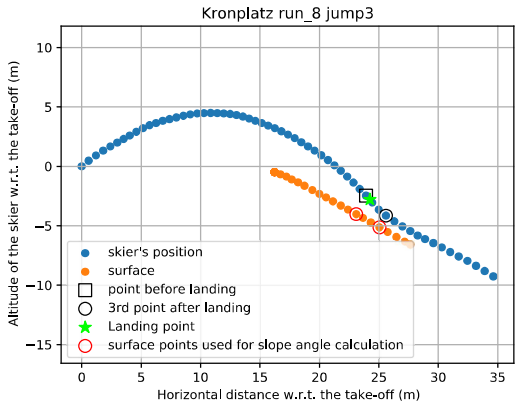
Kronplatz run_8 jump3
Altitude of the skier w.r.t. the take-off (m)
Horizontal distance w.r.t. the take-off (m)
skier's position
surface
point before landing
3rd point after landing
Landing point
surface points used for slope angle calculation

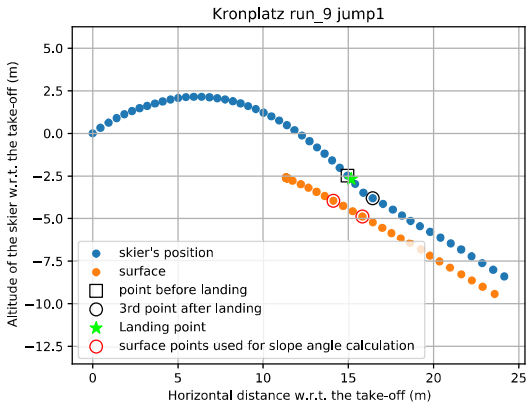
Kronplatz run_9 jump1
Altitude of the skier w.r.t. the take-off (m)
Horizontal distance w.r.t. the take-off (m)
skier's position
surface
point before landing
3rd point after landing
Landing point
surface points used for slope angle calculation

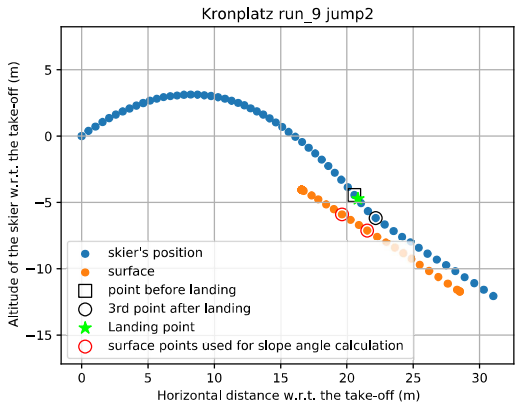
Kronplatz run_9 jump2
Altitude of the skier w.r.t. the take-off (m)
Horizontal distance w.r.t. the take-off (m)
skier's position
surface
point before landing
3rd point after landing
Landing point
surface points used for slope angle calculation

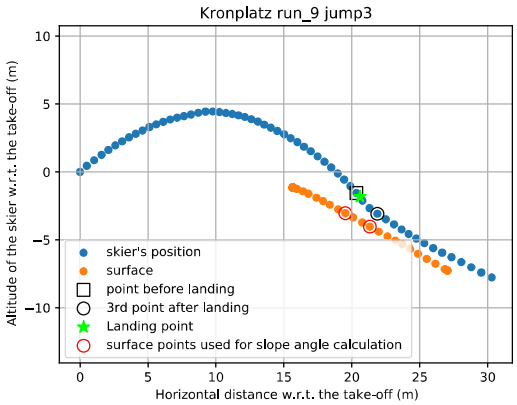
Kronplatz run_9 jump3
Altitude of the skier w.r.t. the take-off (m)
Horizontal distance w.r.t. the take-off (m)
skier's position
surface
point before landing
3rd point after landing
Landing point
surface points used for slope angle calculation

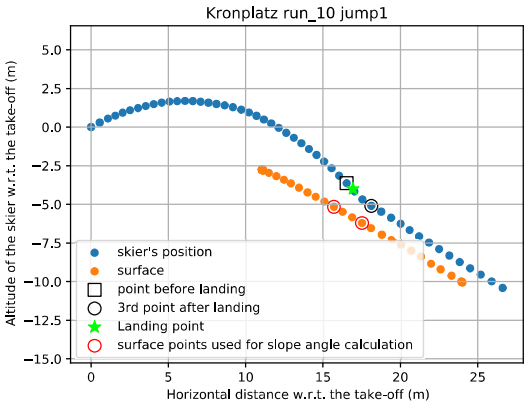
Kronplatz run_10 jump1
Altitude of the skier w.r.t. the take-off (m)
Horizontal distance w.r.t. the take-off (m)
skier's position
surface
point before landing
3rd point after landing
Landing point
surface points used for slope angle calculation

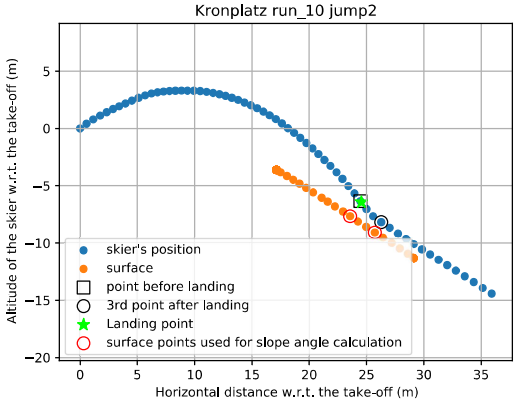
Kronplatz run_10 jump2
Altitude of the skier w.r.t. the take-off (m)
Horizontal distance w.r.t. the take-off (m)
skier's position
surface
point before landing
3rd point after landing
Landing point
surface points used for slope angle calculation

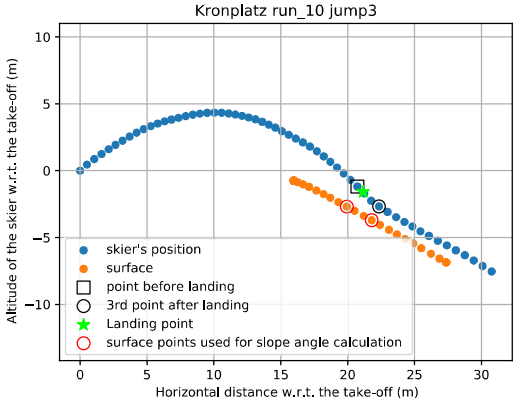
Kronplatz run_10 jump3
Altitude of the skier w.r.t. the take-off (m)
Horizontal distance w.r.t. the take-off (m)
skier's position
surface
point before landing
3rd point after landing
Landing point
surface points used for slope angle calculation

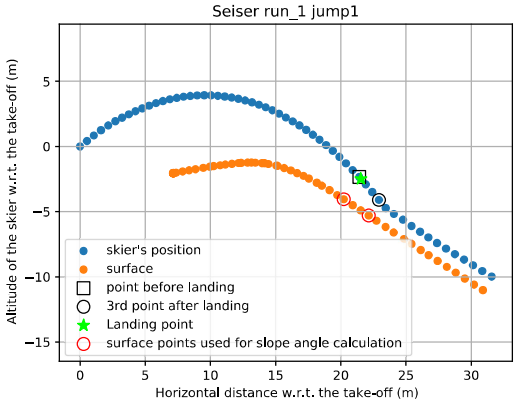
Seiser run_1 jump1
Altitude of the skier w.r.t. the take-off (m)
Horizontal distance w.r.t. the take-off (m)
skier's position
surface
point before landing
3rd point after landing
Landing point
surface points used for slope angle calculation

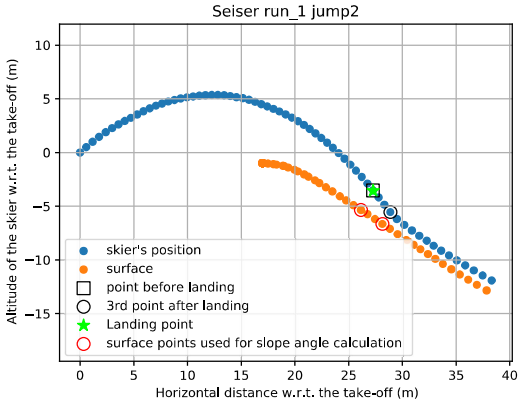
Seiser run_1 jump2
Altitude of the skier w.r.t. the take-off (m)
Horizontal distance w.r.t. the take-off (m)
skier's position
surface
point before landing
3rd point after landing
Landing point
surface points used for slope angle calculation

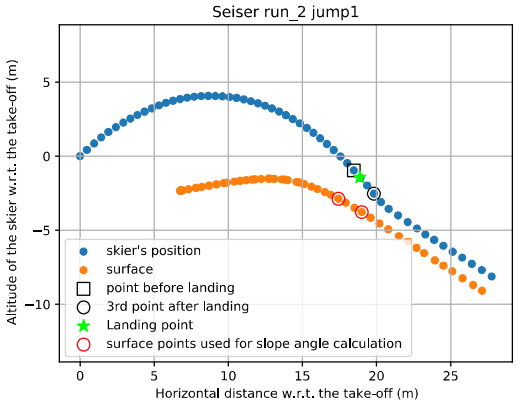
Seiser run_2 jump1
Altitude of the skier w.r.t. the take-off (m)
Horizontal distance w.r.t. the take-off (m)
skier's position
surface
point before landing
3rd point after landing
Landing point
surface points used for slope angle calculation

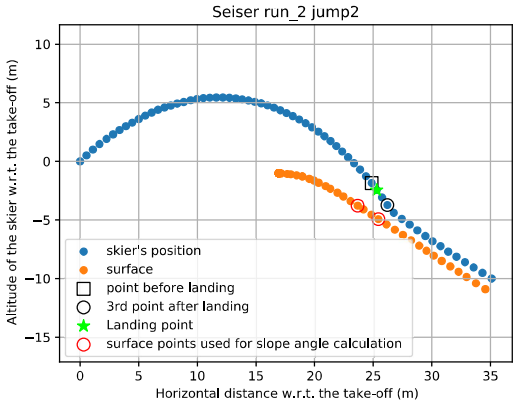
Seiser run_2 jump2
Altitude of the skier w.r.t. the take-off (m)
Horizontal distance w.r.t. the take-off (m)
skier's position
surface
point before landing
3rd point after landing
Landing point
surface points used for slope angle calculation

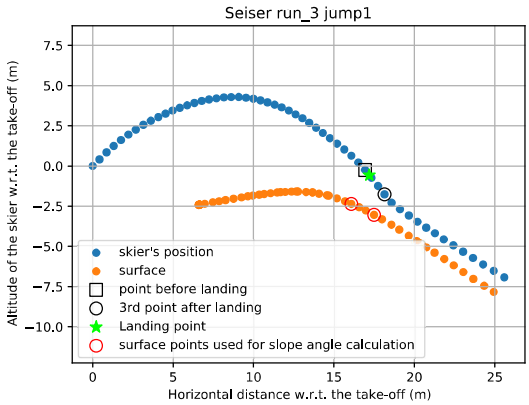
Seiser run_3 jump1
Altitude of the skier w.r.t. the take-off (m)
Horizontal distance w.r.t. the take-off (m)
skier's position
surface
point before landing
3rd point after landing
Landing point
surface points used for slope angle calculation

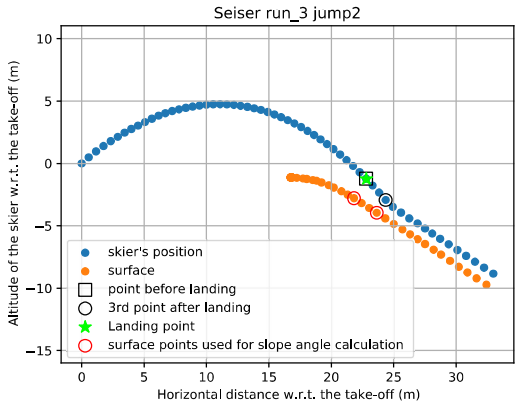
Seiser run_3 jump2
Altitude of the skier w.r.t. the take-off (m)
Horizontal distance w.r.t. the take-off (m)
skier's position
surface
point before landing
3rd point after landing
Landing point
surface points used for slope angle calculation

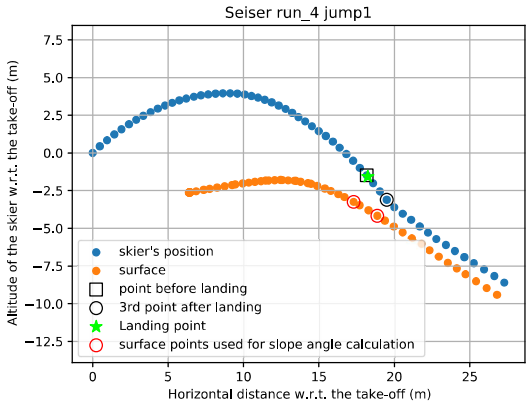
Seiser run_4 jump1
Altitude of the skier w.r.t. the take-off (m)
Horizontal distance w.r.t. the take-off (m)
skier's position
surface
point before landing
3rd point after landing
Landing point
surface points used for slope angle calculation

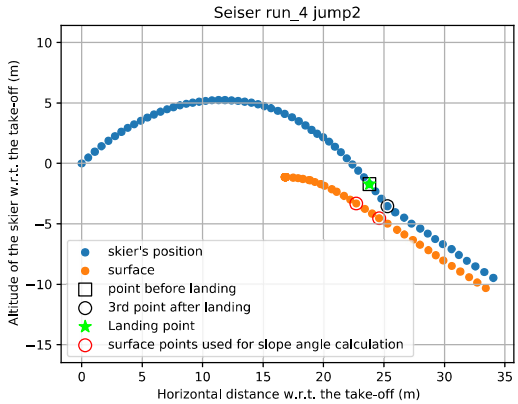
Seiser run_4 jump2
Altitude of the skier w.r.t. the take-off (m)
Horizontal distance w.r.t. the take-off (m)
skier's position
surface
point before landing
3rd point after landing
Landing point
surface points used for slope angle calculation

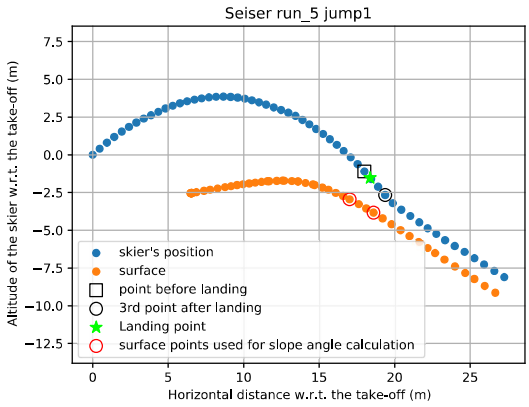
Seiser run_5 jump1
Altitude of the skier w.r.t. the take-off (m)
Horizontal distance w.r.t. the take-off (m)
skier's position
surface
point before landing
3rd point after landing
Landing point
surface points used for slope angle calculation

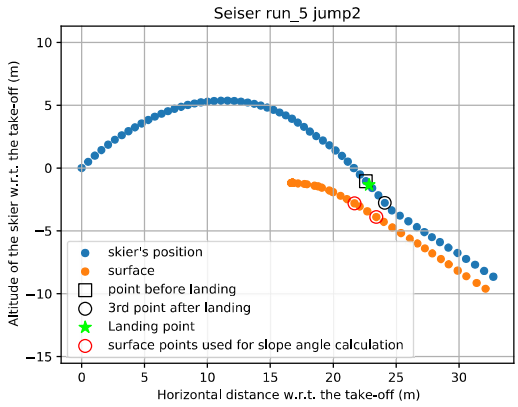
Seiser run_5 jump2
Altitude of the skier w.r.t. the take-off (m)
Horizontal distance w.r.t. the take-off (m)
skier's position
surface
point before landing
3rd point after landing
Landing point
surface points used for slope angle calculation

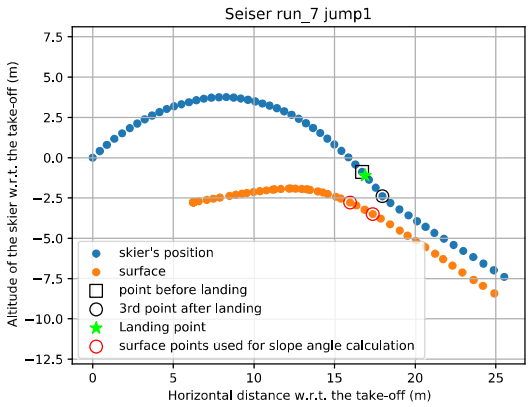
Seiser run_7 jump1
Altitude of the skier w.r.t. the take-off (m)
Horizontal distance w.r.t. the take-off (m)
skier's position
surface
point before landing
3rd point after landing
Landing point
surface points used for slope angle calculation

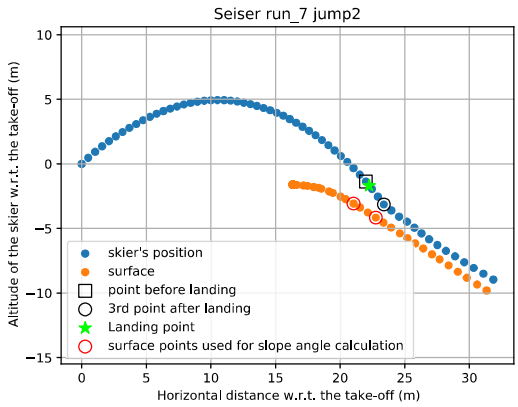
Seiser run_7 jump2
Altitude of the skier w.r.t. the take-off (m)
Horizontal distance w.r.t. the take-off (m)
skier's position
surface
point before landing
3rd point after landing
Landing point
surface points used for slope angle calculation

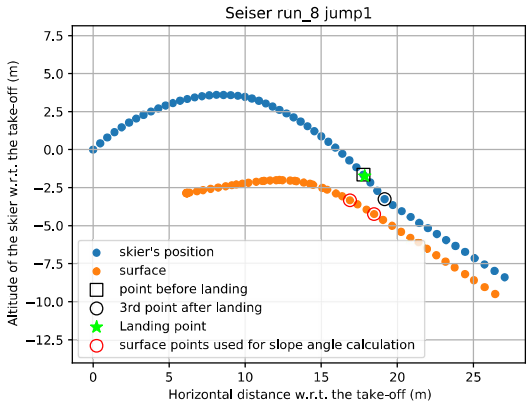
Seiser run_8 jump1
Altitude of the skier w.r.t. the take-off (m)
Horizontal distance w.r.t. the take-off (m)
skier's position
surface
point before landing
3rd point after landing
Landing point
surface points used for slope angle calculation

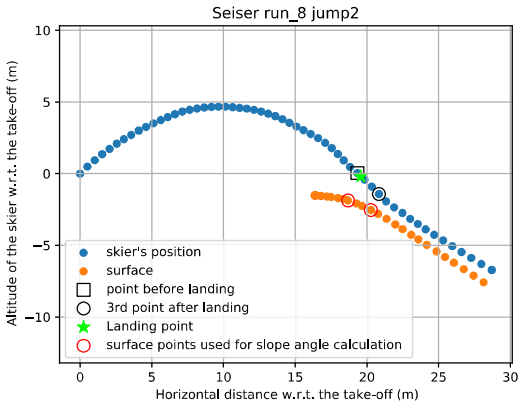
Seiser run_8 jump2
Altitude of the skier w.r.t. the take-off (m)
Horizontal distance w.r.t. the take-off (m)
skier's position
surface
point before landing
3rd point after landing
Landing point
surface points used for slope angle calculation

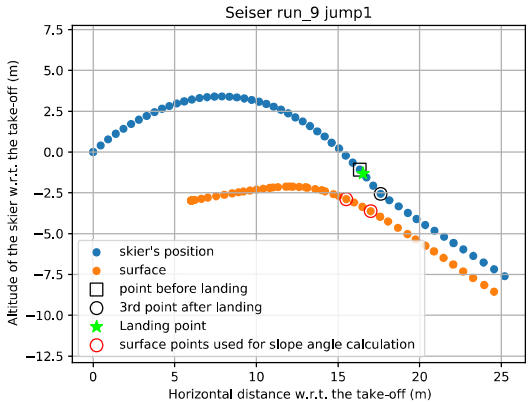
Seiser run_9 jump1
Altitude of the skier w.r.t. the take-off (m)
Horizontal distance w.r.t. the take-off (m)
skier's position
surface
point before landing
3rd point after landing
Landing point
surface points used for slope angle calculation

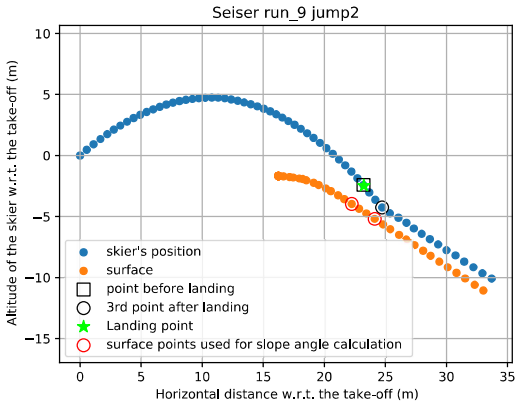
Seiser run_9 jump2
Altitude of the skier w.r.t. the take-off (m)
Horizontal distance w.r.t. the take-off (m)
skier's position
surface
point before landing
3rd point after landing
Landing point
surface points used for slope angle calculation

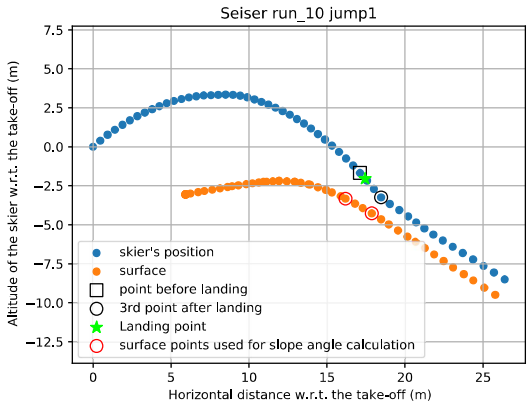
Seiser run_10 jump1
Altitude of the skier w.r.t. the take-off (m)
Horizontal distance w.r.t. the take-off (m)
skier's position
surface
point before landing
3rd point after landing
Landing point
surface points used for slope angle calculation

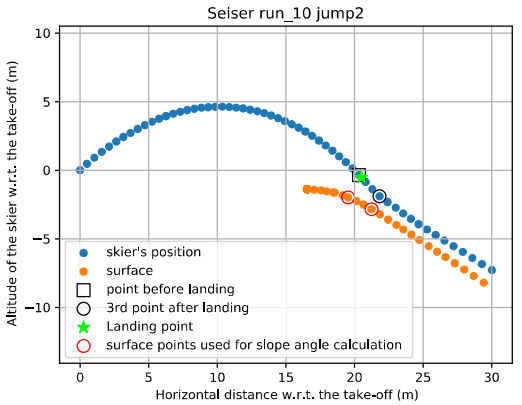
Seiser run_10 jump2
Altitude of the skier w.r.t. the take-off (m)
Horizontal distance w.r.t. the take-off (m)
skier's position
surface
point before landing
3rd point after landing
Landing point
surface points used for slope angle calculation

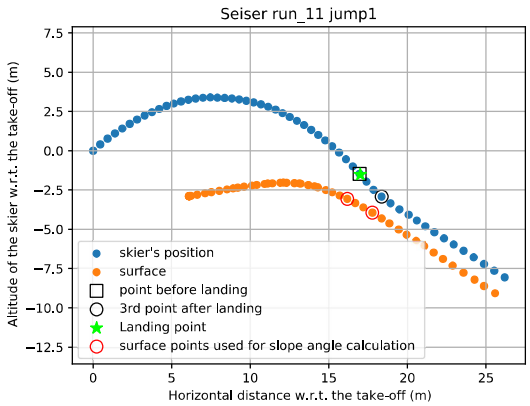
Seiser run_11 jump1
Altitude of the skier w.r.t. the take-off (m)
Horizontal distance w.r.t. the take-off (m)
skier's position
surface
point before landing
3rd point after landing
Landing point
surface points used for slope angle calculation

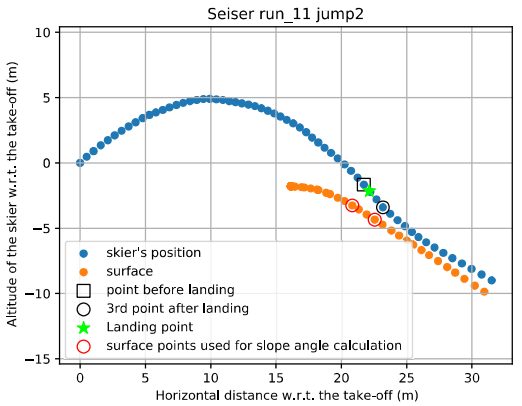
Seiser run_11 jump2
Altitude of the skier w.r.t. the take-off (m)
Horizontal distance w.r.t. the take-off (m)
skier's position
surface
point before landing
3rd point after landing
Landing point
surface points used for slope angle calculation

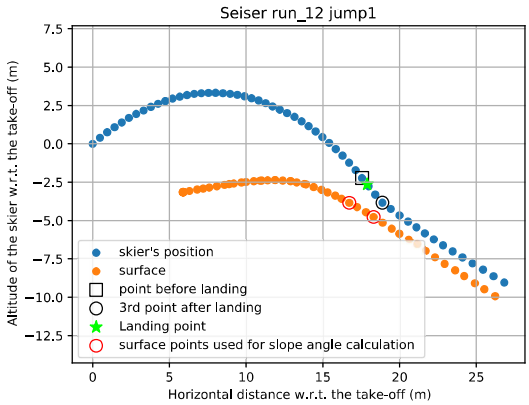
Seiser run_12 jump1
Altitude of the skier w.r.t. the take-off (m)
Horizontal distance w.r.t. the take-off (m)
skier's position
surface
point before landing
3rd point after landing
Landing point
surface points used for slope angle calculation

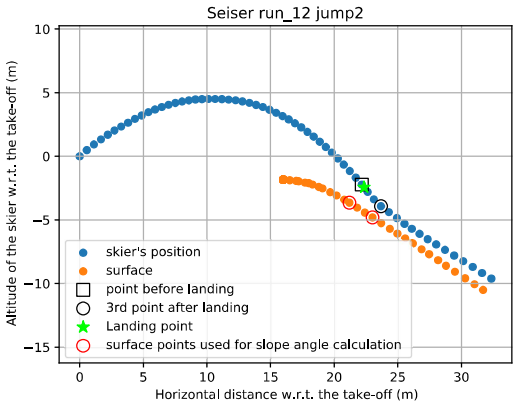
Seiser run_12 jump2
Altitude of the skier w.r.t. the take-off (m)
Horizontal distance w.r.t. the take-off (m)
skier's position
surface
point before landing
3rd point after landing
Landing point
surface points used for slope angle calculation

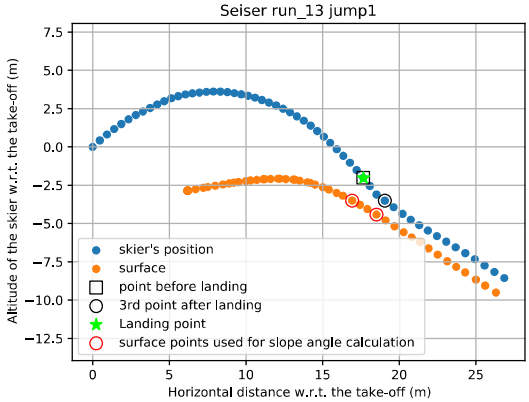
Seiser run_13 jump1
Altitude of the skier w.r.t. the take-off (m)
Horizontal distance w.r.t. the take-off (m)
skier's position
surface
point before landing
3rd point after landing
Landing point
surface points used for slope angle calculation

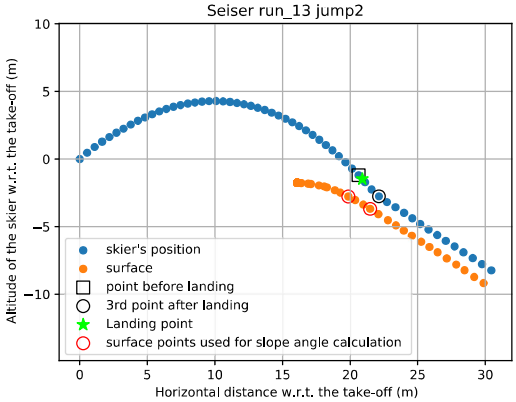
Seiser run_13 jump2
Altitude of the skier w.r.t. the take-off (m)
Horizontal distance w.r.t. the take-off (m)
skier's position
surface
point before landing
3rd point after landing
Landing point
surface points used for slope angle calculation

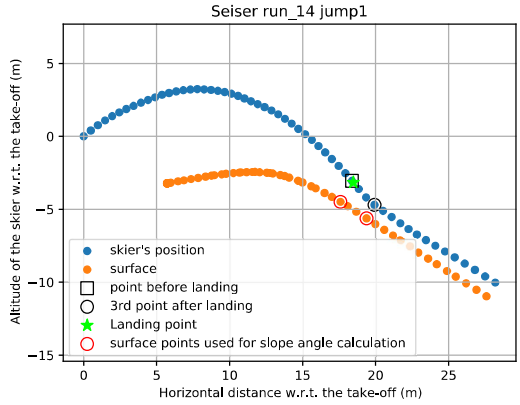
Seiser run_14 jump1
Altitude of the skier w.r.t. the take-off (m)
Horizontal distance w.r.t. the take-off (m)
skier's position
surface
point before landing
3rd point after landing
Landing point
surface points used for slope angle calculation

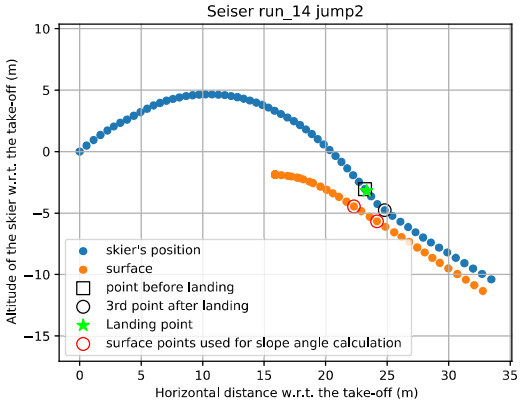
Seiser run_14 jump2
Altitude of the skier w.r.t. the take-off (m)
Horizontal distance w.r.t. the take-off (m)
skier's position
surface
point before landing
3rd point after landing
Landing point
surface points used for slope angle calculation

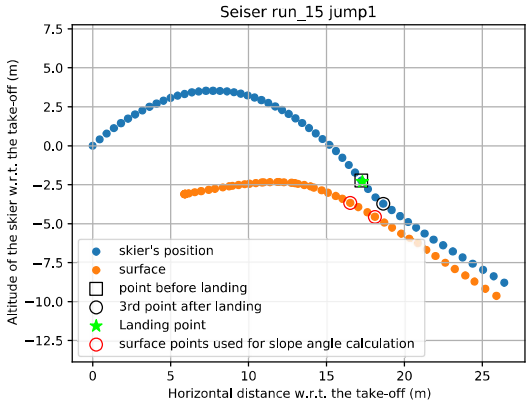
Seiser run_15 jump1
Altitude of the skier w.r.t. the take-off (m)
Horizontal distance w.r.t. the take-off (m)
skier's position
surface
point before landing
3rd point after landing
Landing point
surface points used for slope angle calculation

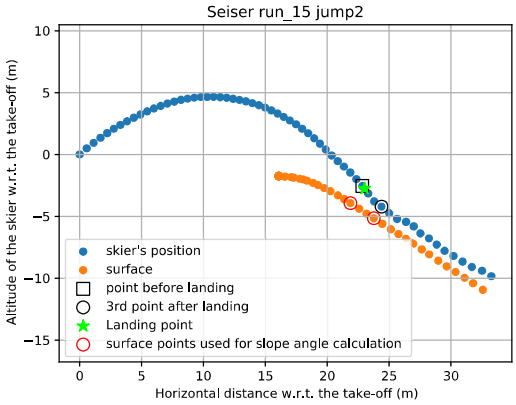
Seiser run_15 jump2
Altitude of the skier w.r.t. the take-off (m)
Horizontal distance w.r.t. the take-off (m)
skier's position
surface
point before landing
3rd point after landing
Landing point
surface points used for slope angle calculation

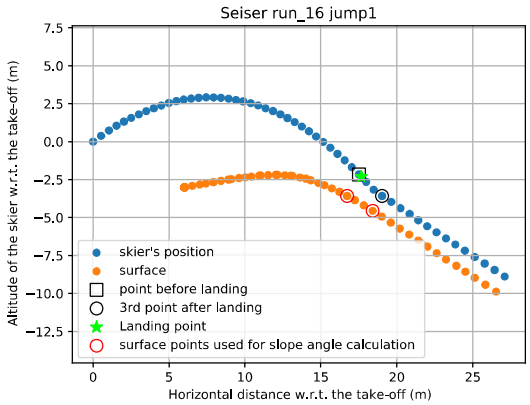
Seiser run_16 jump1
Altitude of the skier w.r.t. the take-off (m)
Horizontal distance w.r.t. the take-off (m)
skier's position
surface
point before landing
3rd point after landing
Landing point
surface points used for slope angle calculation

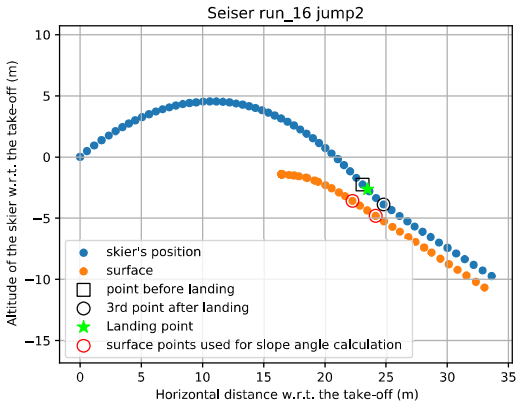
Seiser run_16 jump2
Altitude of the skier w.r.t. the take-off (m)
Horizontal distance w.r.t. the take-off (m)
skier's position
surface
point before landing
3rd point after landing
Landing point
surface points used for slope angle calculation

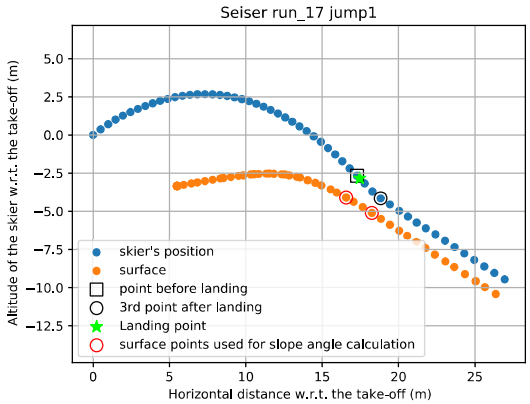
Seiser run_17 jump1
Altitude of the skier w.r.t. the take-off (m)
Horizontal distance w.r.t. the take-off (m)
skier's position
surface
point before landing
3rd point after landing
Landing point
surface points used for slope angle calculation

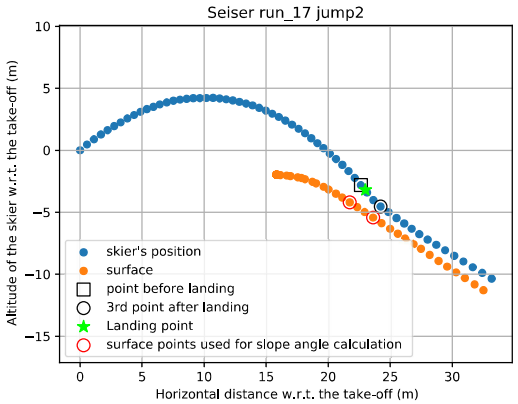
Seiser run_17 jump2
Altitude of the skier w.r.t. the take-off (m)
Horizontal distance w.r.t. the take-off (m)
skier's position
surface
point before landing
3rd point after landing
Landing point
surface points used for slope angle calculation

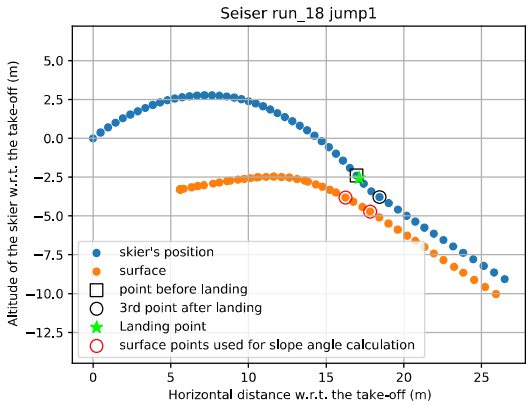
Seiser run_18 jump1
Altitude of the skier w.r.t. the take-off (m)
Horizontal distance w.r.t. the take-off (m)
skier's position
surface
point before landing
3rd point after landing
Landing point
surface points used for slope angle calculation

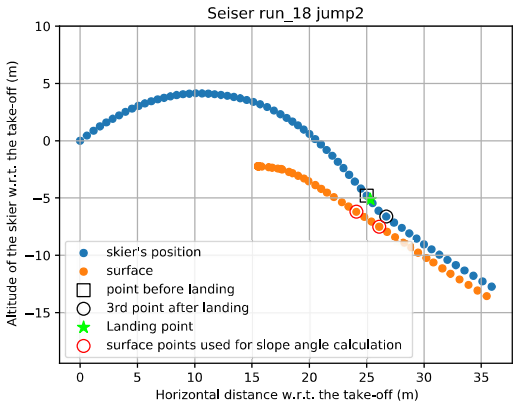
Seiser run_18 jump2
Altitude of the skier w.r.t. the take-off (m)
Horizontal distance w.r.t. the take-off (m)
skier's position
surface
point before landing
3rd point after landing
Landing point
surface points used for slope angle calculation

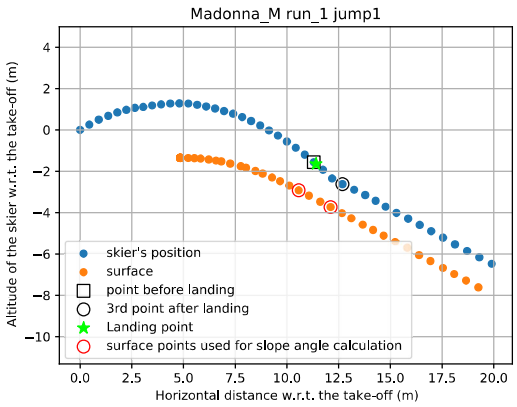
Madonna_M run_1 jump1
Altitude of the skier w.r.t. the take-off (m)
Horizontal distance w.r.t. the take-off (m)
skier's position
surface
point before landing
3rd point after landing
Landing point
surface points used for slope angle calculation

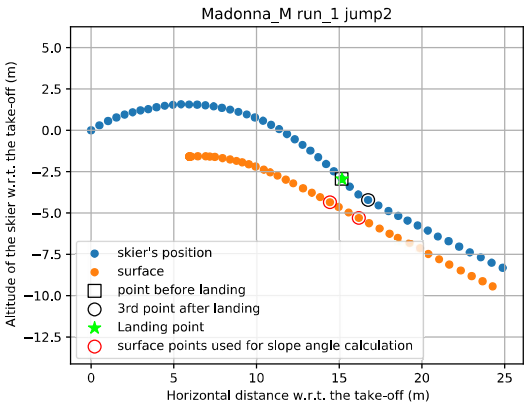
Madonna_M run_1 jump2
Altitude of the skier w.r.t. the take-off (m)
Horizontal distance w.r.t. the take-off (m)
skier's position
surface
point before landing
3rd point after landing
Landing point
surface points used for slope angle calculation

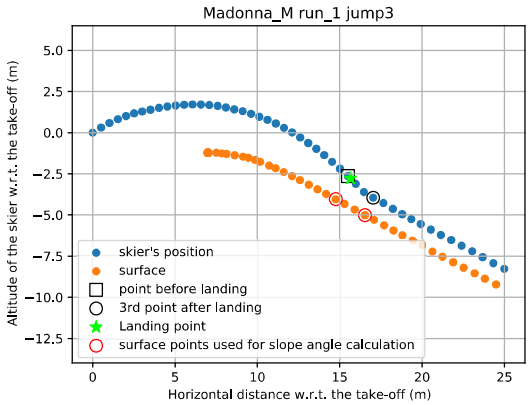
Madonna_M run_1 jump3
Altitude of the skier w.r.t. the take-off (m)
Horizontal distance w.r.t. the take-off (m)
skier's position
surface
point before landing
3rd point after landing
Landing point
surface points used for slope angle calculation

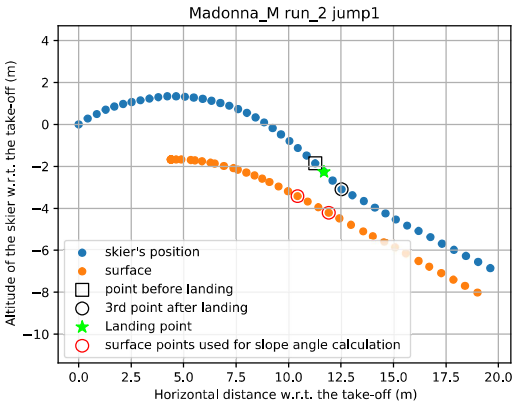
Madonna_M run_2 jump1
Altitude of the skier w.r.t. the take-off (m)
Horizontal distance w.r.t. the take-off (m)
skier's position
surface
point before landing
3rd point after landing
Landing point
surface points used for slope angle calculation

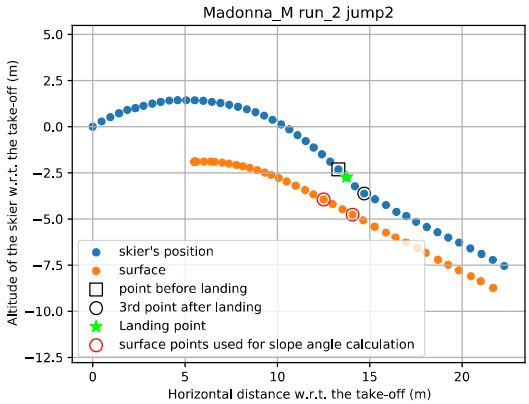
Madonna_M run_2 jump2
Altitude of the skier w.r.t. the take-off (m)
Horizontal distance w.r.t. the take-off (m)
skier's position
surface
point before landing
3rd point after landing
Landing point
surface points used for slope angle calculation

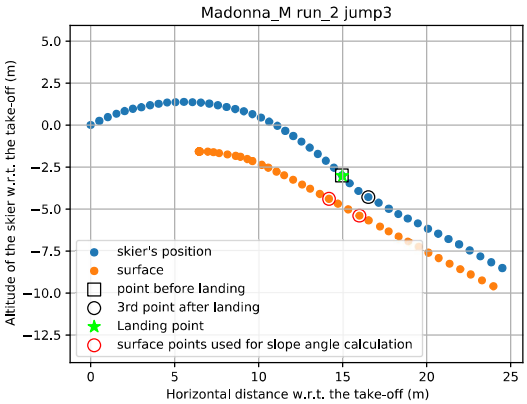
Madonna_M run_2 jump3
Altitude of the skier w.r.t. the take-off (m)
Horizontal distance w.r.t. the take-off (m)
skier's position
surface
point before landing
3rd point after landing
Landing point
surface points used for slope angle calculation

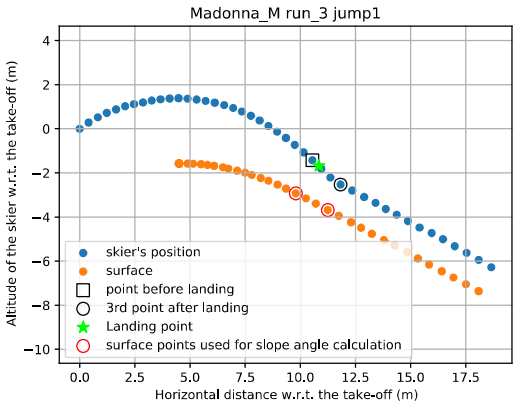
Madonna_M run_3 jump1
Altitude of the skier w.r.t. the take-off (m)
Horizontal distance w.r.t. the take-off (m)
skier's position
surface
point before landing
3rd point after landing
Landing point
surface points used for slope angle calculation

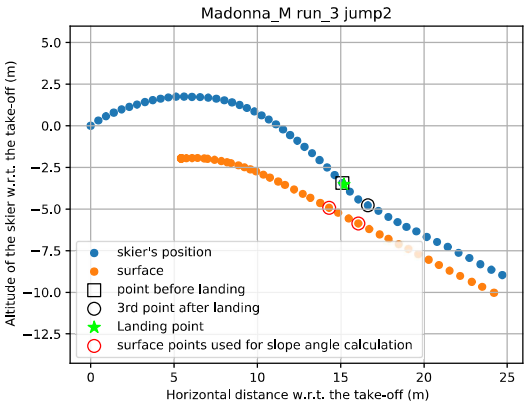
Madonna_M run_3 jump2
Altitude of the skier w.r.t. the take-off (m)
Horizontal distance w.r.t. the take-off (m)
skier's position
surface
point before landing
3rd point after landing
Landing point
surface points used for slope angle calculation

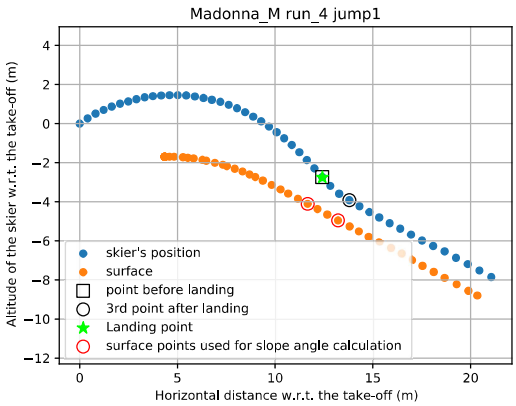
Madonna_M run_4 jump1
Altitude of the skier w.r.t. the take-off (m)
Horizontal distance w.r.t. the take-off (m)
skier's position
surface
point before landing
3rd point after landing
Landing point
surface points used for slope angle calculation

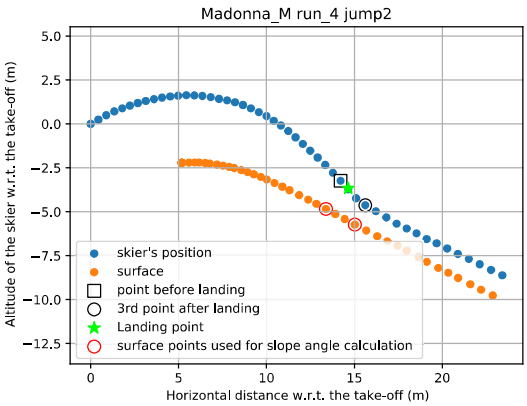
Madonna_M run_4 jump2
Altitude of the skier w.r.t. the take-off (m)
Horizontal distance w.r.t. the take-off (m)
skier's position
surface
point before landing
3rd point after landing
Landing point
surface points used for slope angle calculation

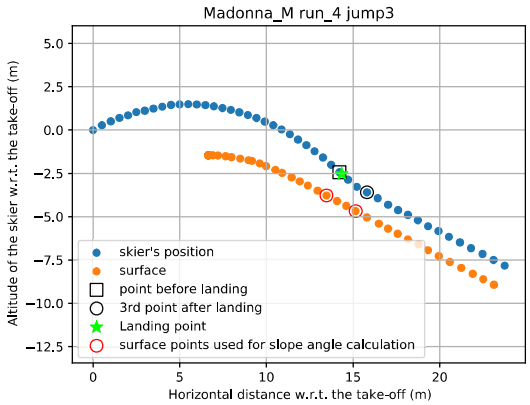
Madonna_M run_4 jump3
Altitude of the skier w.r.t. the take-off (m)
Horizontal distance w.r.t. the take-off (m)
skier's position
surface
point before landing
3rd point after landing
Landing point
surface points used for slope angle calculation

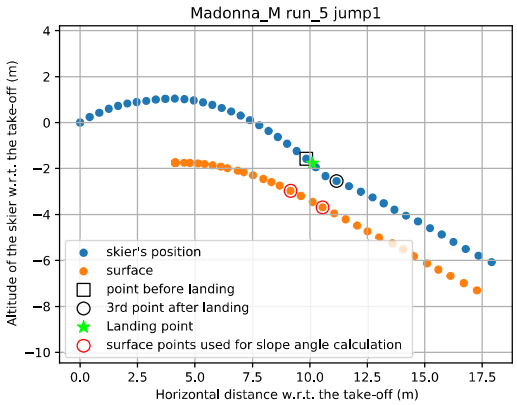
Madonna_M run_5 jump1
Altitude of the skier w.r.t. the take-off (m)
Horizontal distance w.r.t. the take-off (m)
skier's position
surface
point before landing
3rd point after landing
Landing point
surface points used for slope angle calculation

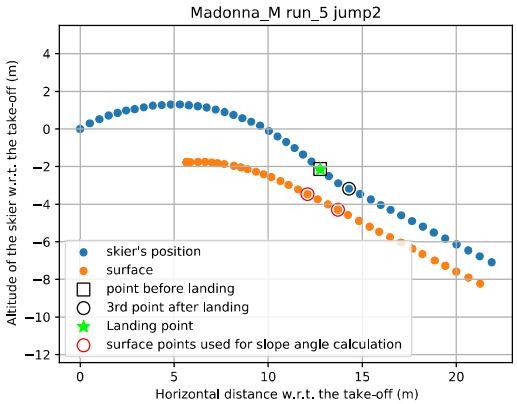
Madonna_M run_5 jump2
Altitude of the skier w.r.t. the take-off (m)
Horizontal distance w.r.t. the take-off (m)
skier's position
surface
point before landing
3rd point after landing
Landing point
surface points used for slope angle calculation

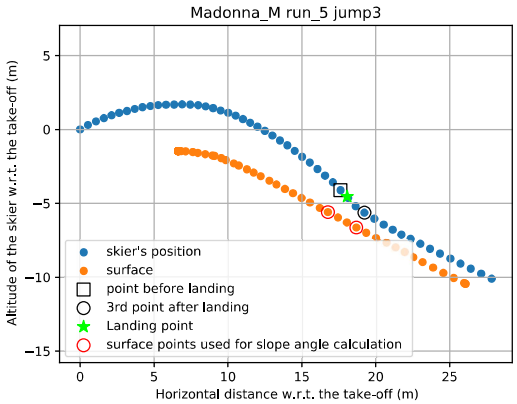
Madonna_M run_5 jump3
Altitude of the skier w.r.t. the take-off (m)
Horizontal distance w.r.t. the take-off (m)
skier's position
surface
point before landing
3rd point after landing
Landing point
surface points used for slope angle calculation

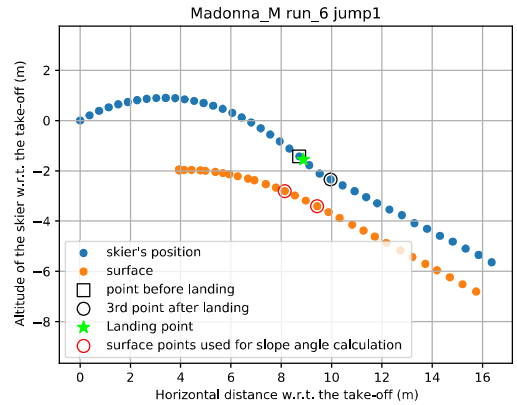
Madonna_M run_6 jump1
Altitude of the skier w.r.t. the take-off (m)
Horizontal distance w.r.t. the take-off (m)
skier's position
surface
point before landing
3rd point after landing
Landing point
surface points used for slope angle calculation

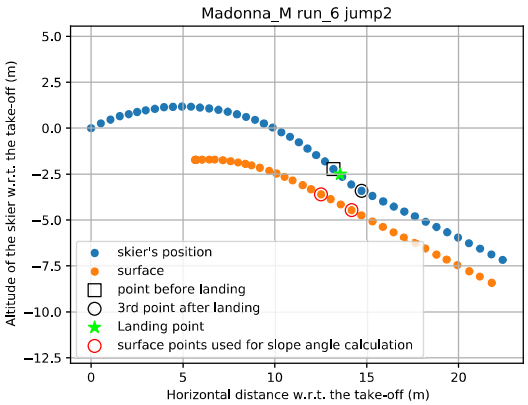
Madonna_M run_6 jump2
Altitude of the skier w.r.t. the take-off (m)
Horizontal distance w.r.t. the take-off (m)
skier's position
surface
point before landing
3rd point after landing
Landing point
surface points used for slope angle calculation

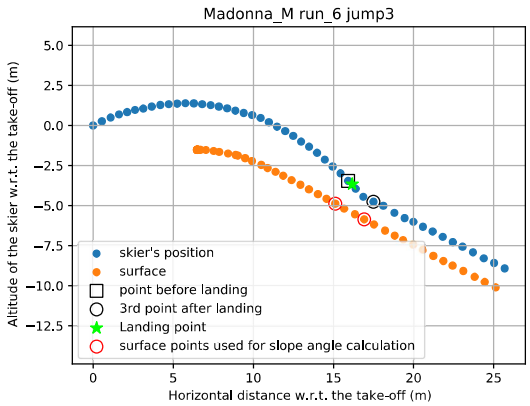
Madonna_M run_6 jump3
Altitude of the skier w.r.t. the take-off (m)
Horizontal distance w.r.t. the take-off (m)
skier's position
surface
point before landing
3rd point after landing
Landing point
surface points used for slope angle calculation

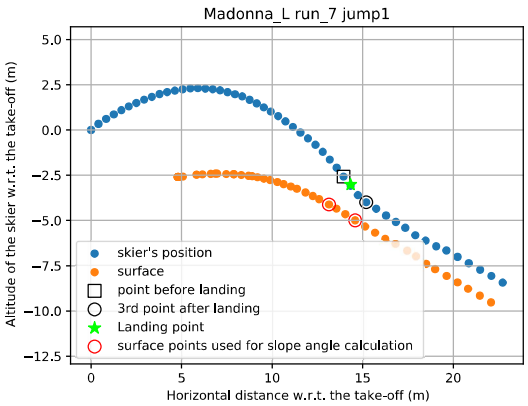
Madonna_L run_7 jump1
Altitude of the skier w.r.t. the take-off (m)
Horizontal distance w.r.t. the take-off (m)
skier's position
surface
point before landing
3rd point after landing
Landing point
surface points used for slope angle calculation

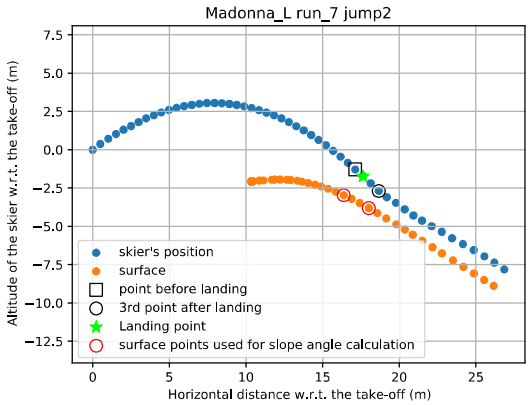
Madonna_L run_7 jump2
Altitude of the skier w.r.t. the take-off (m)
Horizontal distance w.r.t. the take-off (m)
skier's position
surface
point before landing
3rd point after landing
Landing point
surface points used for slope angle calculation

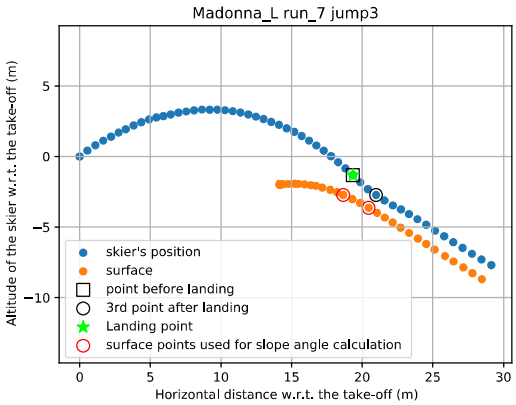
Madonna_L run_7 jump3
Altitude of the skier w.r.t. the take-off (m)
Horizontal distance w.r.t. the take-off (m)
skier's position
surface
point before landing
3rd point after landing
Landing point
surface points used for slope angle calculation

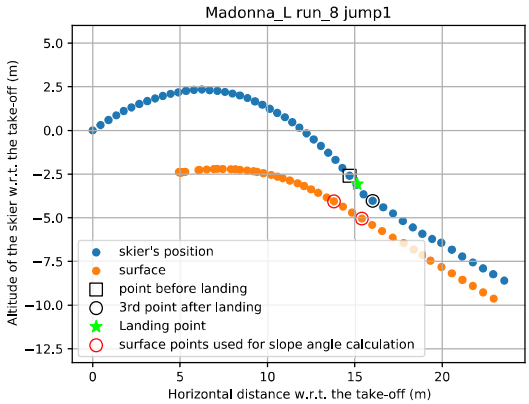
Madonna_L run_8 jump1
Altitude of the skier w.r.t. the take-off (m)
Horizontal distance w.r.t. the take-off (m)
skier's position
surface
point before landing
3rd point after landing
Landing point
surface points used for slope angle calculation

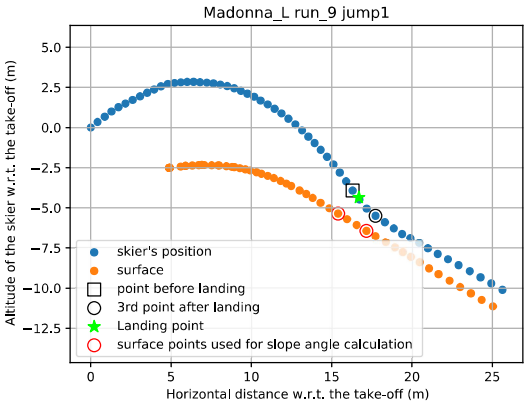
Madonna_L run_9 jump1
Altitude of the skier w.r.t. the take-off (m)
Horizontal distance w.r.t. the take-off (m)
skier's position
surface
point before landing
3rd point after landing
Landing point
surface points used for slope angle calculation

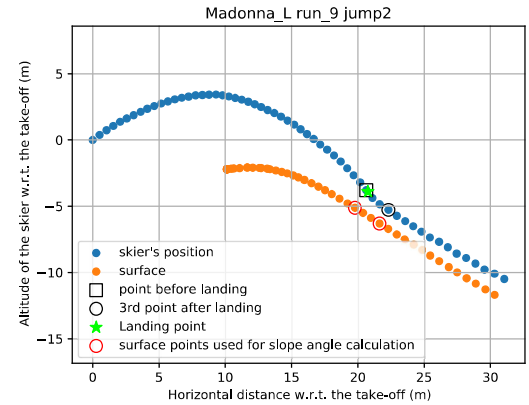
Madonna_L run_9 jump2
Altitude of the skier w.r.t. the take-off (m)
Horizontal distance w.r.t. the take-off (m)
skier's position
surface
point before landing
3rd point after landing
Landing point
surface points used for slope angle calculation

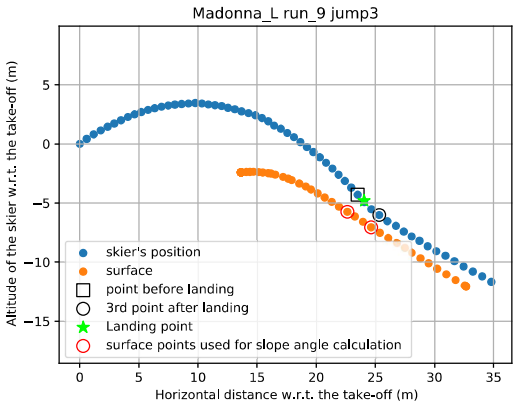
Madonna_L run_9 jump3
Altitude of the skier w.r.t. the take-off (m)
Horizontal distance w.r.t. the take-off (m)
skier's position
surface
point before landing
3rd point after landing
Landing point
surface points used for slope angle calculation

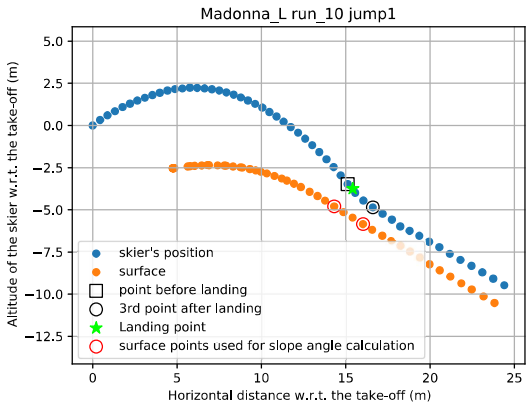
Madonna_L run_10 jump1
Altitude of the skier w.r.t. the take-off (m)
Horizontal distance w.r.t. the take-off (m)
skier's position
surface
point before landing
3rd point after landing
Landing point
surface points used for slope angle calculation

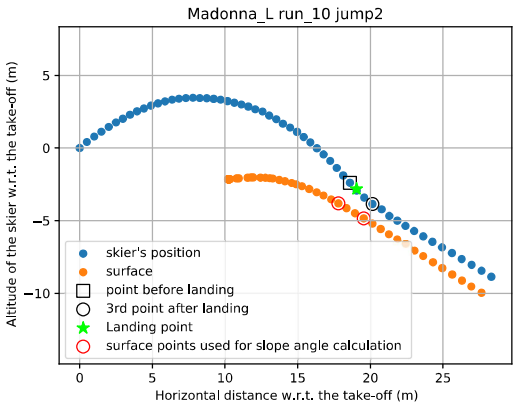
Madonna_L run_10 jump2
Altitude of the skier w.r.t. the take-off (m)
Horizontal distance w.r.t. the take-off (m)
skier's position
surface
point before landing
3rd point after landing
Landing point
surface points used for slope angle calculation

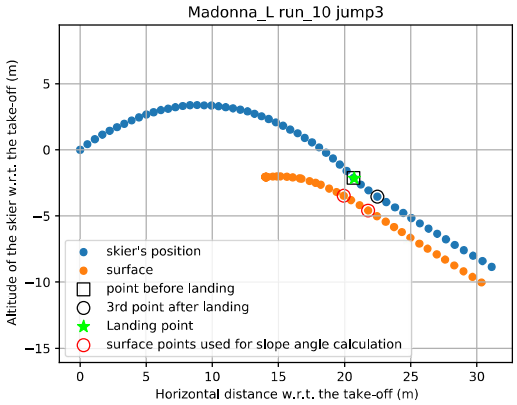
Madonna_L run_10 jump3
Altitude of the skier w.r.t. the take-off (m)
Horizontal distance w.r.t. the take-off (m)
skier's position
surface
point before landing
3rd point after landing
Landing point
surface points used for slope angle calculation

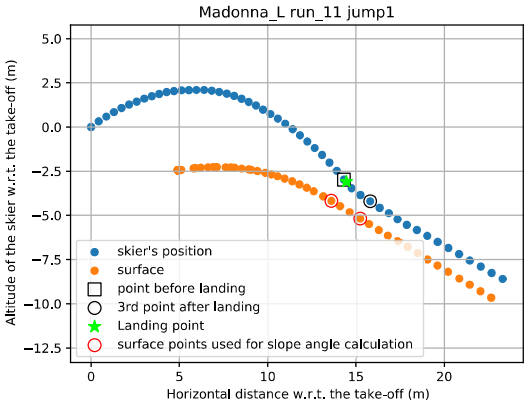
Madonna_L run_11 jump1
Altitude of the skier w.r.t. the take-off (m)
Horizontal distance w.r.t. the take-off (m)
skier's position
surface
point before landing
3rd point after landing
Landing point
surface points used for slope angle calculation

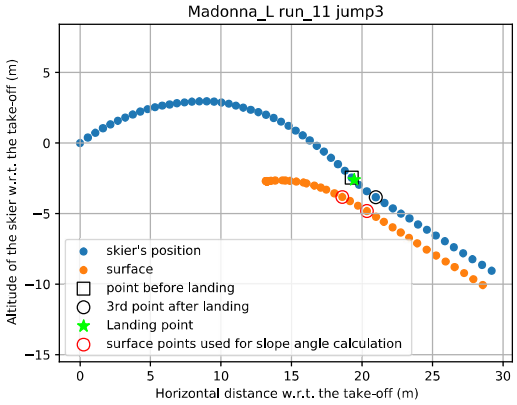
Madonna_L run_11 jump3
Altitude of the skier w.r.t. the take-off (m)
Horizontal distance w.r.t. the take-off (m)
skier's position
surface
point before landing
3rd point after landing
Landing point
surface points used for slope angle calculation

H

GRF plots

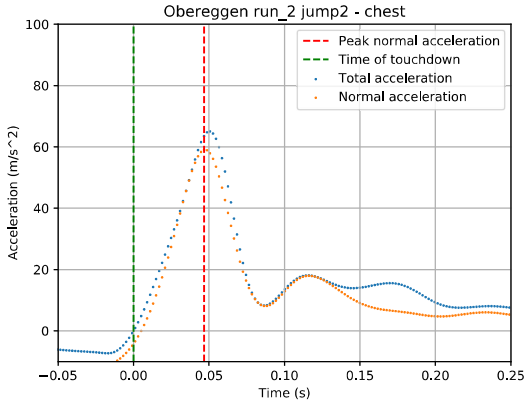
Obereggen run_2 jump2 - chest
Peak normal acceleration
Time of touchdown
Total acceleration
Normal acceleration
Acceleration (m/s^2)
Time (s)

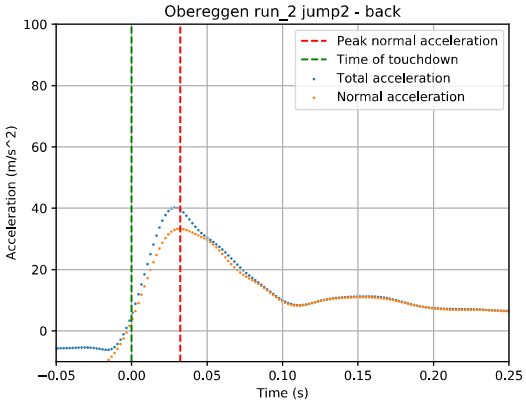
Obereggen run_2 jump2 - back
Peak normal acceleration
Time of touchdown
Total acceleration
Normal acceleration
Acceleration (m/s^2)
Time (s)

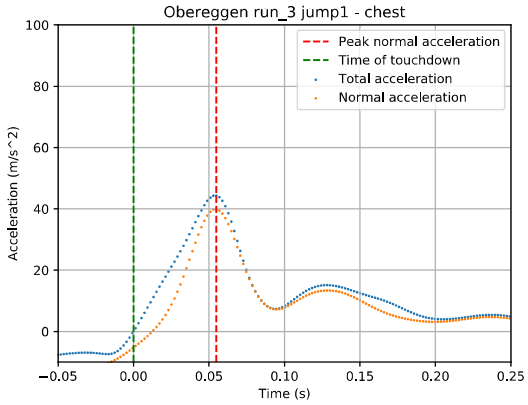
Obereggen run_3 jump1 - chest
Peak normal acceleration
Time of touchdown
Total acceleration
Normal acceleration
Acceleration (m/s^2)
Time (s)

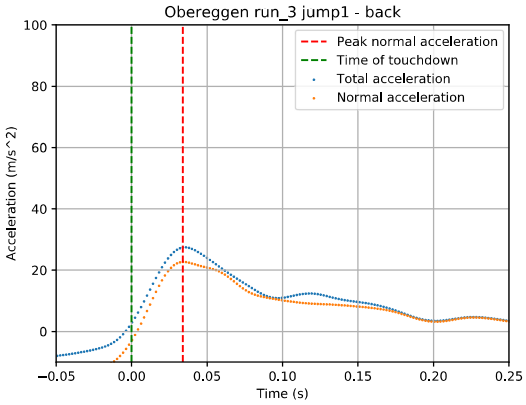
Obereggen run_3 jump1 - back
Peak normal acceleration
Time of touchdown
Total acceleration
Normal acceleration
Acceleration (m/s^2)
Time (s)

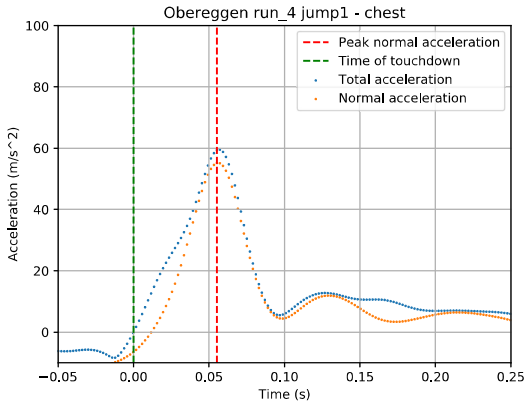
Obereggen run_4 jump1 - chest
Peak normal acceleration
Time of touchdown
Total acceleration
Normal acceleration
Acceleration (m/s^2)
Time (s)

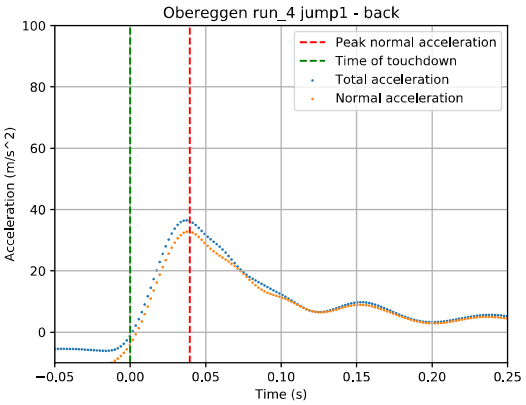
Obereggen run_4 jump1 - back
Peak normal acceleration
Time of touchdown
Total acceleration
Normal acceleration
Acceleration (m/s^2)
Time (s)

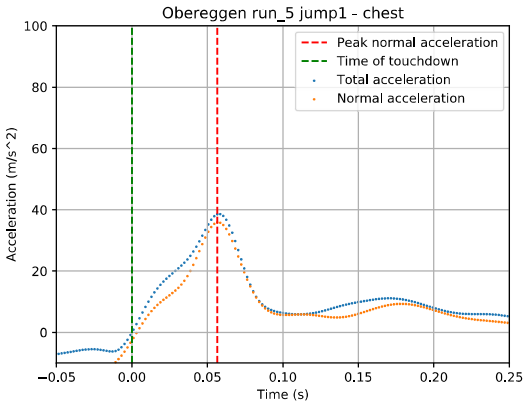
Obereggen run_5 jump1 - chest
Peak normal acceleration
Time of touchdown
Total acceleration
Normal acceleration
Acceleration (m/s^2)
Time (s)

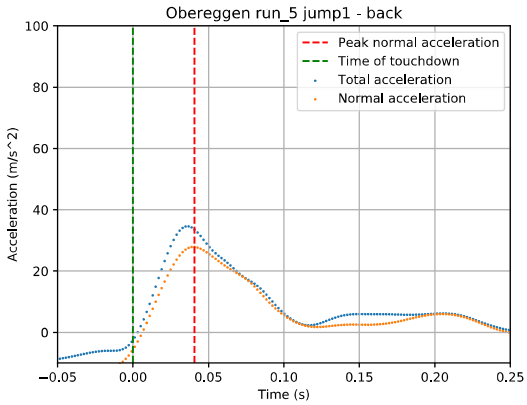
Obereggen run_5 jump1 - back
Peak normal acceleration
Time of touchdown
Total acceleration
Normal acceleration
Acceleration (m/s^2)
Time (s)

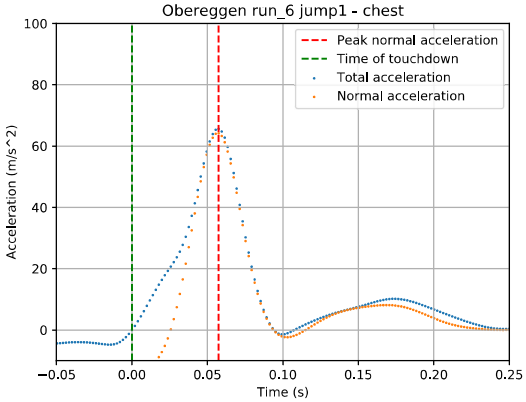
Obereggen run_6 jump1 - chest
Peak normal acceleration
Time of touchdown
Total acceleration
Normal acceleration
Acceleration (m/s^2)
Time (s)

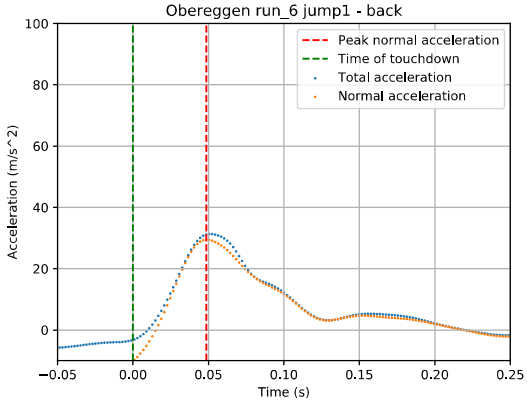
Obereggen run_6 jump1 - back
Peak normal acceleration
Time of touchdown
Total acceleration
Normal acceleration
Acceleration (m/s^2)
Time (s)

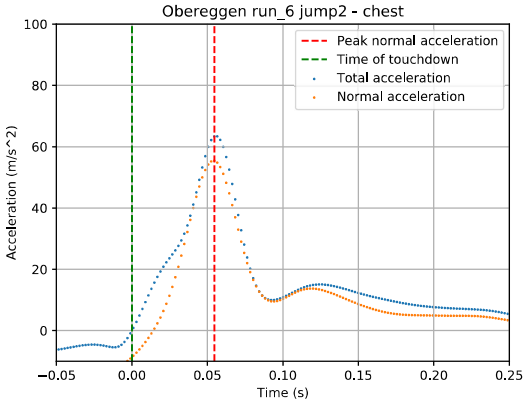
Obereggen run_6 jump2 - chest
Peak normal acceleration
Time of touchdown
Total acceleration
Normal acceleration
Acceleration (m/s^2)
Time (s)

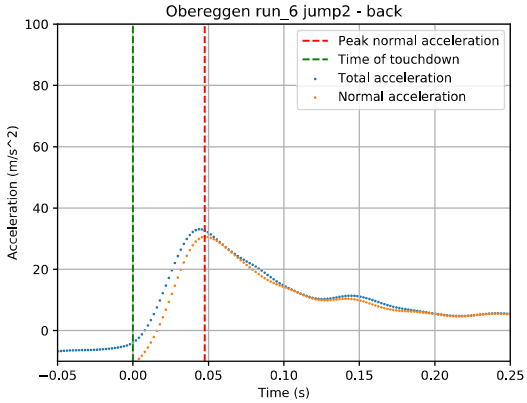
Obereggen run_6 jump2 - back
Peak normal acceleration
Time of touchdown
Total acceleration
Normal acceleration
Acceleration (m/s^2)
Time (s)

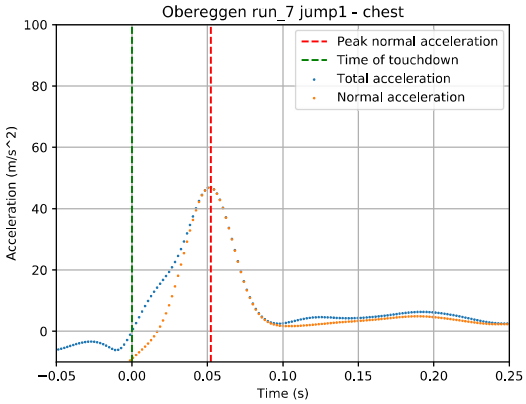
Obereggen run_7 jump1 - chest
Peak normal acceleration
Time of touchdown
Total acceleration
Normal acceleration
Acceleration (m/s^2)
Time (s)

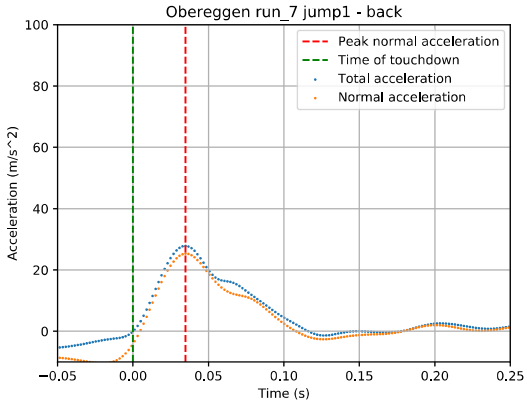
Obereggen run_7 jump1 - back
Peak normal acceleration
Time of touchdown
Total acceleration
Normal acceleration
Acceleration (m/s^2)
Time (s)

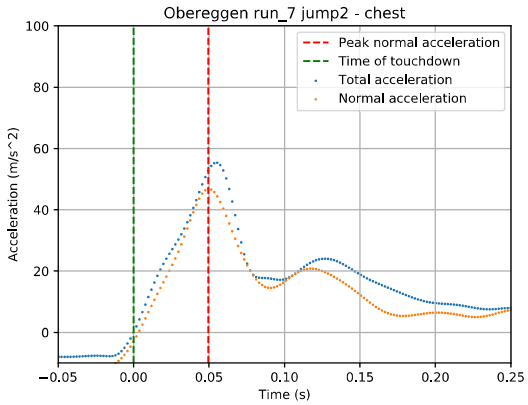
Obereggen run_7 jump2 - chest
Peak normal acceleration
Time of touchdown
Total acceleration
Normal acceleration
Acceleration (m/s^2)
Time (s)

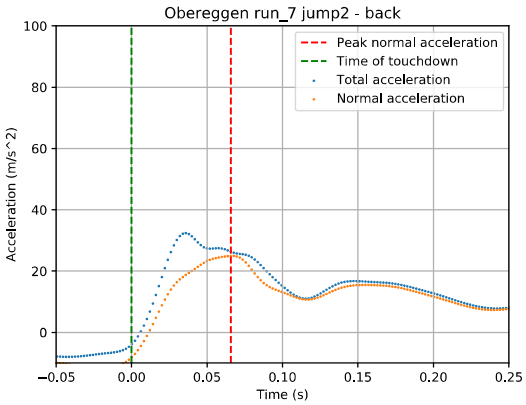
Obereggen run_7 jump2 - back
Peak normal acceleration
Time of touchdown
Total acceleration
Normal acceleration
Acceleration (m/s^2)
Time (s)

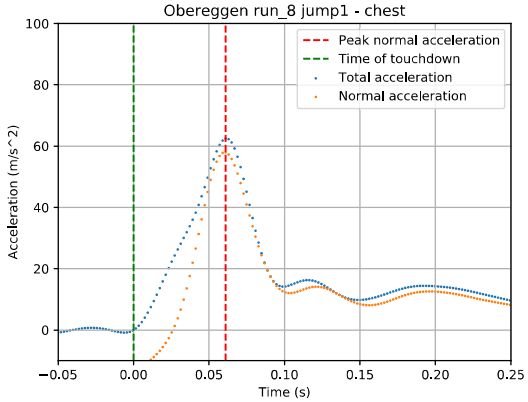
Obereggen run_8 jump1 - chest
Peak normal acceleration
Time of touchdown
Total acceleration
Normal acceleration
Acceleration (m/s^2)
Time (s)

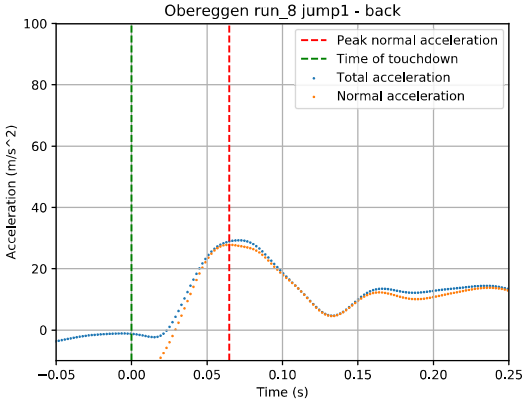
Obereggen run_8 jump1 - back
Peak normal acceleration
Time of touchdown
Total acceleration
Normal acceleration
Acceleration (m/s^2)
Time (s)

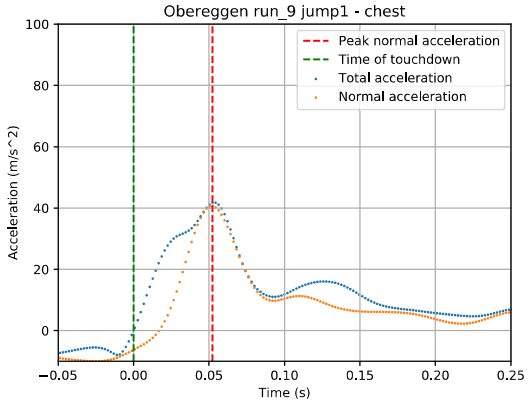
Obereggen run_9 jump1 - chest
Peak normal acceleration
Time of touchdown
Total acceleration
Normal acceleration
Acceleration (m/s^2)
Time (s)

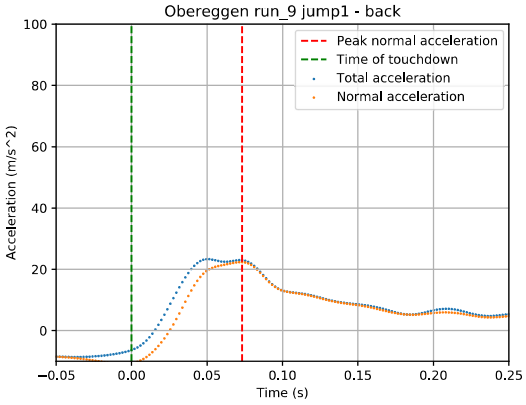
Obereggen run_9 jump1 - back
Peak normal acceleration
Time of touchdown
Total acceleration
Normal acceleration
Acceleration (m/s^2)
Time (s)

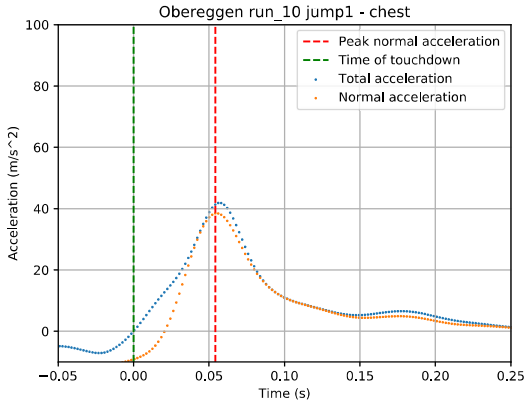
Obereggen run_10 jump1 - chest
Peak normal acceleration
Time of touchdown
Total acceleration
Normal acceleration
Acceleration (m/s^2)
Time (s)

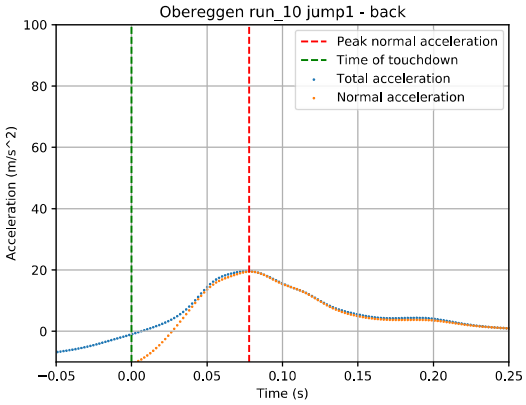
Obereggen run_10 jump1 - back
Peak normal acceleration
Time of touchdown
Total acceleration
Normal acceleration
Acceleration (m/s^2)
Time (s)

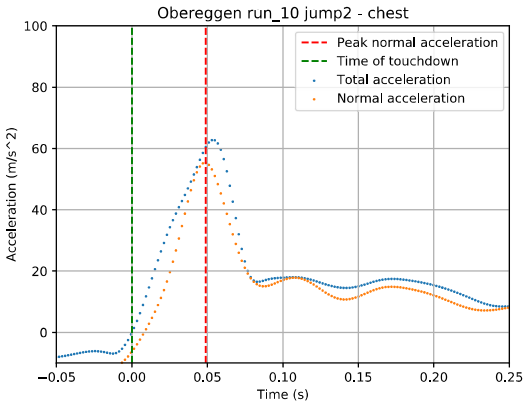
Obereggen run_10 jump2 - chest
Peak normal acceleration
Time of touchdown
Total acceleration
Normal acceleration
Acceleration (m/s^2)
Time (s)

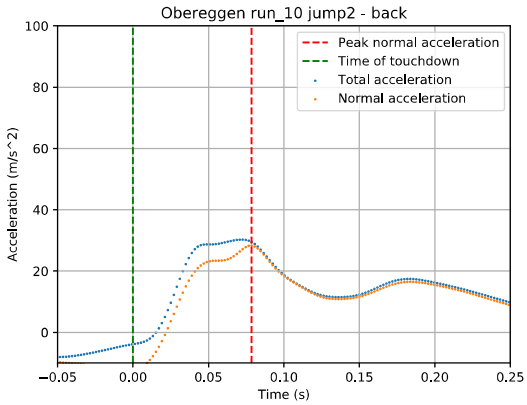
Obereggen run_10 jump2 - back
Peak normal acceleration
Time of touchdown
Total acceleration
Normal acceleration
Acceleration (m/s^2)
Time (s)

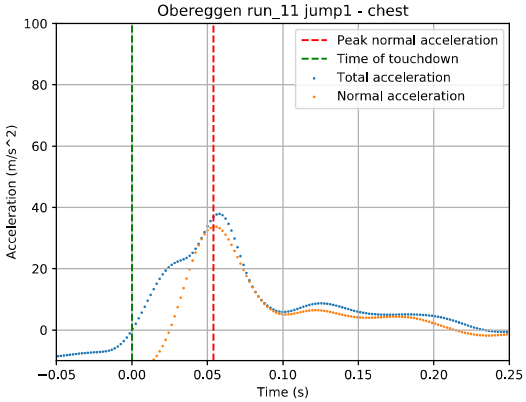
Obereggen run_11 jump1 - chest
Peak normal acceleration
Time of touchdown
Total acceleration
Normal acceleration
Acceleration (m/s^2)
Time (s)

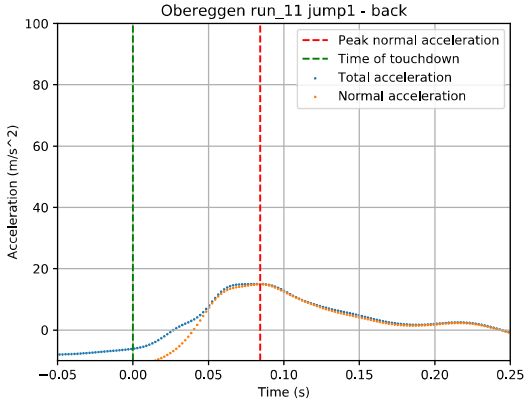
Obereggen run_11 jump1 - back
Peak normal acceleration
Time of touchdown
Total acceleration
Normal acceleration
Acceleration (m/s^2)
Time (s)

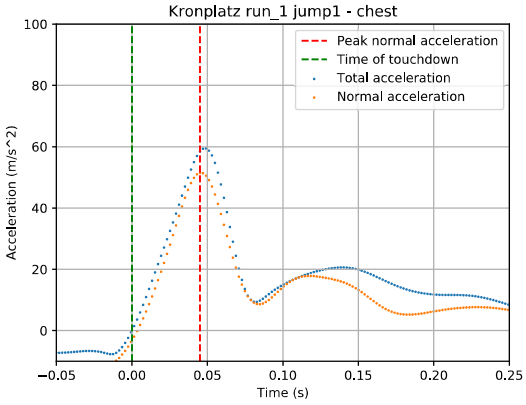
Kronplatz run_1 jump1 - chest
Peak normal acceleration
Time of touchdown
Total acceleration
Normal acceleration
Acceleration (m/s^2)
Time (s)

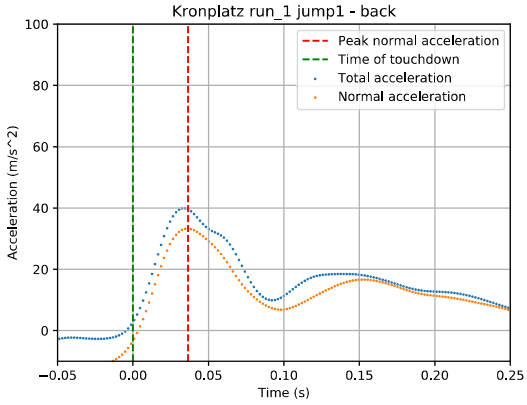
Kronplatz run_1 jump1 - back
Peak normal acceleration
Time of touchdown
Total acceleration
Normal acceleration
Acceleration (m/s^2)
Time (s)

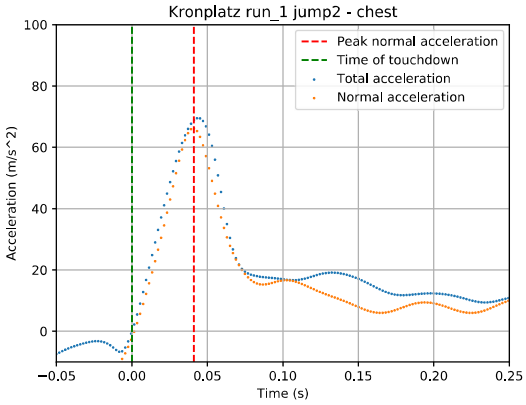
Kronplatz run_1 jump2 - chest
Peak normal acceleration
Time of touchdown
Total acceleration
Normal acceleration
Acceleration (m/s^2)
Time (s)

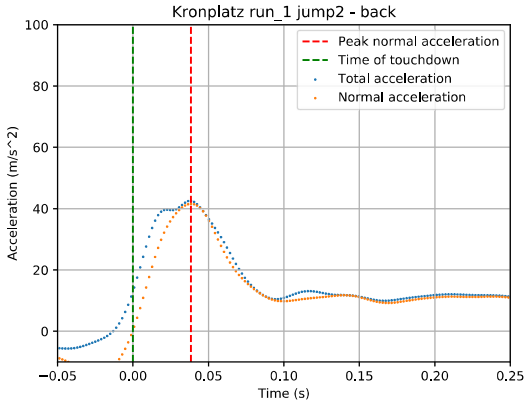
Kronplatz run_1 jump2 - back
Peak normal acceleration
Time of touchdown
Total acceleration
Normal acceleration
Acceleration (m/s^2)
Time (s)

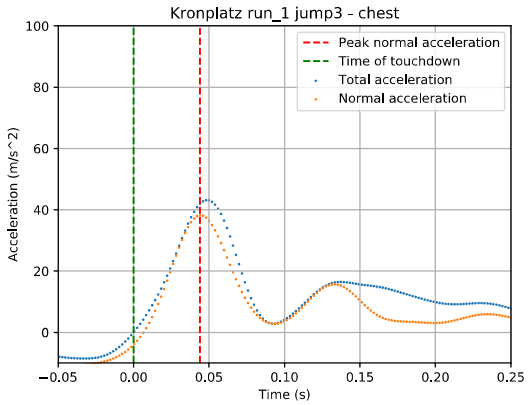
Kronplatz run_1 jump3 - chest
Peak normal acceleration
Time of touchdown
Total acceleration
Normal acceleration
Acceleration (m/s^2)
Time (s)

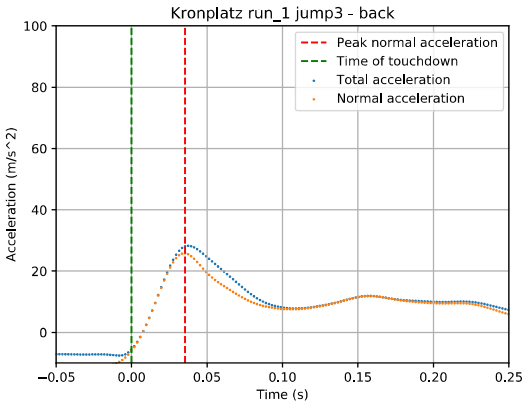
Kronplatz run_1 jump3 - back
Peak normal acceleration
Time of touchdown
Total acceleration
Normal acceleration
Acceleration (m/s^2)
Time (s)

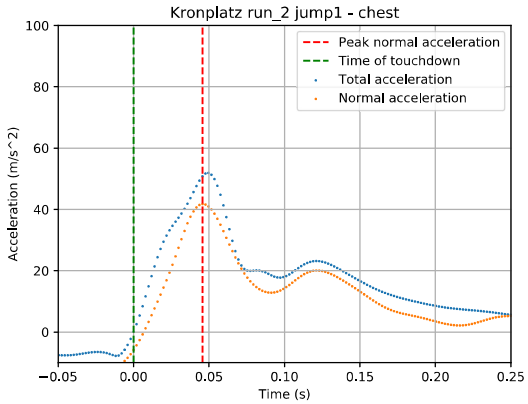
Kronplatz run_2 jump1 - chest
Peak normal acceleration
Time of touchdown
Total acceleration
Normal acceleration
Acceleration (m/s^2)
Time (s)

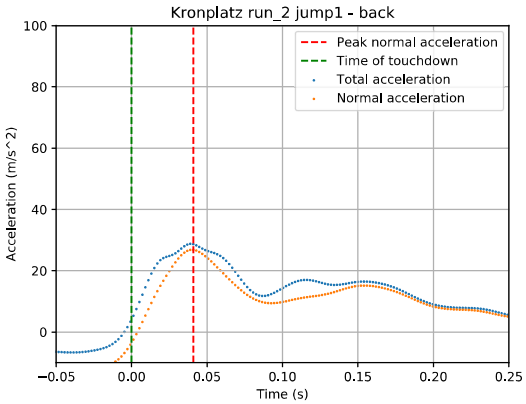
Kronplatz run_2 jump1 - back
Peak normal acceleration
Time of touchdown
Total acceleration
Normal acceleration
Acceleration (m/s^2)
Time (s)

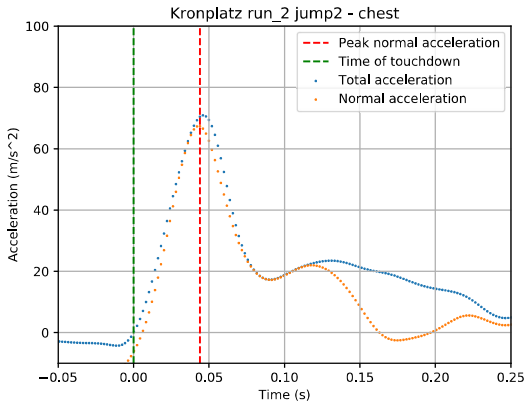
Kronplatz run_2 jump2 - chest
Peak normal acceleration
Time of touchdown
Total acceleration
Normal acceleration
Acceleration (m/s^2)
Time (s)

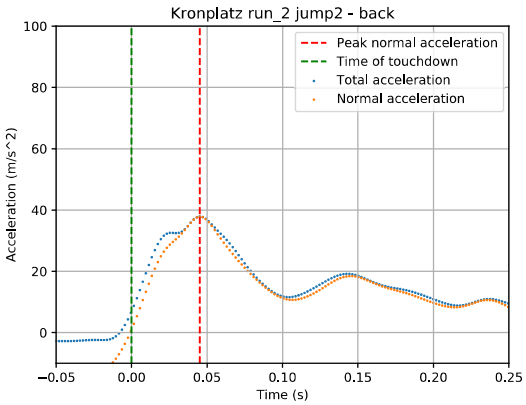
Kronplatz run_2 jump2 - back
Peak normal acceleration
Time of touchdown
Total acceleration
Normal acceleration
Acceleration (m/s^2)
Time (s)

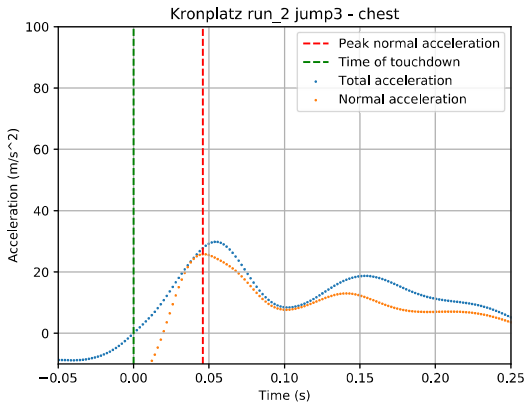
Kronplatz run_2 jump3 - chest
Peak normal acceleration
Time of touchdown
Total acceleration
Normal acceleration
Acceleration (m/s^2)
Time (s)

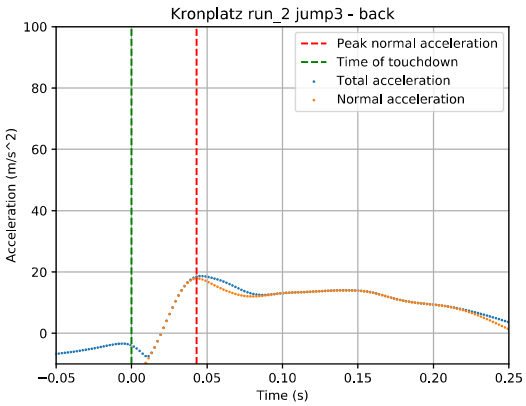
Kronplatz run_2 jump3 - back
Peak normal acceleration
Time of touchdown
Total acceleration
Normal acceleration
Acceleration (m/s^2)
Time (s)

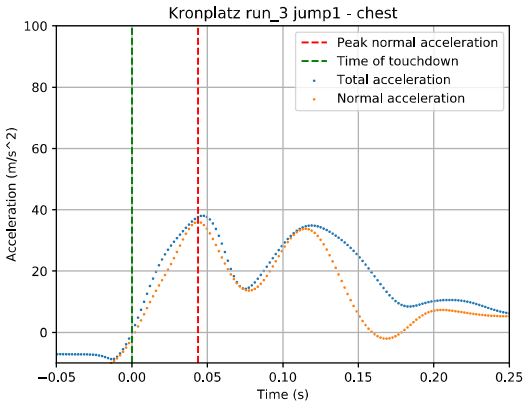
Kronplatz run_3 jump1 - chest
Peak normal acceleration
Time of touchdown
Total acceleration
Normal acceleration
Acceleration (m/s^2)
Time (s)

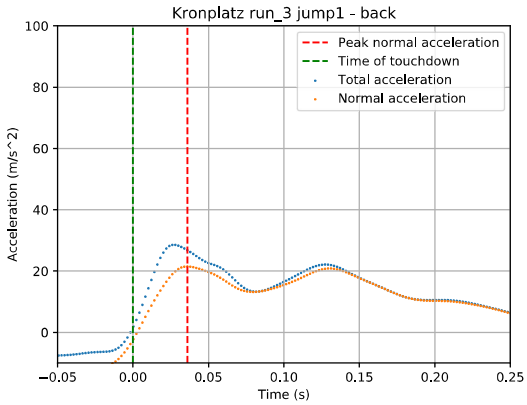
Kronplatz run_3 jump1 - back
Peak normal acceleration
Time of touchdown
Total acceleration
Normal acceleration
Acceleration (m/s^2)
Time (s)

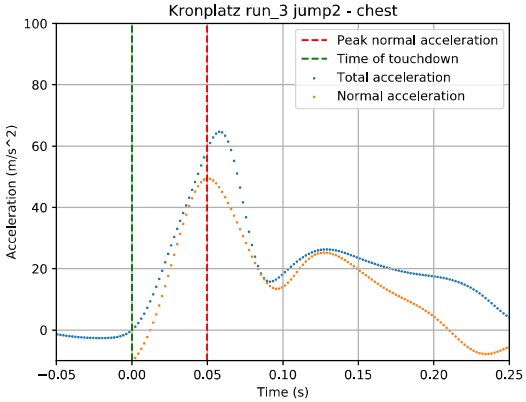
Kronplatz run_3 jump2 - chest
Peak normal acceleration
Time of touchdown
Total acceleration
Normal acceleration
Acceleration (m/s^2)
Time (s)

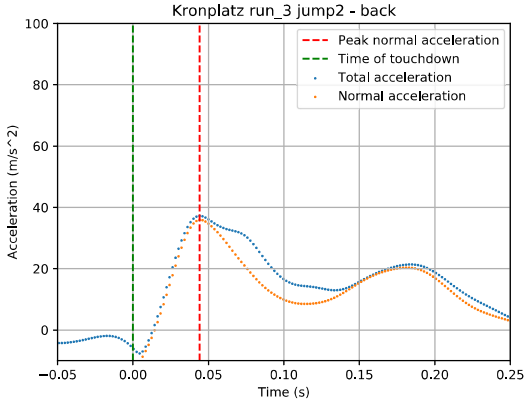
Kronplatz run_3 jump2 - back
Peak normal acceleration
Time of touchdown
Total acceleration
Normal acceleration
Acceleration (m/s^2)
Time (s)

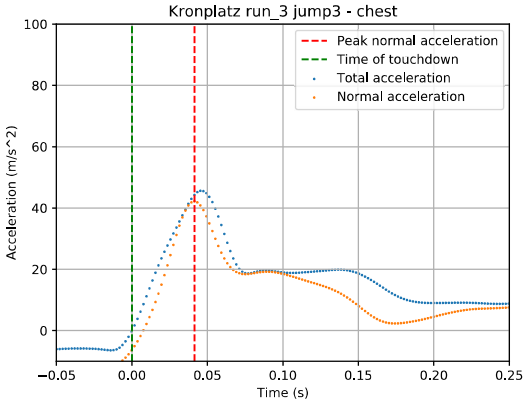
Kronplatz run_3 jump3 - chest
Peak normal acceleration
Time of touchdown
Total acceleration
Normal acceleration
Acceleration (m/s^2)
Time (s)

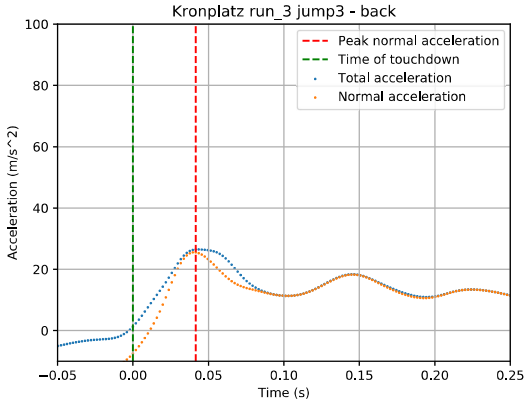
Kronplatz run_3 jump3 - back
Peak normal acceleration
Time of touchdown
Total acceleration
Normal acceleration
Acceleration (m/s^2)
Time (s)

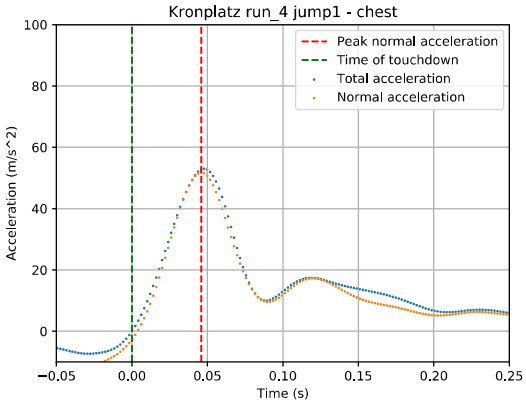
Kronplatz run_4 jump1 - chest
Peak normal acceleration
Time of touchdown
Total acceleration
Normal acceleration
Acceleration (m/s^2)
Time (s)

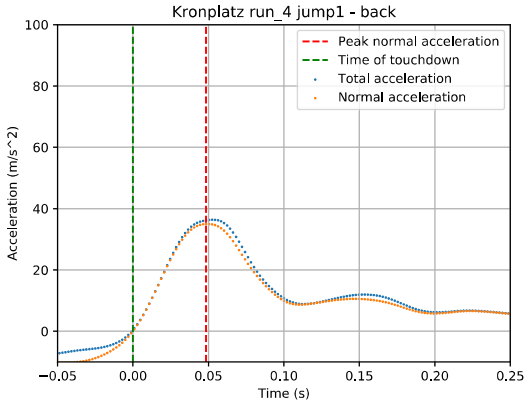
Kronplatz run_4 jump1 - back
Peak normal acceleration
Time of touchdown
Total acceleration
Normal acceleration
Acceleration (m/s^2)
Time (s)

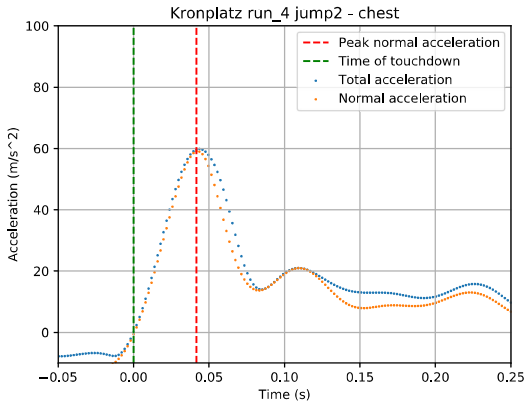
Kronplatz run_4 jump2 - chest
Peak normal acceleration
Time of touchdown
Total acceleration
Normal acceleration
Acceleration (m/s^2)
Time (s)

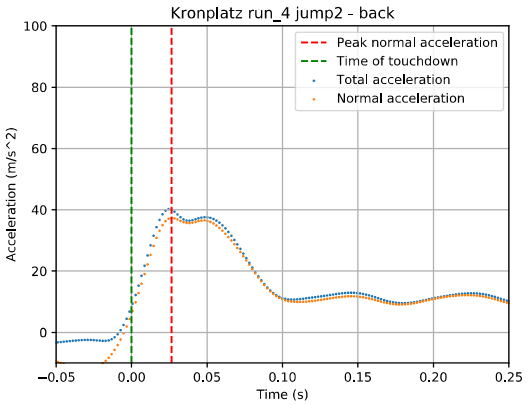
Kronplatz run_4 jump2 - back
Peak normal acceleration
Time of touchdown
Total acceleration
Normal acceleration
Acceleration (m/s^2)
Time (s)

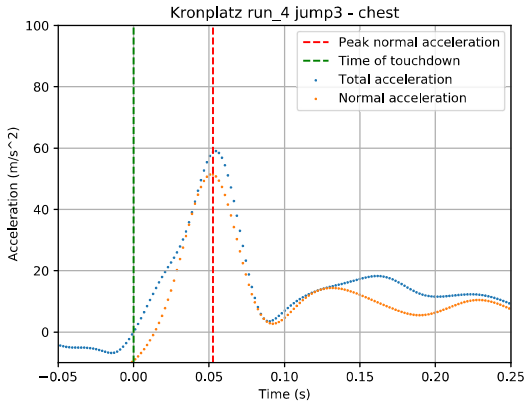
Kronplatz run_4 jump3 - chest
Peak normal acceleration
Time of touchdown
Total acceleration
Normal acceleration
Acceleration (m/s^2)
Time (s)

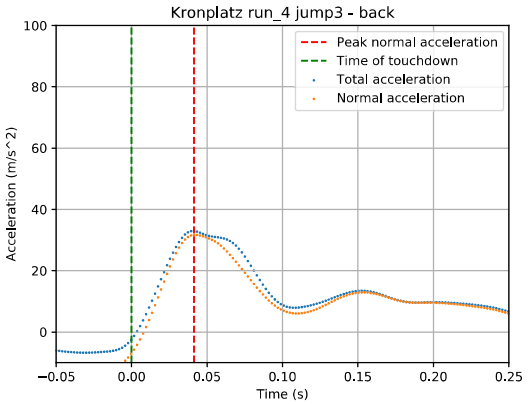
Kronplatz run_4 jump3 - back
Peak normal acceleration
Time of touchdown
Total acceleration
Normal acceleration
Acceleration (m/s^2)
Time (s)

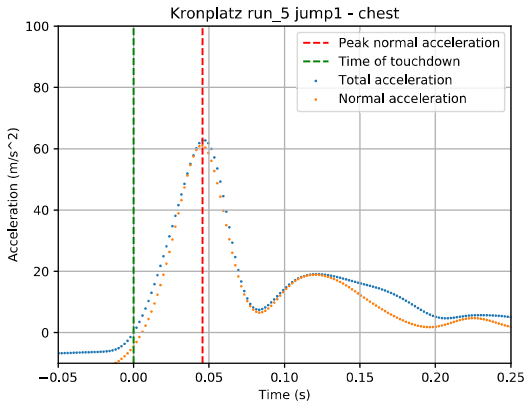
Kronplatz run_5 jump1 - chest
Peak normal acceleration
Time of touchdown
Total acceleration
Normal acceleration
Acceleration (m/s^2)
Time (s)

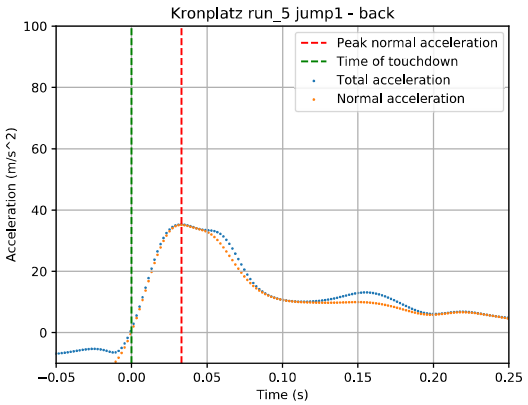
Kronplatz run_5 jump1 - back
Peak normal acceleration
Time of touchdown
Total acceleration
Normal acceleration
Acceleration (m/s^2)
Time (s)

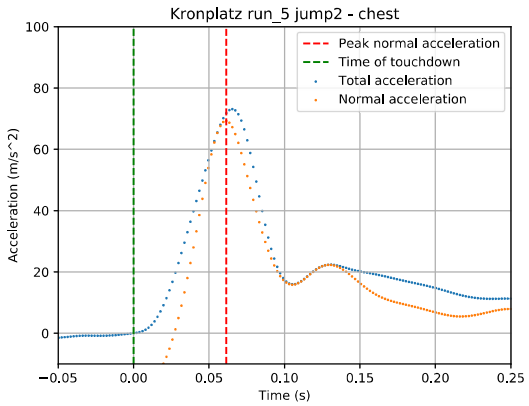
Kronplatz run_5 jump2 - chest
Peak normal acceleration
Time of touchdown
Total acceleration
Normal acceleration
Acceleration (m/s^2)
Time (s)

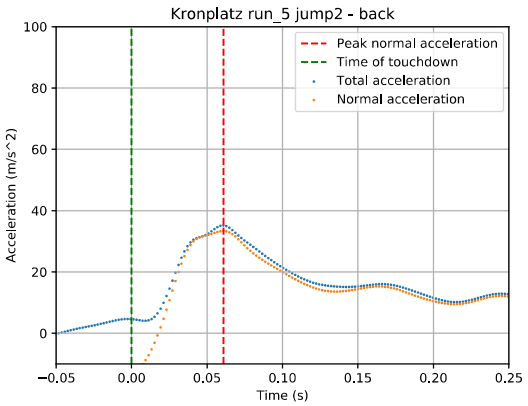
Kronplatz run_5 jump2 - back
Peak normal acceleration
Time of touchdown
Total acceleration
Normal acceleration
Acceleration (m/s^2)
Time (s)

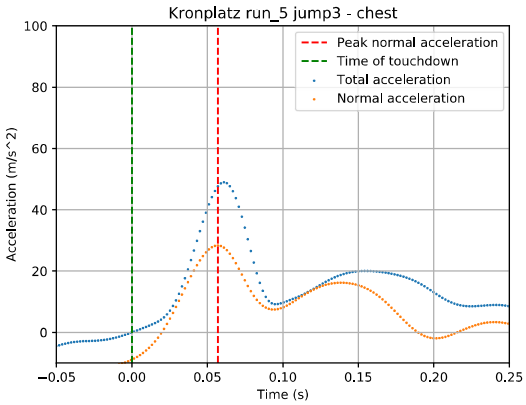
Kronplatz run_5 jump3 - chest
Peak normal acceleration
Time of touchdown
Total acceleration
Normal acceleration
Acceleration (m/s^2)
Time (s)

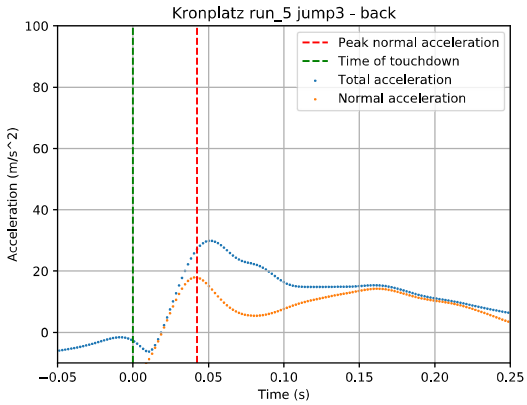
Kronplatz run_5 jump3 - back
Peak normal acceleration
Time of touchdown
Total acceleration
Normal acceleration
Acceleration (m/s^2)
Time (s)

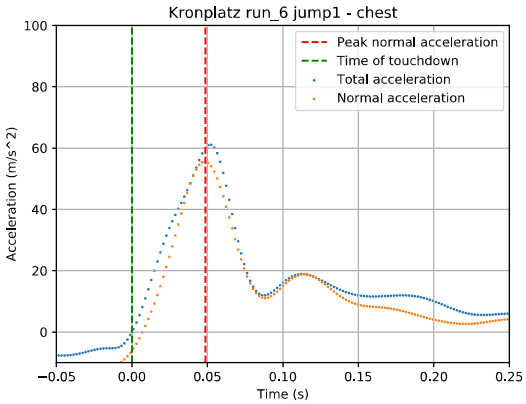
Kronplatz run_6 jump1 - chest
Peak normal acceleration
Time of touchdown
Total acceleration
Normal acceleration
Acceleration (m/s^2)
Time (s)

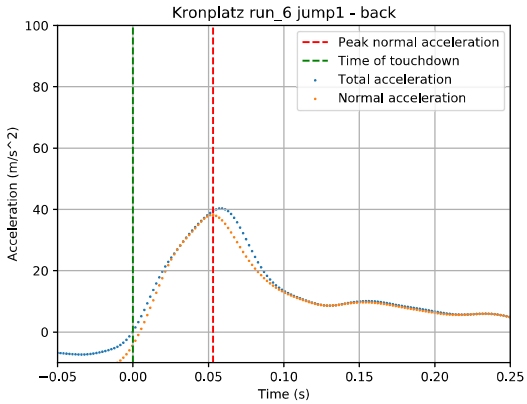
Kronplatz run_6 jump1 - back
Peak normal acceleration
Time of touchdown
Total acceleration
Normal acceleration
Acceleration (m/s^2)
Time (s)

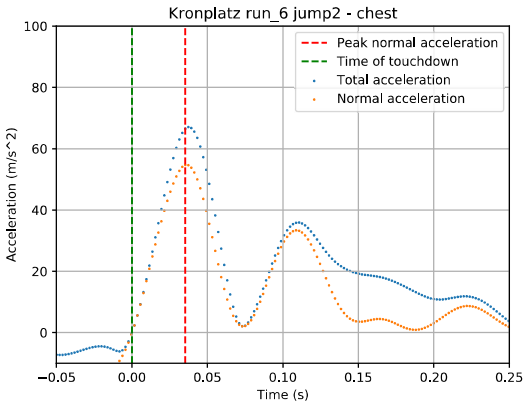
Kronplatz run_6 jump2 - chest
Peak normal acceleration
Time of touchdown
Total acceleration
Normal acceleration
Acceleration (m/s^2)
Time (s)

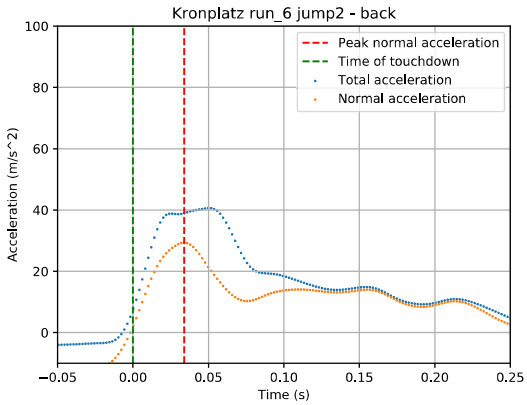
Kronplatz run_6 jump2 - back
Peak normal acceleration
Time of touchdown
Total acceleration
Normal acceleration
Acceleration (m/s^2)
Time (s)

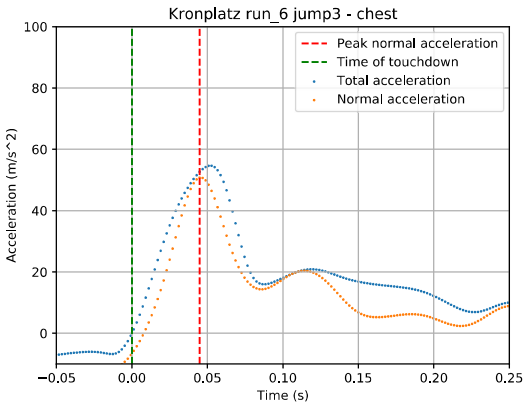
Kronplatz run_6 jump3 - chest
Peak normal acceleration
Time of touchdown
Total acceleration
Normal acceleration
Acceleration (m/s^2)
Time (s)

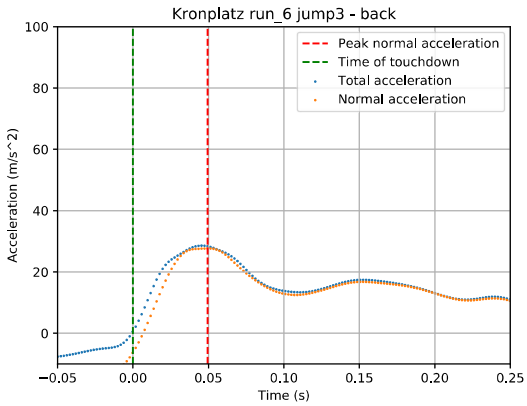
Kronplatz run_6 jump3 - back
Peak normal acceleration
Time of touchdown
Total acceleration
Normal acceleration
Acceleration (m/s^2)
Time (s)

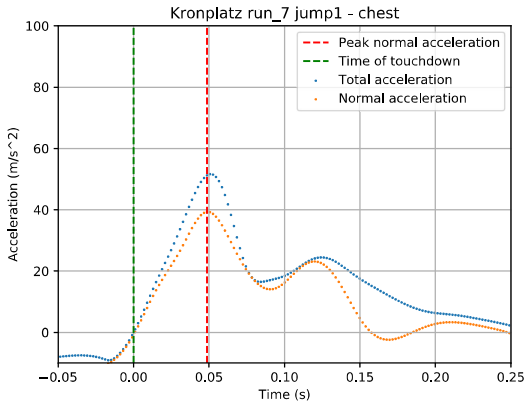
Kronplatz run_7 jump1 - chest
Peak normal acceleration
Time of touchdown
Total acceleration
Normal acceleration
Acceleration (m/s^2)
Time (s)

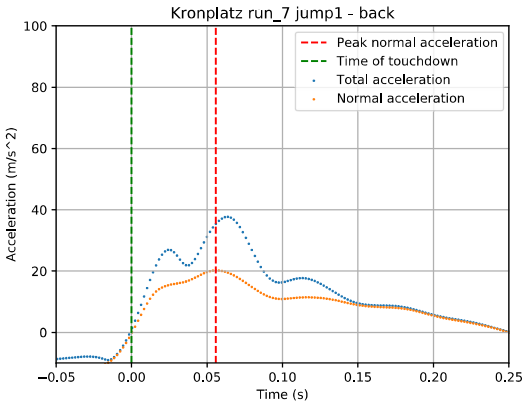
Kronplatz run_7 jump1 - back
Peak normal acceleration
Time of touchdown
Total acceleration
Normal acceleration
Acceleration (m/s^2)
Time (s)

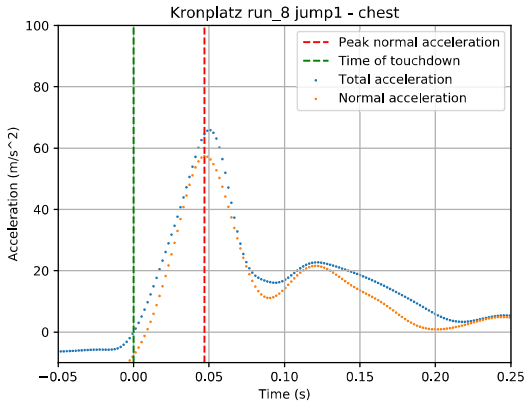
Kronplatz run_8 jump1 - chest
Peak normal acceleration
Time of touchdown
Total acceleration
Normal acceleration
Acceleration (m/s^2)
Time (s)

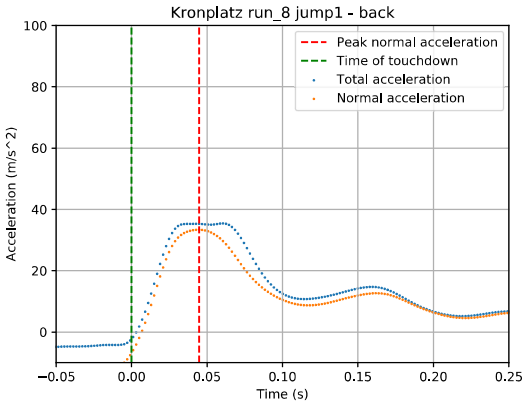
Kronplatz run_8 jump1 - back
Peak normal acceleration
Time of touchdown
Total acceleration
Normal acceleration
Acceleration (m/s^2)
Time (s)

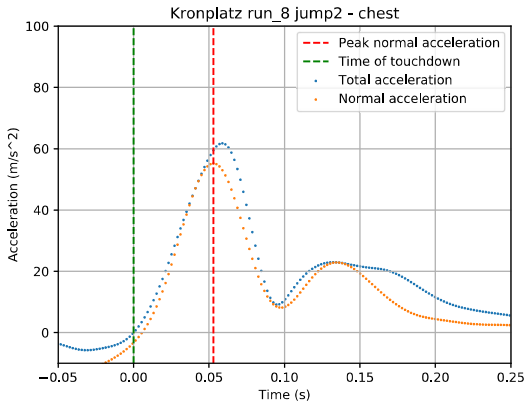
Kronplatz run_8 jump2 - chest
Peak normal acceleration
Time of touchdown
Total acceleration
Normal acceleration
Acceleration (m/s^2)
Time (s)

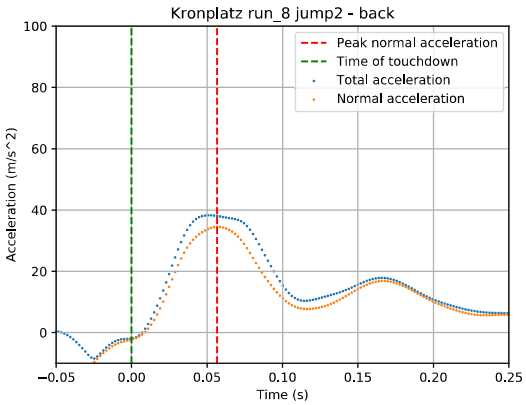
Kronplatz run_8 jump2 - back
Peak normal acceleration
Time of touchdown
Total acceleration
Normal acceleration
Acceleration (m/s^2)
Time (s)

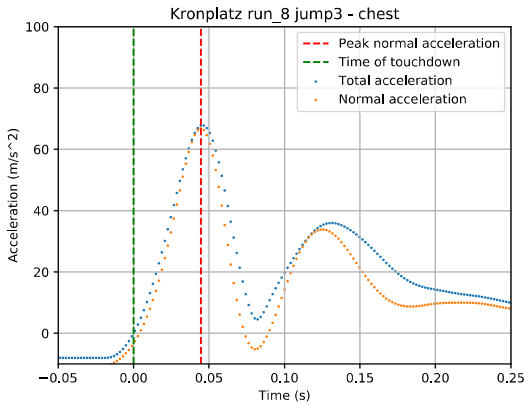
Kronplatz run_8 jump3 - chest
Peak normal acceleration
Time of touchdown
Total acceleration
Normal acceleration
Acceleration (m/s^2)
Time (s)

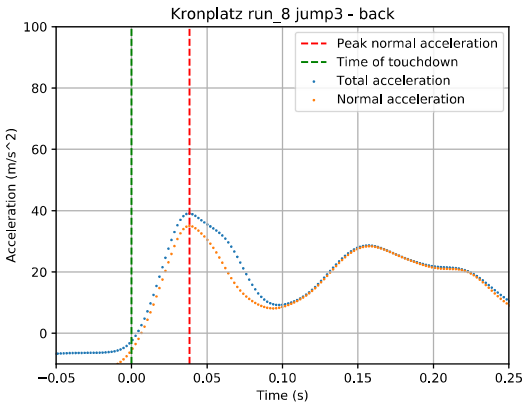
Kronplatz run_8 jump3 - back
Peak normal acceleration
Time of touchdown
Total acceleration
Normal acceleration
Acceleration (m/s^2)
Time (s)

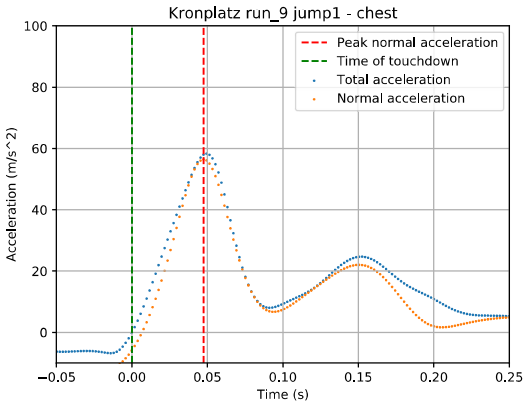
Kronplatz run_9 jump1 - chest
Peak normal acceleration
Time of touchdown
Total acceleration
Normal acceleration
Acceleration (m/s^2)
Time (s)

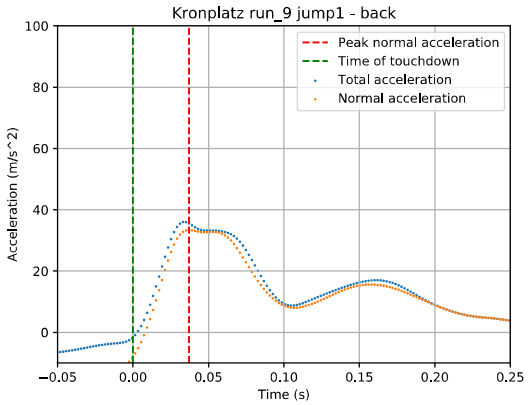
Kronplatz run_9 jump1 - back
Peak normal acceleration
Time of touchdown
Total acceleration
Normal acceleration
Acceleration (m/s^2)
Time (s)

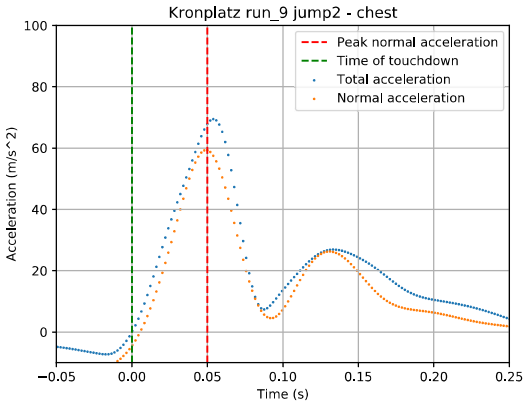
Kronplatz run_9 jump2 - chest
Peak normal acceleration
Time of touchdown
Total acceleration
Normal acceleration
Acceleration (m/s^2)
Time (s)

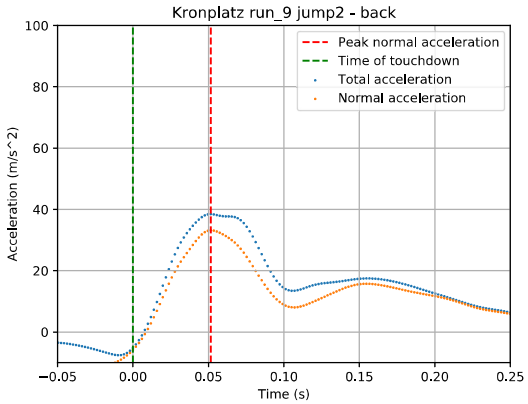
Kronplatz run_9 jump2 - back
Peak normal acceleration
Time of touchdown
Total acceleration
Normal acceleration
Acceleration (m/s^2)
Time (s)

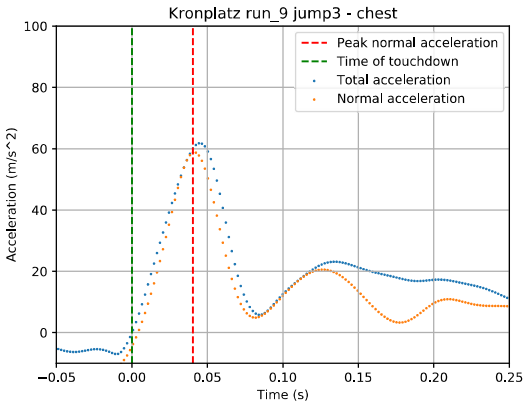
Kronplatz run_9 jump3 - chest
Peak normal acceleration
Time of touchdown
Total acceleration
Normal acceleration
Acceleration (m/s^2)
Time (s)

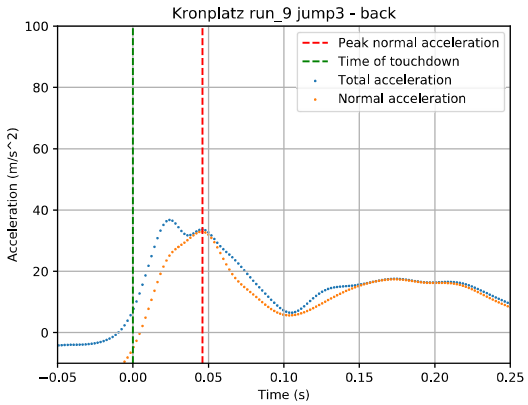
Kronplatz run_9 jump3 - back
Peak normal acceleration
Time of touchdown
Total acceleration
Normal acceleration
Acceleration (m/s^2)
Time (s)

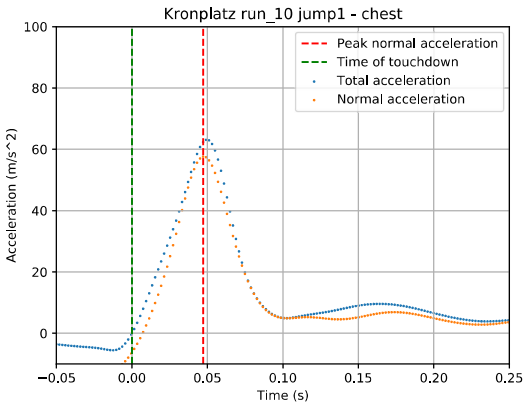
Kronplatz run_10 jump1 - chest
Peak normal acceleration
Time of touchdown
Total acceleration
Normal acceleration
Acceleration (m/s^2)
Time (s)

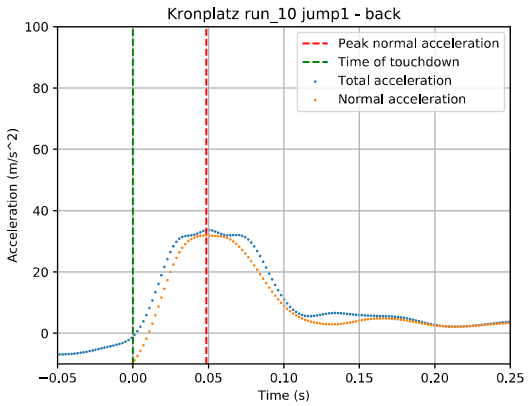
Kronplatz run_10 jump1 - back
Peak normal acceleration
Time of touchdown
Total acceleration
Normal acceleration
Acceleration (m/s^2)
Time (s)

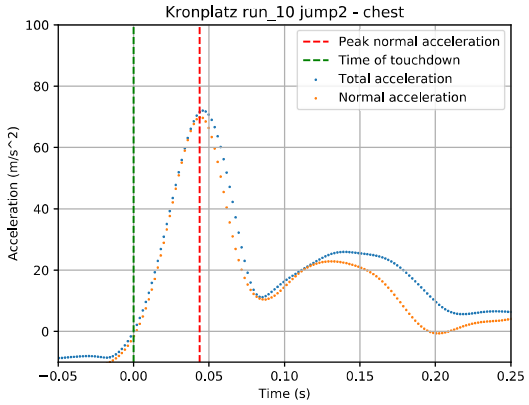
Kronplatz run_10 jump2 - chest
Peak normal acceleration
Time of touchdown
Total acceleration
Normal acceleration
Acceleration (m/s^2)
Time (s)

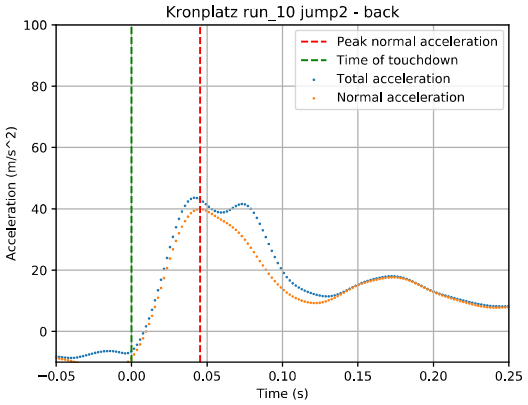
Kronplatz run_10 jump2 - back
Peak normal acceleration
Time of touchdown
Total acceleration
Normal acceleration
Acceleration (m/s^2)
Time (s)

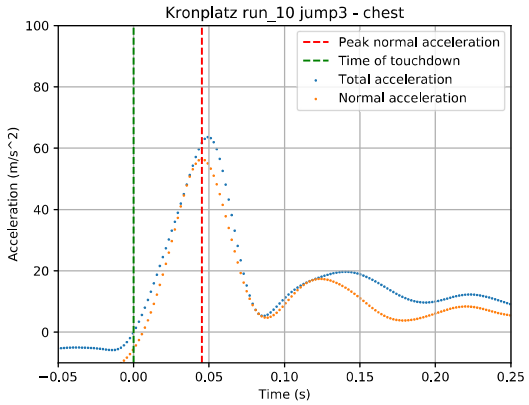
Kronplatz run_10 jump3 - chest
Peak normal acceleration
Time of touchdown
Total acceleration
Normal acceleration
Acceleration (m/s^2)
Time (s)

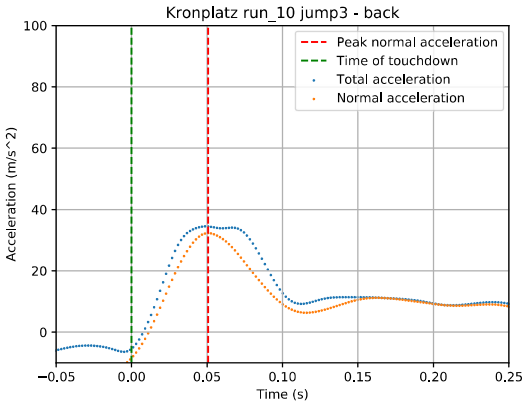
Kronplatz run_10 jump3 - back
Peak normal acceleration
Time of touchdown
Total acceleration
Normal acceleration
Acceleration (m/s^2)
Time (s)

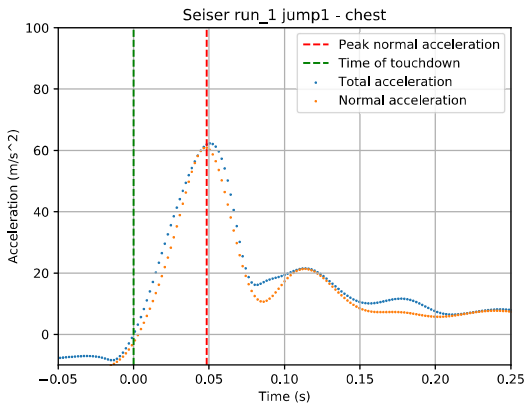
Seiser run_1 jump1 - chest
Peak normal acceleration
Time of touchdown
Total acceleration
Normal acceleration
Acceleration (m/s^2)
Time (s)

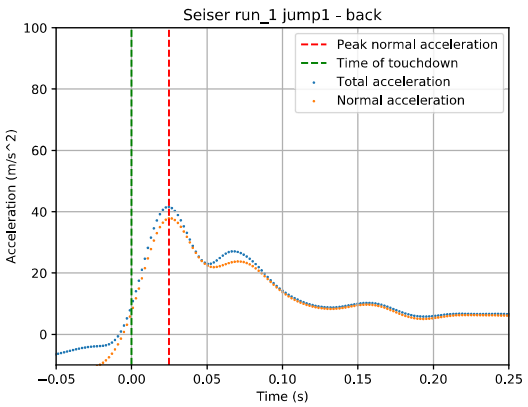
Seiser run_1 jump1 - back
Peak normal acceleration
Time of touchdown
Total acceleration
Normal acceleration
Acceleration (m/s^2)
Time (s)

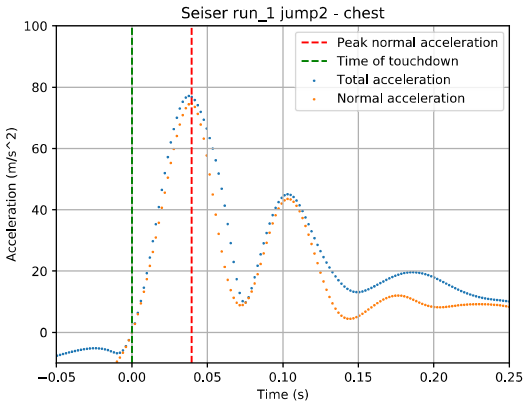
Seiser run_1 jump2 - chest
Peak normal acceleration
Time of touchdown
Total acceleration
Normal acceleration
Acceleration (m/s^2)
Time (s)

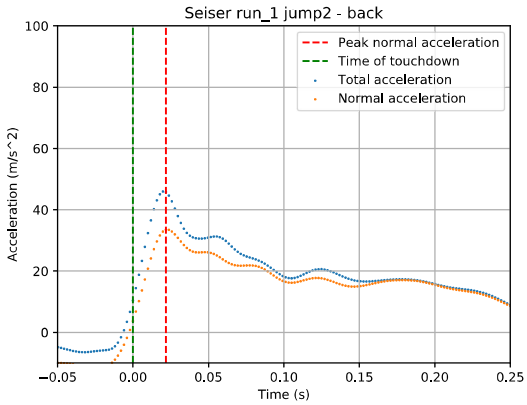
Seiser run_1 jump2 - back
Peak normal acceleration
Time of touchdown
Total acceleration
Normal acceleration
Acceleration (m/s^2)
Time (s)

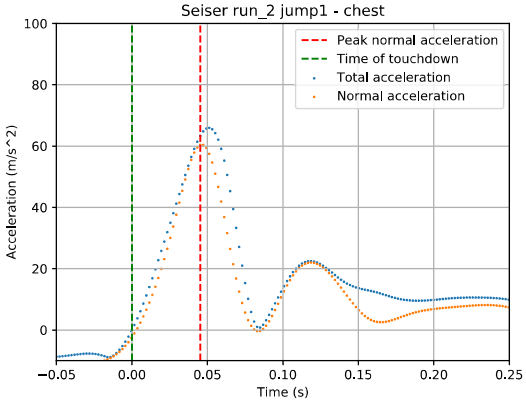
Seiser run_2 jump1 - chest
Peak normal acceleration
Time of touchdown
Total acceleration
Normal acceleration
Acceleration (m/s^2)
Time (s)

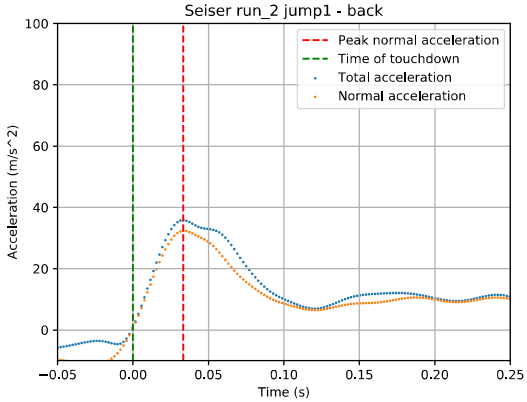
Seiser run_2 jump1 - back
Peak normal acceleration
Time of touchdown
Total acceleration
Normal acceleration
Acceleration (m/s^2)
Time (s)

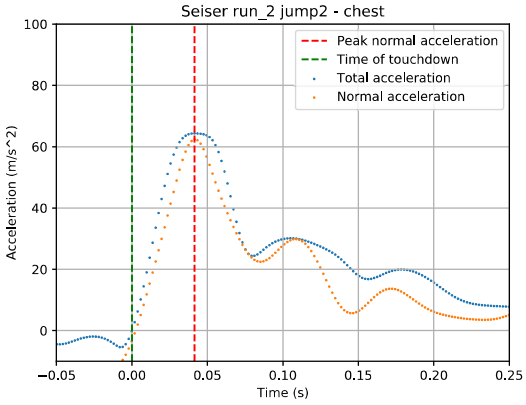
Seiser run_2 jump2 - chest
Peak normal acceleration
Time of touchdown
Total acceleration
Normal acceleration
Acceleration (m/s^2)
Time (s)

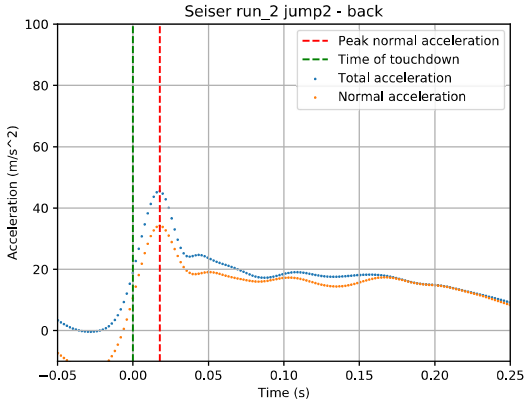
Seiser run_2 jump2 - back
Peak normal acceleration
Time of touchdown
Total acceleration
Normal acceleration
Acceleration (m/s^2)
Time (s)

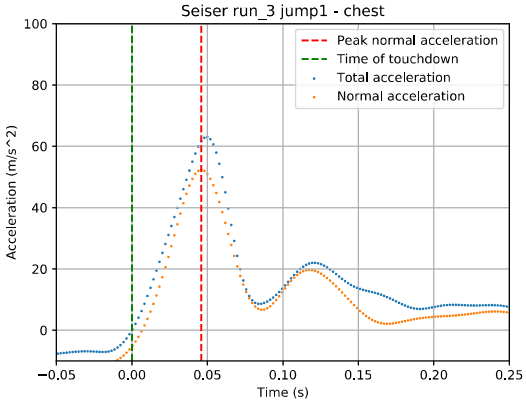
Seiser run_3 jump1 - chest
Peak normal acceleration
Time of touchdown
Total acceleration
Normal acceleration
Acceleration (m/s^2)
Time (s)

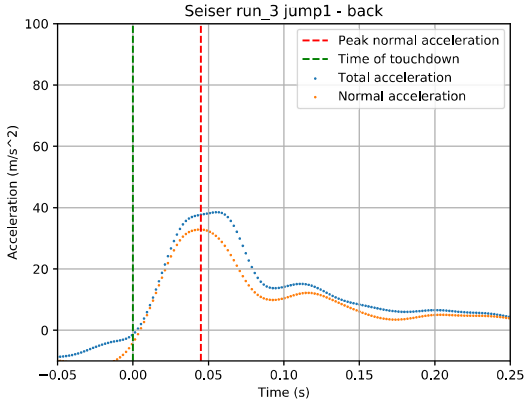
Seiser run_3 jump1 - back
Peak normal acceleration
Time of touchdown
Total acceleration
Normal acceleration
Acceleration (m/s^2)
Time (s)

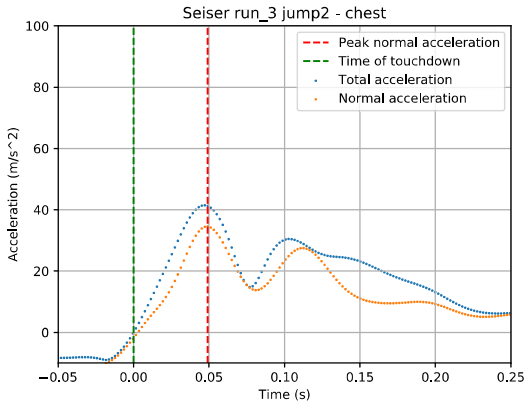
Seiser run_3 jump2 - chest
Peak normal acceleration
Time of touchdown
Total acceleration
Normal acceleration
Acceleration (m/s^2)
Time (s)

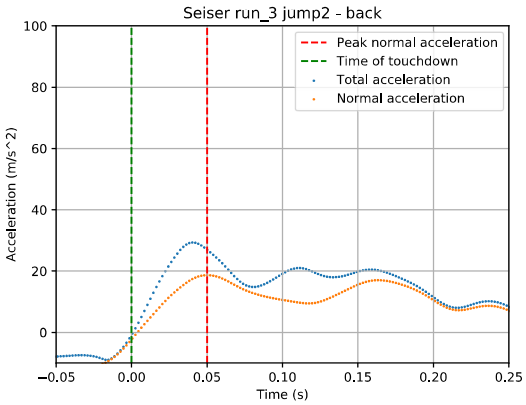
Seiser run_3 jump2 - back
Peak normal acceleration
Time of touchdown
Total acceleration
Normal acceleration
Acceleration (m/s^2)
Time (s)

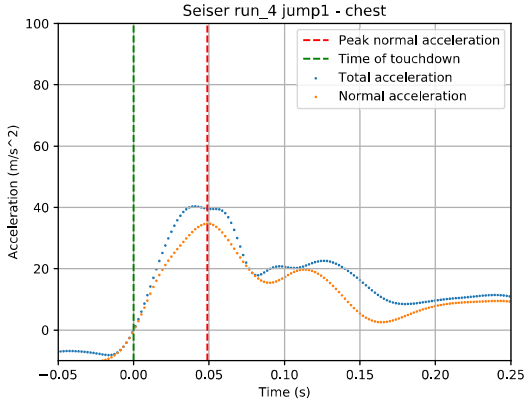
Seiser run_4 jump1 - chest
Peak normal acceleration
Time of touchdown
Total acceleration
Normal acceleration
Acceleration (m/s^2)
Time (s)

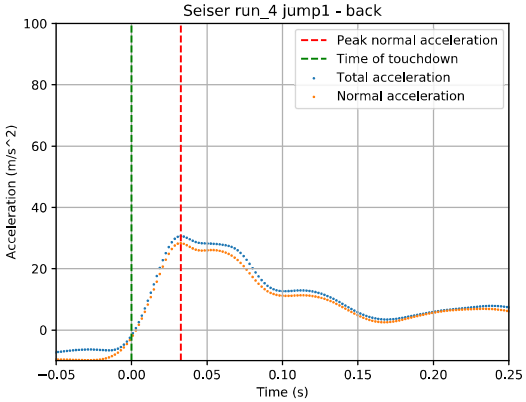
Seiser run_4 jump1 - back
Peak normal acceleration
Time of touchdown
Total acceleration
Normal acceleration
Acceleration (m/s^2)
Time (s)

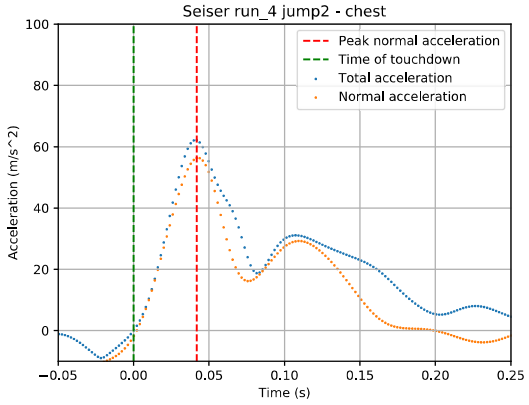
Seiser run_4 jump2 - chest
Peak normal acceleration
Time of touchdown
Total acceleration
Normal acceleration
Acceleration (m/s^2)
Time (s)

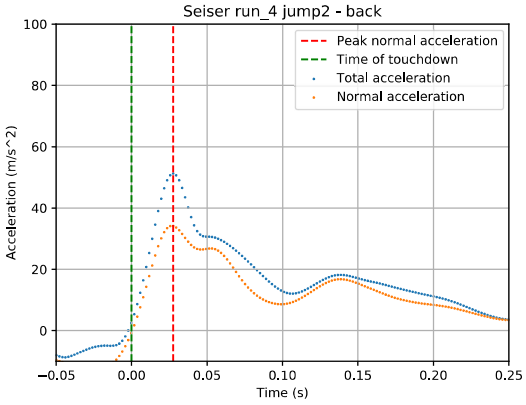
Seiser run_4 jump2 - back
Peak normal acceleration
Time of touchdown
Total acceleration
Normal acceleration
Acceleration (m/s^2)
Time (s)

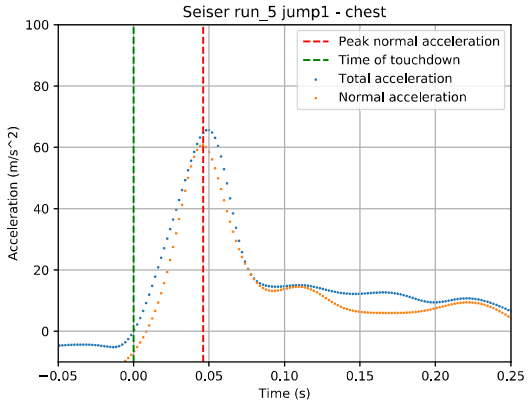
Seiser run_5 jump1 - chest
Peak normal acceleration
Time of touchdown
Total acceleration
Normal acceleration
Acceleration (m/s^2)
Time (s)

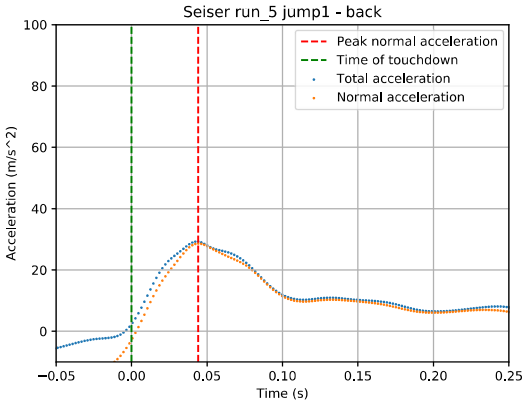
Seiser run_5 jump1 - back
Peak normal acceleration
Time of touchdown
Total acceleration
Normal acceleration
Acceleration (m/s^2)
Time (s)

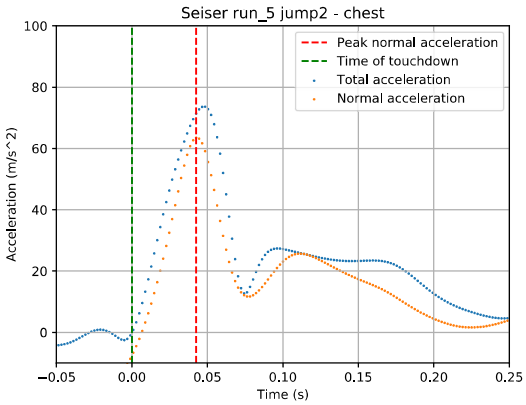
Seiser run_5 jump2 - chest
Peak normal acceleration
Time of touchdown
Total acceleration
Normal acceleration
Acceleration (m/s^2)
Time (s)

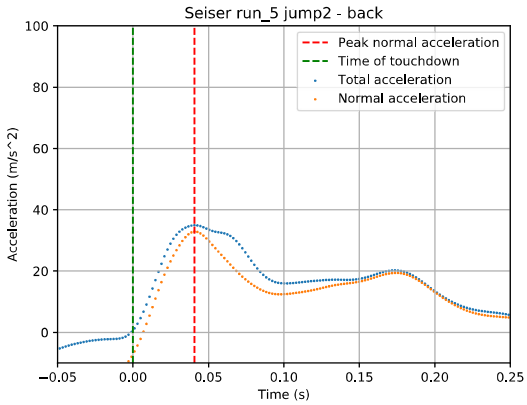
Seiser run_5 jump2 - back
Peak normal acceleration
Time of touchdown
Total acceleration
Normal acceleration
Acceleration (m/s^2)
Time (s)

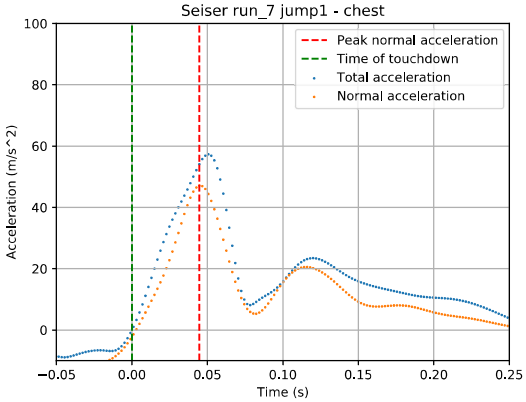
Seiser run_7 jump1 - chest
Peak normal acceleration
Time of touchdown
Total acceleration
Normal acceleration
Acceleration (m/s^2)
Time (s)

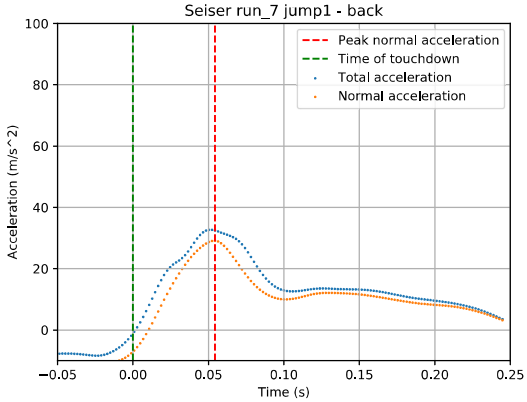
Seiser run_7 jump1 - back
Peak normal acceleration
Time of touchdown
Total acceleration
Normal acceleration
Acceleration (m/s^2)
Time (s)

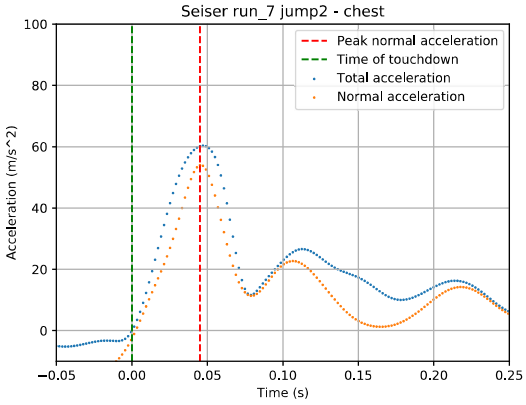
Seiser run_7 jump2 - chest
Peak normal acceleration
Time of touchdown
Total acceleration
Normal acceleration
Acceleration (m/s^2)
Time (s)

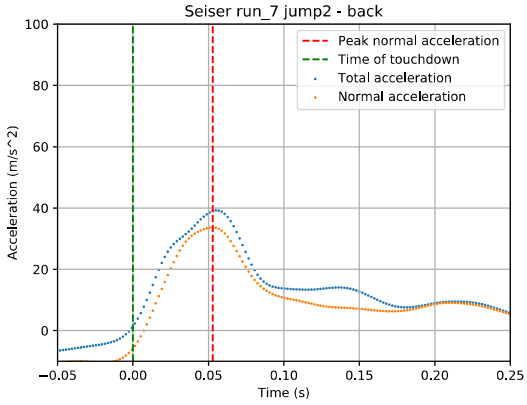
Seiser run_7 jump2 - back
Peak normal acceleration
Time of touchdown
Total acceleration
Normal acceleration
Acceleration (m/s^2)
Time (s)

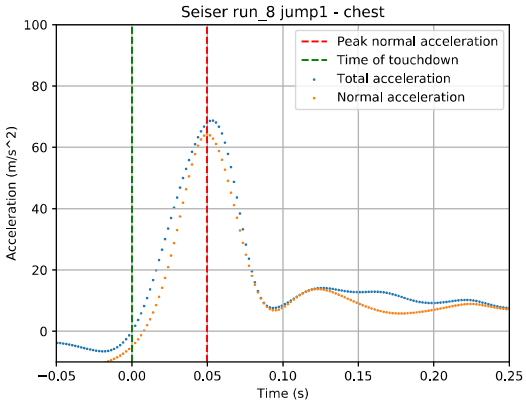
Seiser run_8 jump1 - chest
Peak normal acceleration
Time of touchdown
Total acceleration
Normal acceleration
Acceleration (m/s^2)
Time (s)

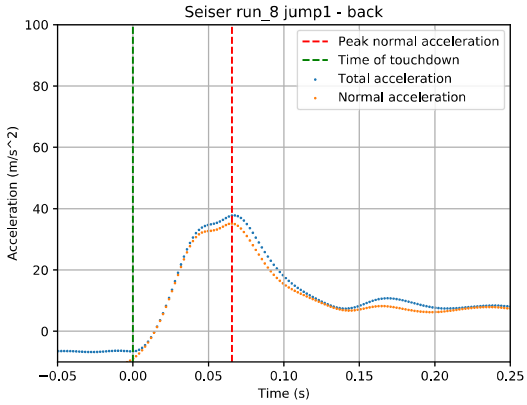
Seiser run_8 jump1 - back
Peak normal acceleration
Time of touchdown
Total acceleration
Normal acceleration
Acceleration (m/s^2)
Time (s)

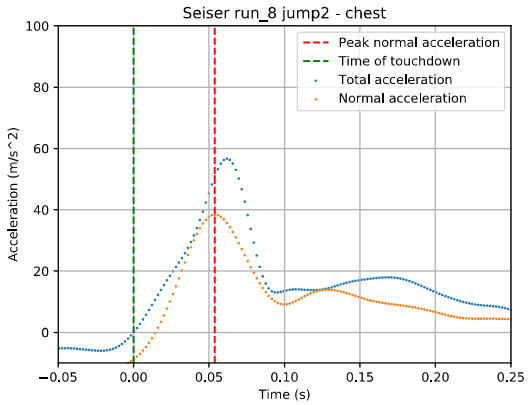
Seiser run_8 jump2 - chest
Peak normal acceleration
Time of touchdown
Total acceleration
Normal acceleration
Acceleration (m/s^2)
Time (s)

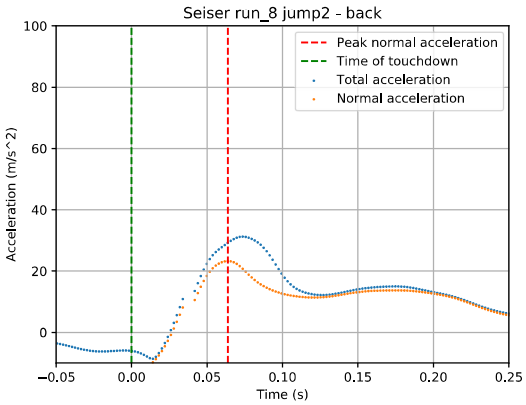
Seiser run_8 jump2 - back
Peak normal acceleration
Time of touchdown
Total acceleration
Normal acceleration
Acceleration (m/s^2)
Time (s)

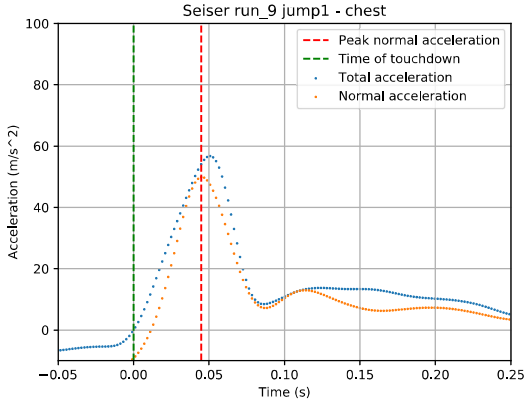
Seiser run_9 jump1 - chest
Peak normal acceleration
Time of touchdown
Total acceleration
Normal acceleration
Acceleration (m/s^2)
Time (s)

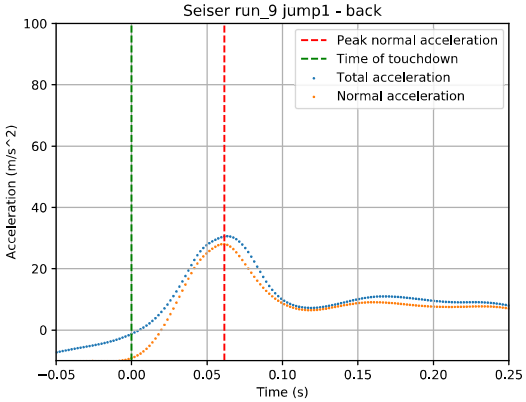
Seiser run_9 jump1 - back
Peak normal acceleration
Time of touchdown
Total acceleration
Normal acceleration
Acceleration (m/s^2)
Time (s)

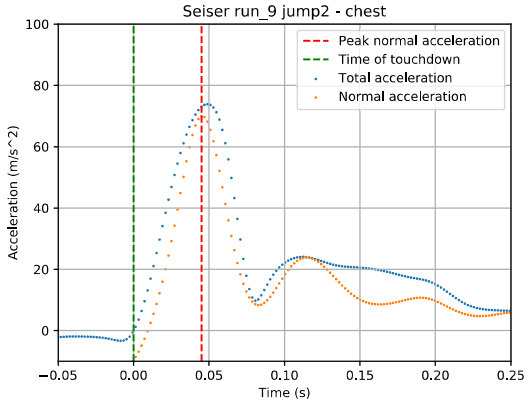
Seiser run_9 jump2 - chest
Peak normal acceleration
Time of touchdown
Total acceleration
Normal acceleration
Acceleration (m/s^2)
Time (s)

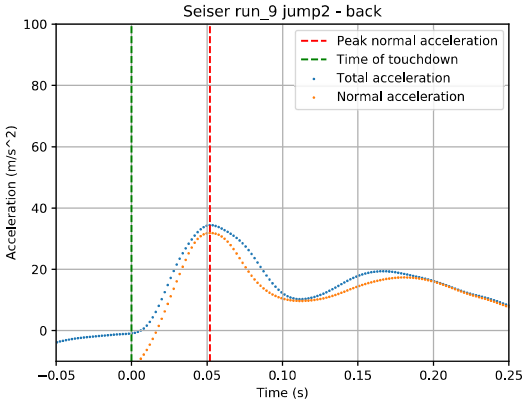
Seiser run_9 jump2 - back
Peak normal acceleration
Time of touchdown
Total acceleration
Normal acceleration
Acceleration (m/s^2)
Time (s)

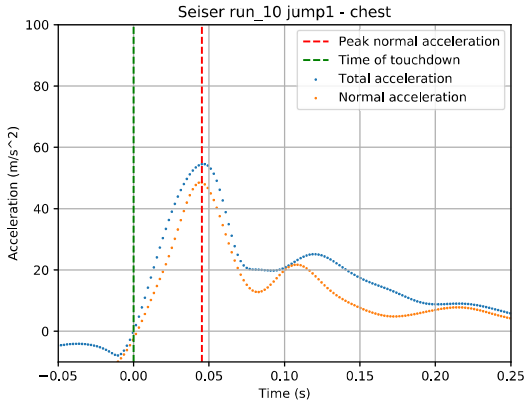
Seiser run_10 jump1 - chest
Peak normal acceleration
Time of touchdown
Total acceleration
Normal acceleration
Acceleration (m/s^2)
Time (s)

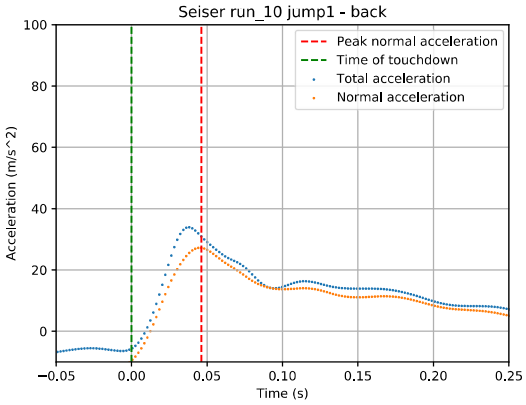
Seiser run_10 jump1 - back
Peak normal acceleration
Time of touchdown
Total acceleration
Normal acceleration
Acceleration (m/s^2)
Time (s)

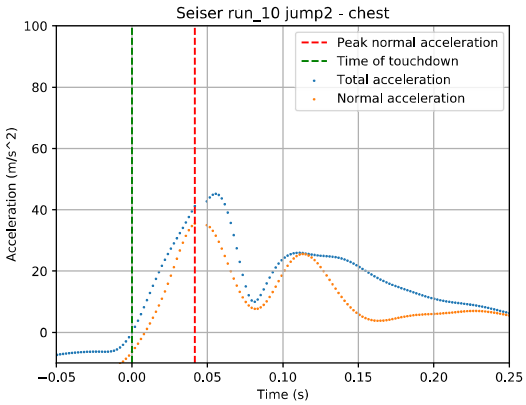
Seiser run_10 jump2 - chest
Peak normal acceleration
Time of touchdown
Total acceleration
Normal acceleration
Acceleration (m/s^2)
Time (s)

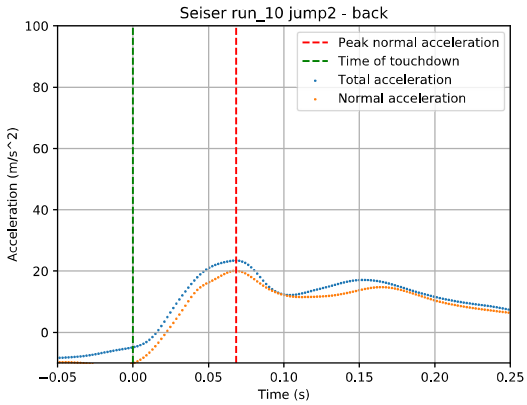
Seiser run_10 jump2 - back
Peak normal acceleration
Time of touchdown
Total acceleration
Normal acceleration
Acceleration (m/s^2)
Time (s)

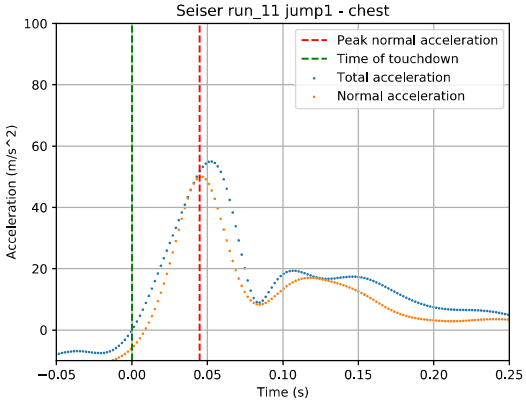
Seiser run_11 jump1 - chest
Peak normal acceleration
Time of touchdown
Total acceleration
Normal acceleration
Acceleration (m/s^2)
Time (s)

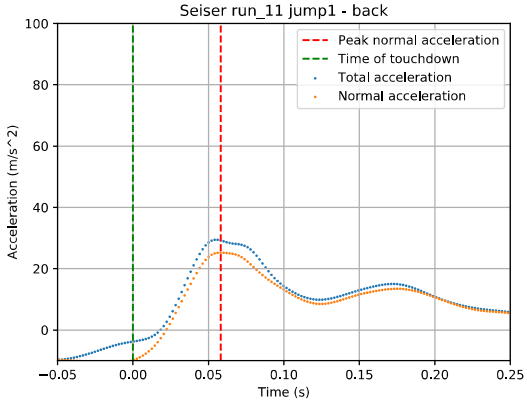
Seiser run_11 jump1 - back
Peak normal acceleration
Time of touchdown
Total acceleration
Normal acceleration
Acceleration (m/s^2)
Time (s)

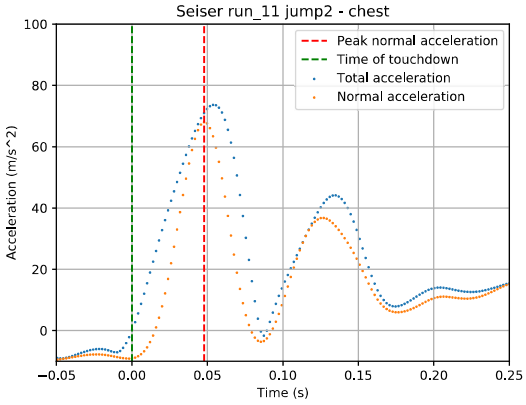
Seiser run_11 jump2 - chest
Peak normal acceleration
Time of touchdown
Total acceleration
Normal acceleration
Acceleration (m/s^2)
Time (s)

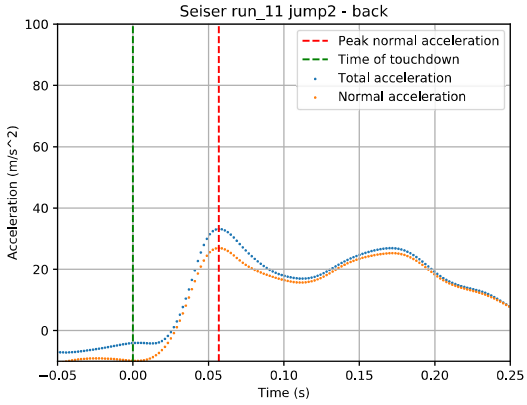
Seiser run_11 jump2 - back
Peak normal acceleration
Time of touchdown
Total acceleration
Normal acceleration
Acceleration (m/s^2)
Time (s)

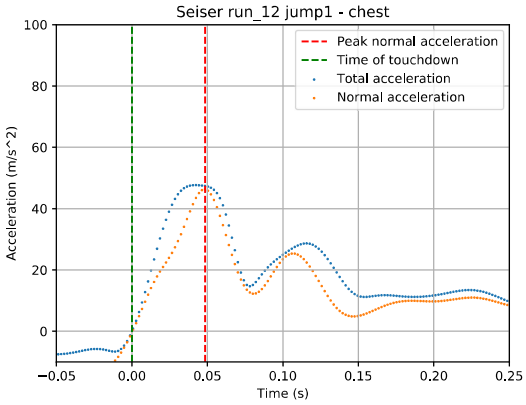
Seiser run_12 jump1 - chest
Peak normal acceleration
Time of touchdown
Total acceleration
Normal acceleration
Acceleration (m/s^2)
Time (s)

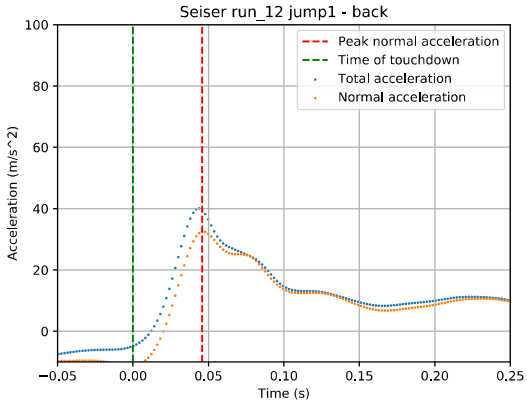
Seiser run_12 jump1 - back
Peak normal acceleration
Time of touchdown
Total acceleration
Normal acceleration
Acceleration (m/s^2)
Time (s)

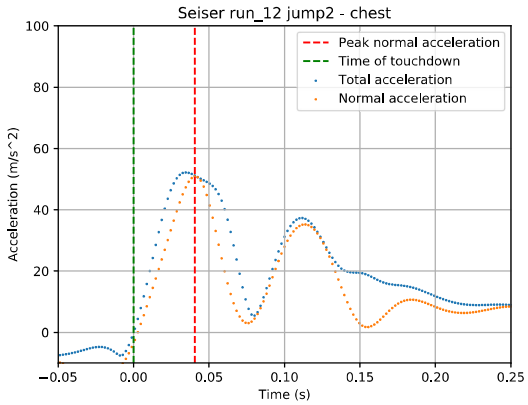
Seiser run_12 jump2 - chest
Peak normal acceleration
Time of touchdown
Total acceleration
Normal acceleration
Acceleration (m/s^2)
Time (s)

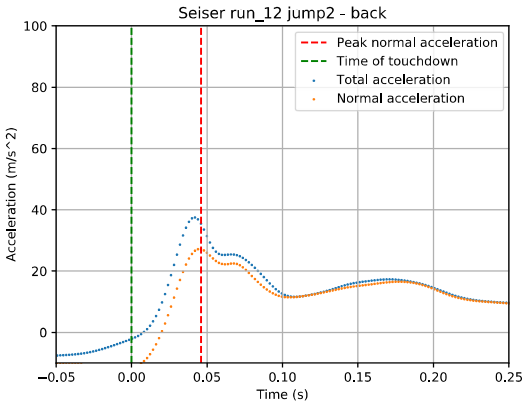
Seiser run_12 jump2 - back
Peak normal acceleration
Time of touchdown
Total acceleration
Normal acceleration
Acceleration (m/s^2)
Time (s)

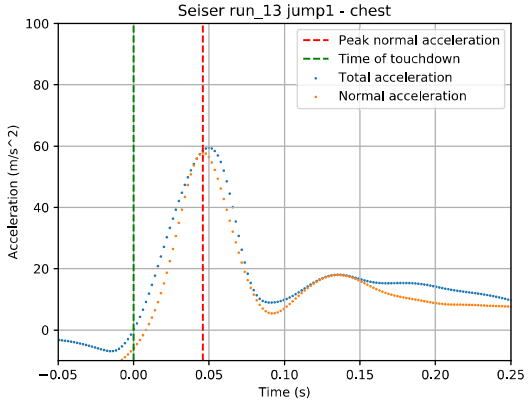
Seiser run_13 jump1 - chest
Peak normal acceleration
Time of touchdown
Total acceleration
Normal acceleration
Acceleration (m/s^2)
Time (s)

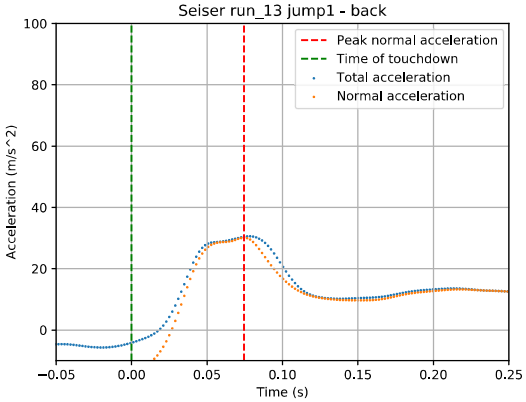
Seiser run_13 jump1 - back
Peak normal acceleration
Time of touchdown
Total acceleration
Normal acceleration
Acceleration (m/s^2)
Time (s)

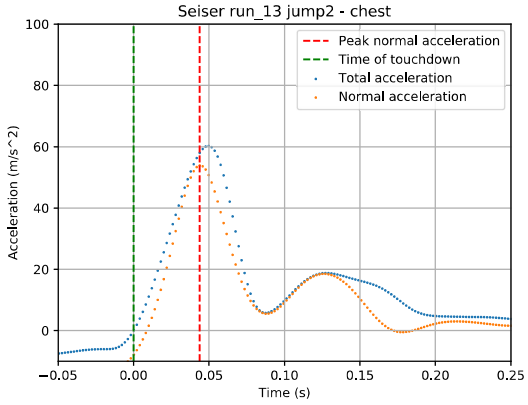
Seiser run_13 jump2 - chest
Peak normal acceleration
Time of touchdown
Total acceleration
Normal acceleration
Acceleration (m/s^2)
Time (s)

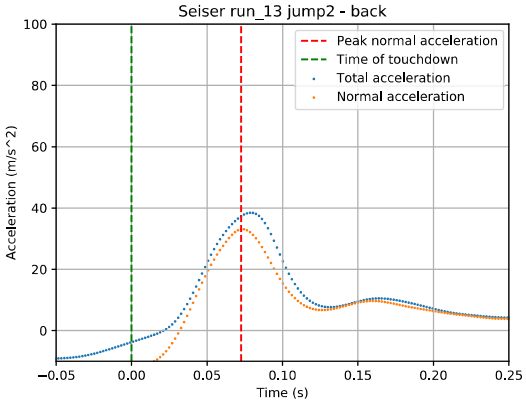
Seiser run_13 jump2 - back
Peak normal acceleration
Time of touchdown
Total acceleration
Normal acceleration
Acceleration (m/s^2)
Time (s)

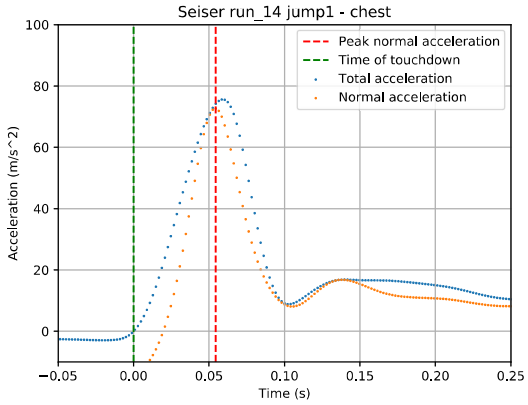
Seiser run_14 jump1 - chest
Peak normal acceleration
Time of touchdown
Total acceleration
Normal acceleration
Acceleration (m/s^2)
Time (s)

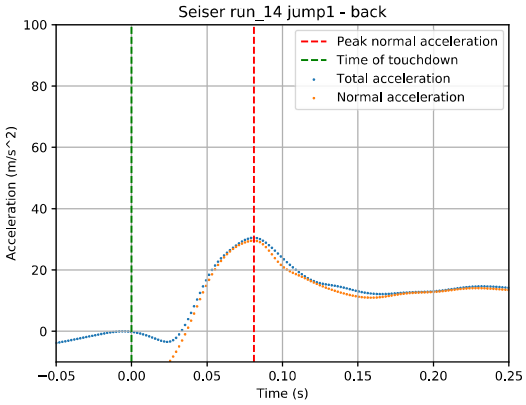
Seiser run_14 jump1 - back
Peak normal acceleration
Time of touchdown
Total acceleration
Normal acceleration
Acceleration (m/s^2)
Time (s)

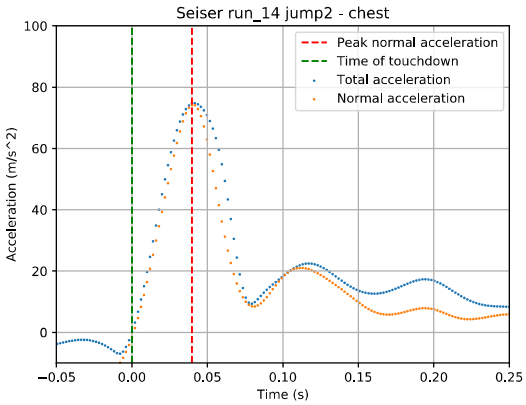
Seiser run_14 jump2 - chest
Peak normal acceleration
Time of touchdown
Total acceleration
Normal acceleration
Acceleration (m/s^2)
Time (s)

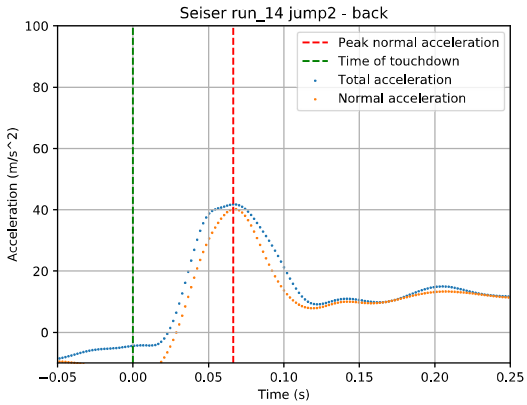
Seiser run_14 jump2 - back
Peak normal acceleration
Time of touchdown
Total acceleration
Normal acceleration
Acceleration (m/s^2)
Time (s)

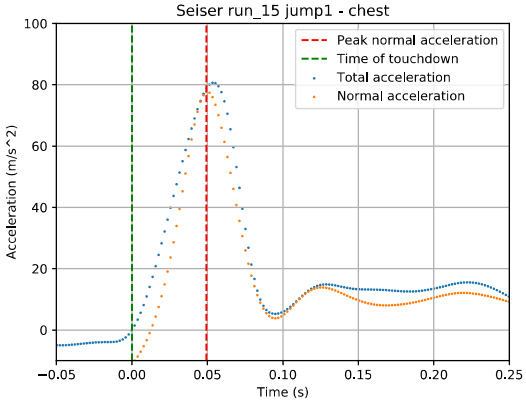
Seiser run_15 jump1 - chest
Peak normal acceleration
Time of touchdown
Total acceleration
Normal acceleration
Acceleration (m/s^2)
Time (s)

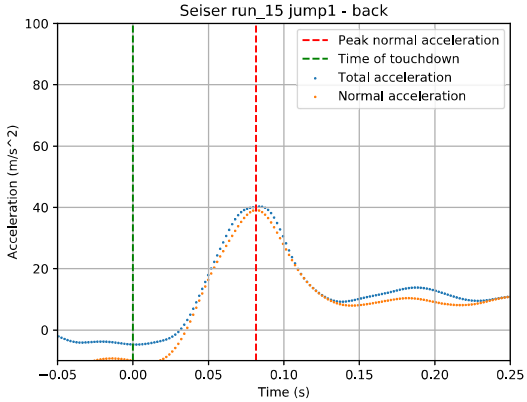
Seiser run_15 jump1 - back
Peak normal acceleration
Time of touchdown
Total acceleration
Normal acceleration
Acceleration (m/s^2)
Time (s)

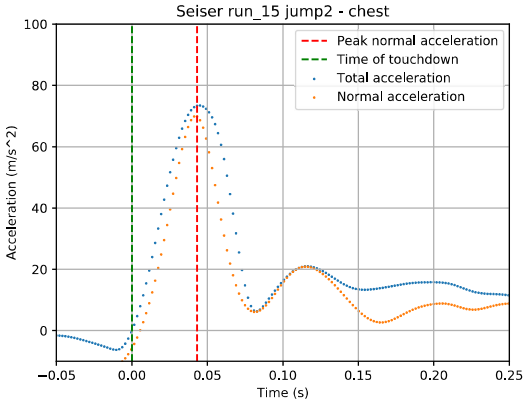
Seiser run_15 jump2 - chest
Peak normal acceleration
Time of touchdown
Total acceleration
Normal acceleration
Acceleration (m/s^2)
Time (s)

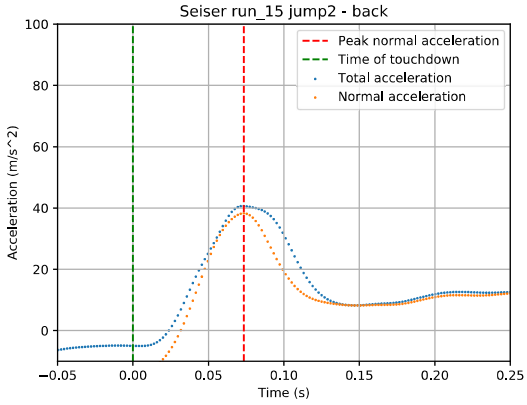
Seiser run_15 jump2 - back
Peak normal acceleration
Time of touchdown
Total acceleration
Normal acceleration
Acceleration (m/s^2)
Time (s)

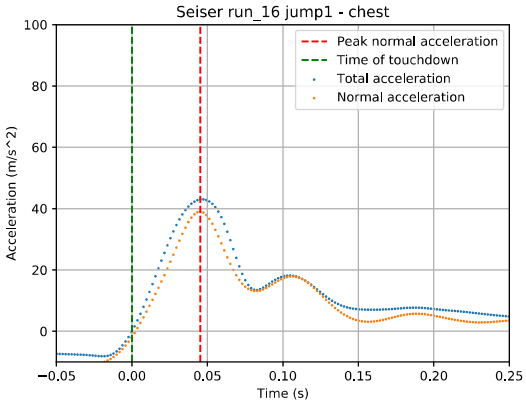
Seiser run_16 jump1 - chest
Peak normal acceleration
Time of touchdown
Total acceleration
Normal acceleration
Acceleration (m/s^2)
Time (s)

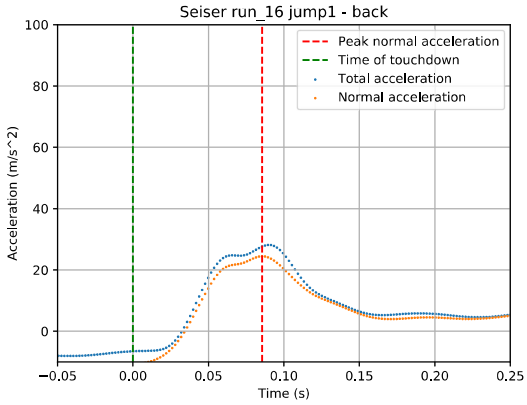
Seiser run_16 jump1 - back
Peak normal acceleration
Time of touchdown
Total acceleration
Normal acceleration
Acceleration (m/s^2)
Time (s)

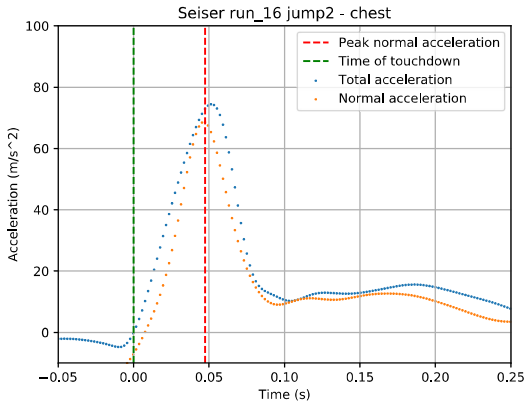
Seiser run_16 jump2 - chest
Peak normal acceleration
Time of touchdown
Total acceleration
Normal acceleration
Acceleration (m/s^2)
Time (s)

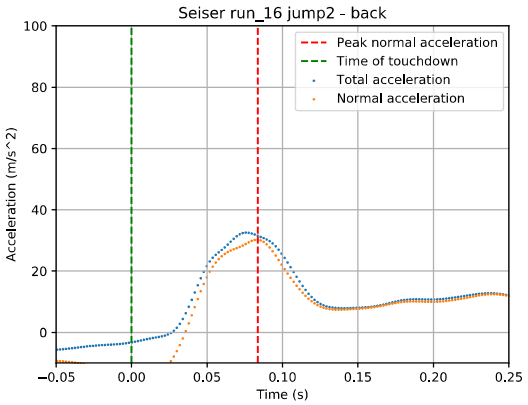
Seiser run_16 jump2 - back
Peak normal acceleration
Time of touchdown
Total acceleration
Normal acceleration
Acceleration (m/s^2)
Time (s)

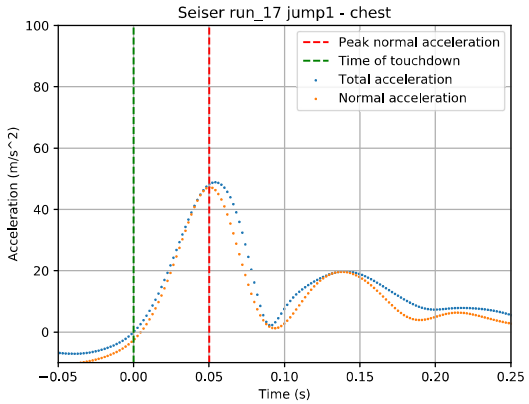
Seiser run_17 jump1 - chest
Peak normal acceleration
Time of touchdown
Total acceleration
Normal acceleration
Acceleration (m/s^2)
Time (s)

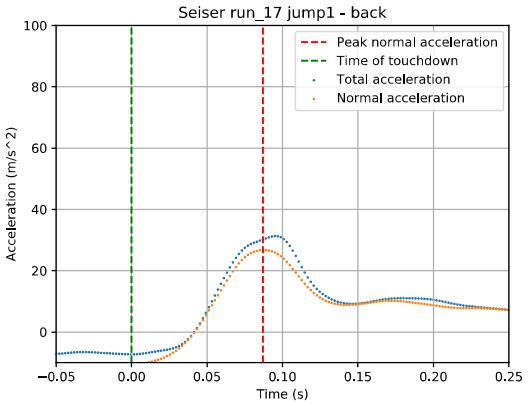
Seiser run_17 jump1 - back
Peak normal acceleration
Time of touchdown
Total acceleration
Normal acceleration
Acceleration (m/s^2)
Time (s)

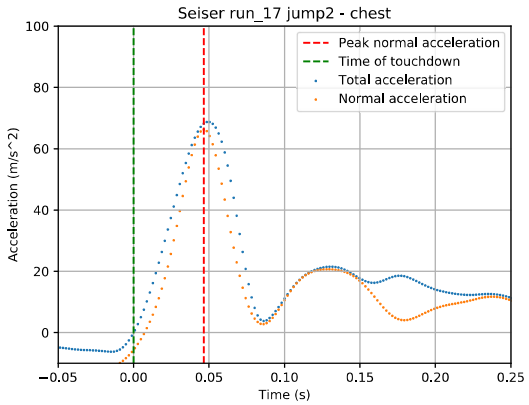
Seiser run_17 jump2 - chest
Peak normal acceleration
Time of touchdown
Total acceleration
Normal acceleration
Acceleration (m/s^2)
Time (s)

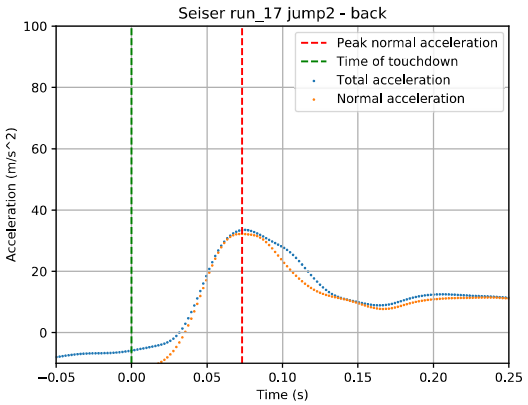
Seiser run_17 jump2 - back
Peak normal acceleration
Time of touchdown
Total acceleration
Normal acceleration
Acceleration (m/s^2)
Time (s)

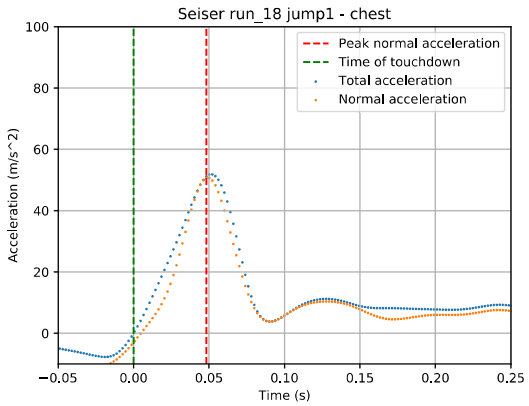
Seiser run_18 jump1 - chest
Peak normal acceleration
Time of touchdown
Total acceleration
Normal acceleration
Acceleration (m/s^2)
Time (s)

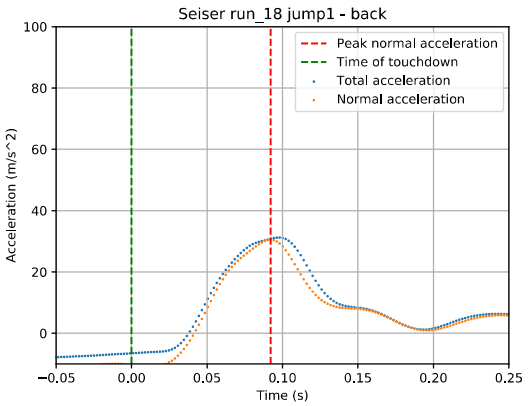
Seiser run_18 jump1 - back
Peak normal acceleration
Time of touchdown
Total acceleration
Normal acceleration
Acceleration (m/s^2)
Time (s)

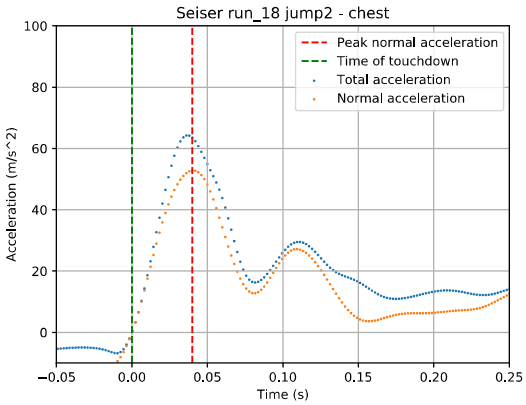
Seiser run_18 jump2 - chest
Peak normal acceleration
Time of touchdown
Total acceleration
Normal acceleration
Acceleration (m/s^2)
Time (s)

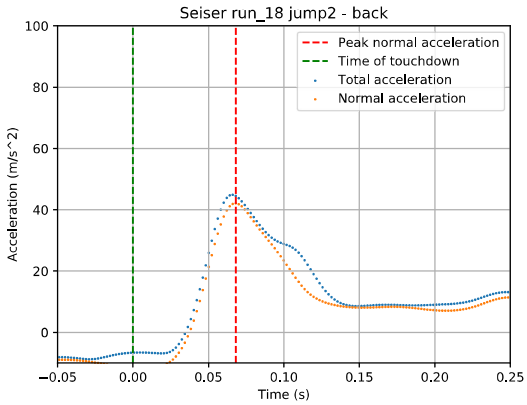
Seiser run_18 jump2 - back
Peak normal acceleration
Time of touchdown
Total acceleration
Normal acceleration
Acceleration (m/s^2)
Time (s)

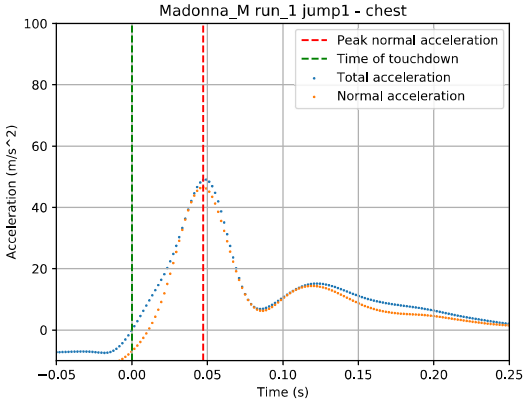
Madonna_M run_1 jump1 - chest
Peak normal acceleration
Time of touchdown
Total acceleration
Normal acceleration
Acceleration (m/s^2)
Time (s)

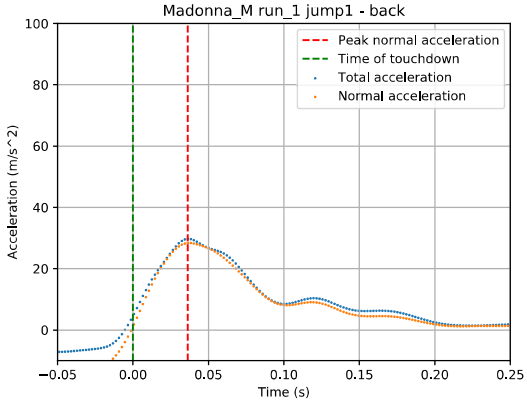
Madonna_M run_1 jump1 - back
Peak normal acceleration
Time of touchdown
Total acceleration
Normal acceleration
Acceleration (m/s^2)
Time (s)

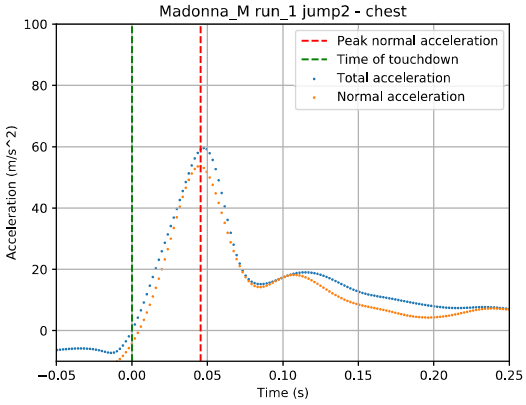
Madonna_M run_1 jump2 - chest
Peak normal acceleration
Time of touchdown
Total acceleration
Normal acceleration
Acceleration (m/s^2)
Time (s)

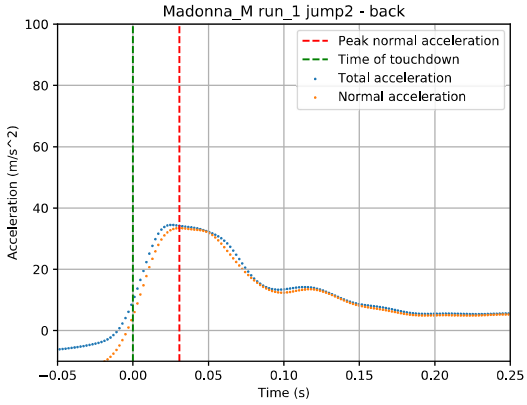
Madonna_M run_1 jump2 - back
Peak normal acceleration
Time of touchdown
Total acceleration
Normal acceleration
Acceleration (m/s^2)
Time (s)

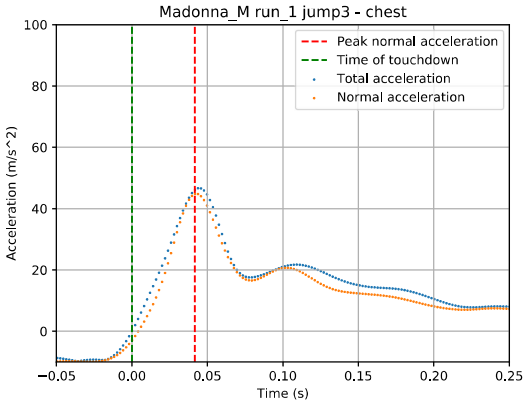
Madonna_M run_1 jump3 - chest
Peak normal acceleration
Time of touchdown
Total acceleration
Normal acceleration
Acceleration (m/s^2)
Time (s)

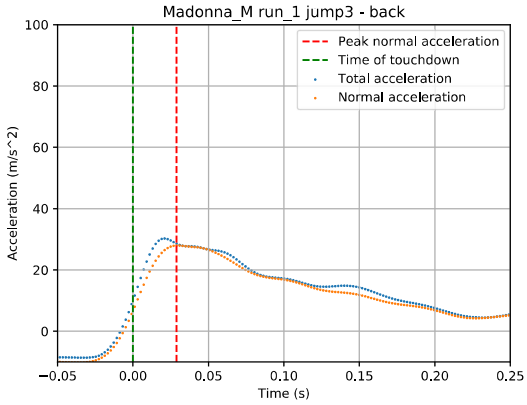
Madonna_M run_1 jump3 - back
Peak normal acceleration
Time of touchdown
Total acceleration
Normal acceleration
Acceleration (m/s^2)
Time (s)

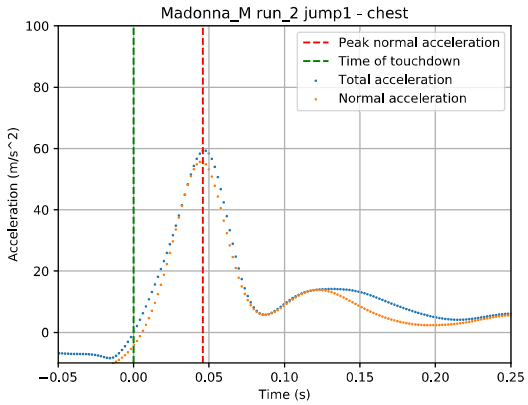
Madonna_M run_2 jump1 - chest
Peak normal acceleration
Time of touchdown
Total acceleration
Normal acceleration
Acceleration (m/s^2)
Time (s)

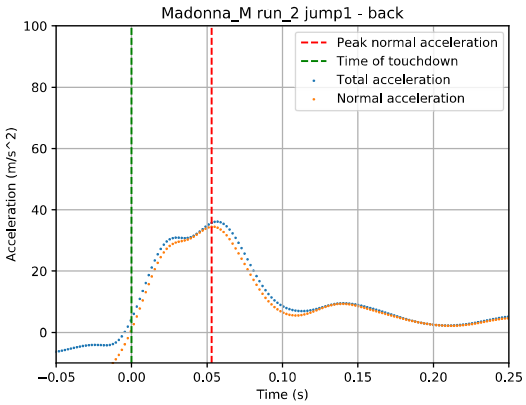
Madonna_M run_2 jump1 - back
Peak normal acceleration
Time of touchdown
Total acceleration
Normal acceleration
Acceleration (m/s^2)
Time (s)

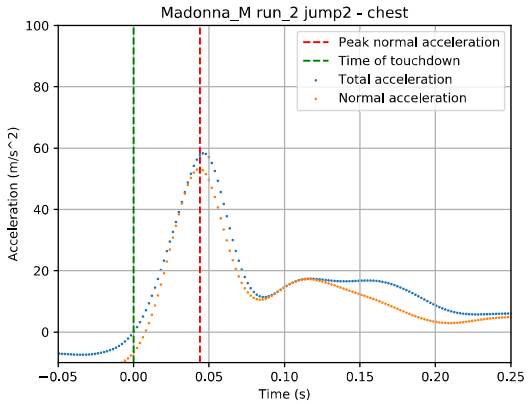
Madonna_M run_2 jump2 - chest
Peak normal acceleration
Time of touchdown
Total acceleration
Normal acceleration
Acceleration (m/s^2)
Time (s)

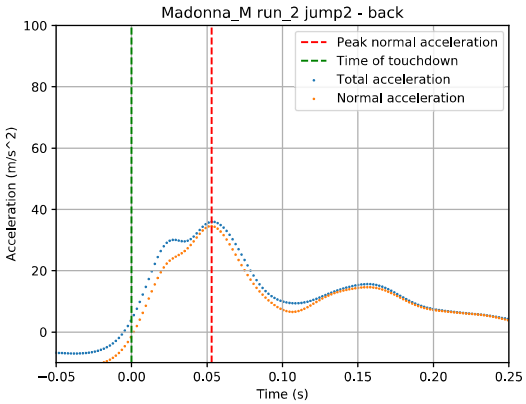
Madonna_M run_2 jump2 - back
Peak normal acceleration
Time of touchdown
Total acceleration
Normal acceleration
Acceleration (m/s^2)
Time (s)

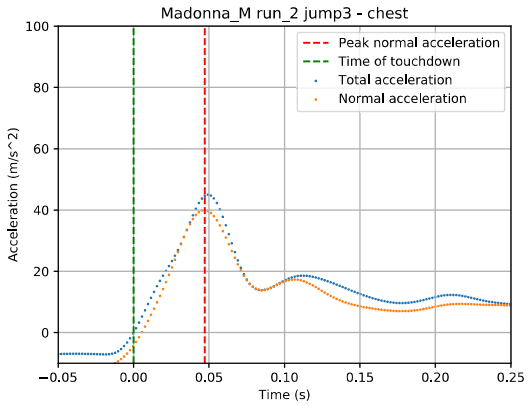
Madonna_M run_2 jump3 - chest
Peak normal acceleration
Time of touchdown
Total acceleration
Normal acceleration
Acceleration (m/s^2)
Time (s)

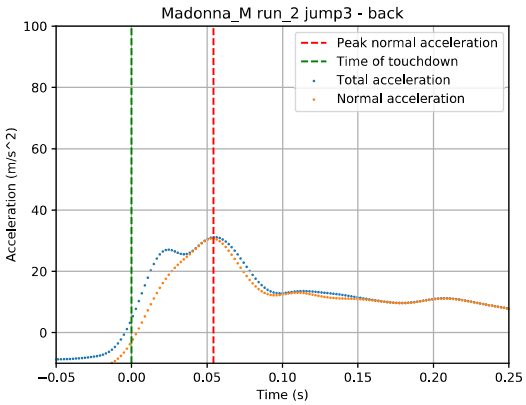
Madonna_M run_2 jump3 - back
Peak normal acceleration
Time of touchdown
Total acceleration
Normal acceleration
Acceleration (m/s^2)
Time (s)

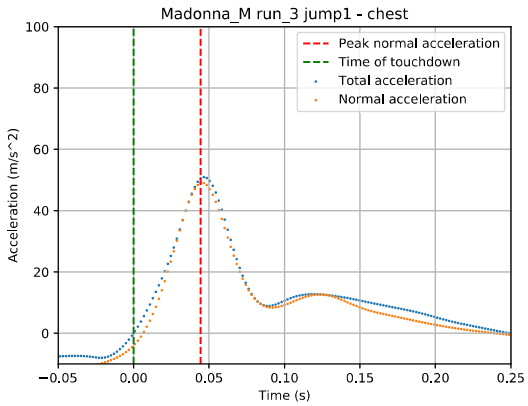
Madonna_M run_3 jump1 - chest
Peak normal acceleration
Time of touchdown
Total acceleration
Normal acceleration
Acceleration (m/s^2)
Time (s)

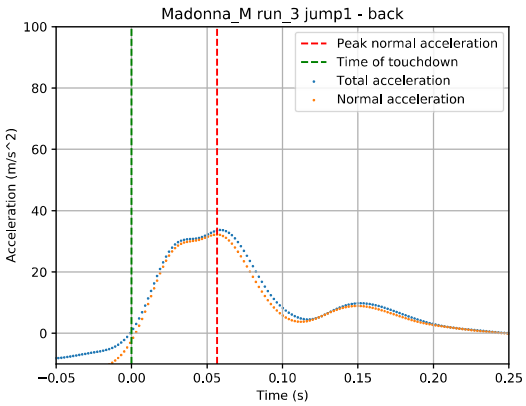
Madonna_M run_3 jump1 - back
Peak normal acceleration
Time of touchdown
Total acceleration
Normal acceleration
Acceleration (m/s^2)
Time (s)

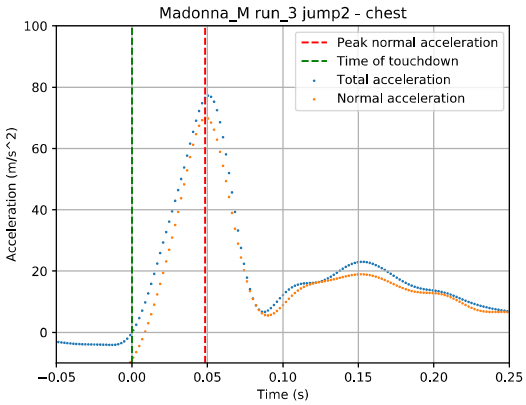
Madonna_M run_3 jump2 - chest
Peak normal acceleration
Time of touchdown
Total acceleration
Normal acceleration
Acceleration (m/s^2)
Time (s)

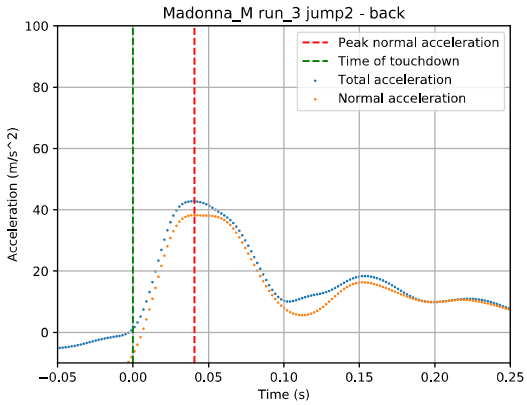
Madonna_M run_3 jump2 - back
Peak normal acceleration
Time of touchdown
Total acceleration
Normal acceleration
Acceleration (m/s^2)
Time (s)

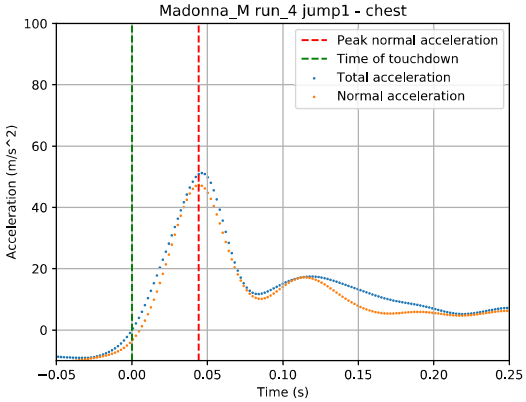
Madonna_M run_4 jump1 - chest
Peak normal acceleration
Time of touchdown
Total acceleration
Normal acceleration
Acceleration (m/s^2)
Time (s)

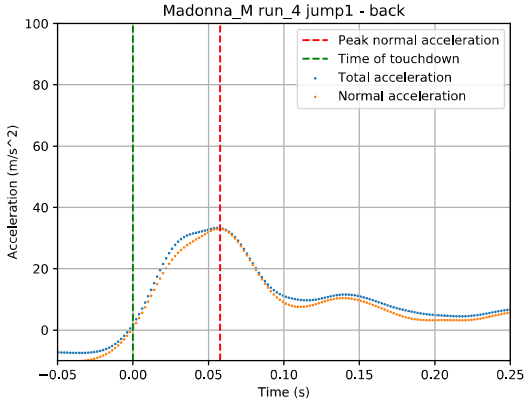
Madonna_M run_4 jump1 - back
Peak normal acceleration
Time of touchdown
Total acceleration
Normal acceleration
Acceleration (m/s^2)
Time (s)

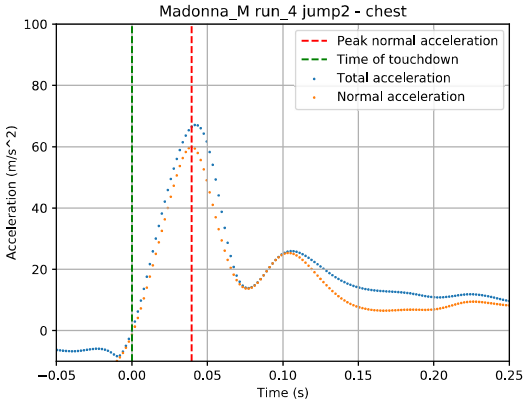
Madonna_M run_4 jump2 - chest
Peak normal acceleration
Time of touchdown
Total acceleration
Normal acceleration
Acceleration (m/s^2)
Time (s)

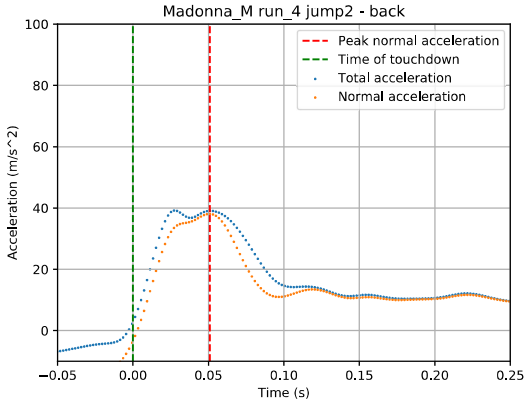
Madonna_M run_4 jump2 - back
Peak normal acceleration
Time of touchdown
Total acceleration
Normal acceleration
Acceleration (m/s^2)
Time (s)

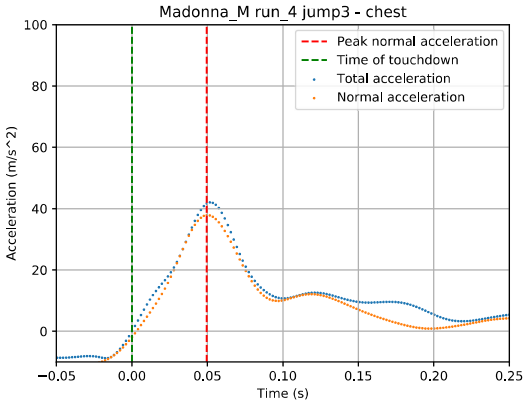
Madonna_M run_4 jump3 - chest
Peak normal acceleration
Time of touchdown
Total acceleration
Normal acceleration
Acceleration (m/s^2)
Time (s)

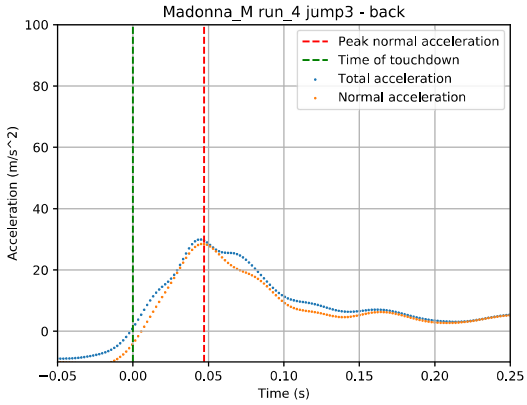
Madonna_M run_4 jump3 - back
Peak normal acceleration
Time of touchdown
Total acceleration
Normal acceleration
Acceleration (m/s^2)
Time (s)

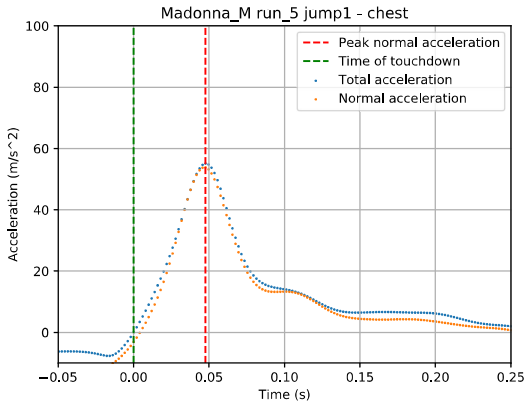
Madonna_M run_5 jump1 - chest
Peak normal acceleration
Time of touchdown
Total acceleration
Normal acceleration
Acceleration (m/s^2)
Time (s)

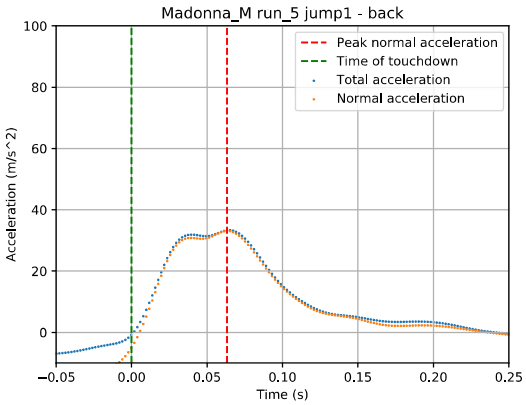
Madonna_M run_5 jump1 - back
Peak normal acceleration
Time of touchdown
Total acceleration
Normal acceleration
Acceleration (m/s^2)
Time (s)

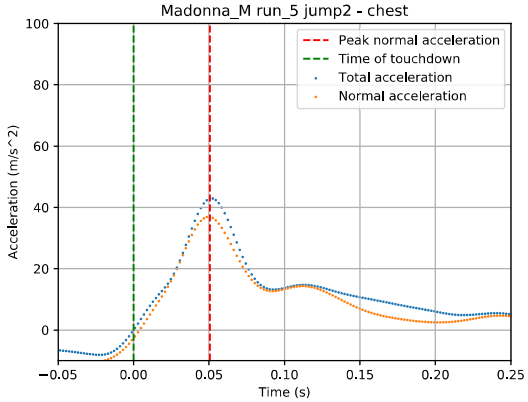
Madonna_M run_5 jump2 - chest
Peak normal acceleration
Time of touchdown
Total acceleration
Normal acceleration
Acceleration (m/s^2)
Time (s)

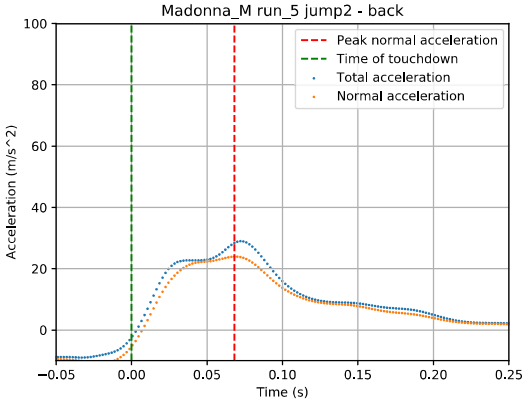
Madonna_M run_5 jump2 - back
Peak normal acceleration
Time of touchdown
Total acceleration
Normal acceleration
Acceleration (m/s^2)
Time (s)

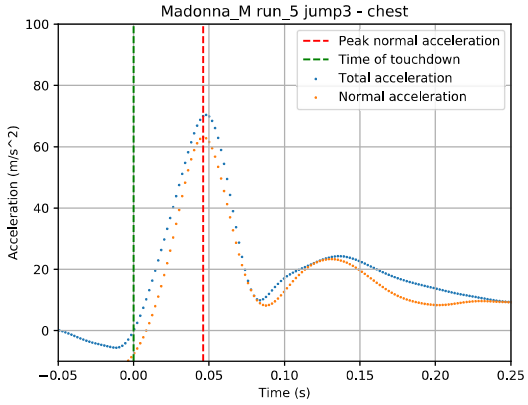
Madonna_M run_5 jump3 - chest
Peak normal acceleration
Time of touchdown
Total acceleration
Normal acceleration
Acceleration (m/s^2)
Time (s)

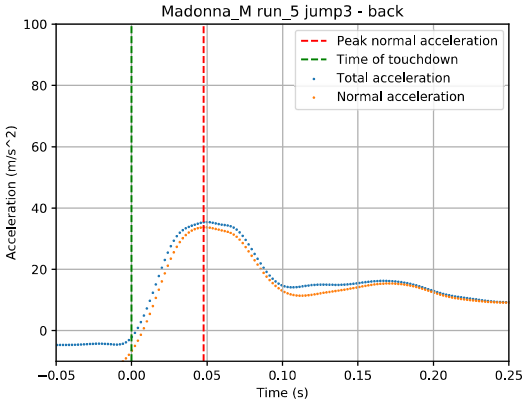
Madonna_M run_5 jump3 - back
Peak normal acceleration
Time of touchdown
Total acceleration
Normal acceleration
Acceleration (m/s^2)
Time (s)

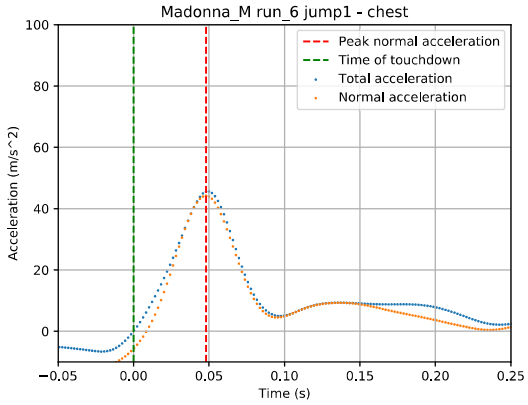
Madonna_M run_6 jump1 - chest
Peak normal acceleration
Time of touchdown
Total acceleration
Normal acceleration
Acceleration (m/s^2)
Time (s)

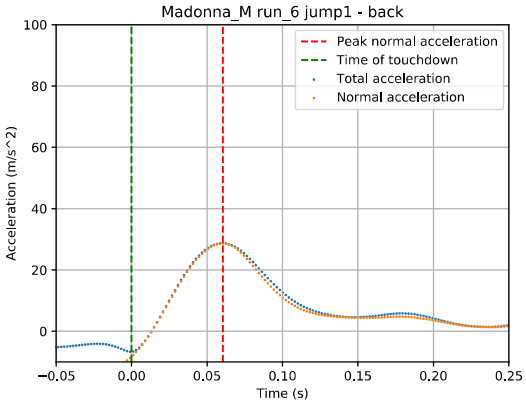
Madonna_M run_6 jump1 - back
Peak normal acceleration
Time of touchdown
Total acceleration
Normal acceleration
Acceleration (m/s^2)
Time (s)

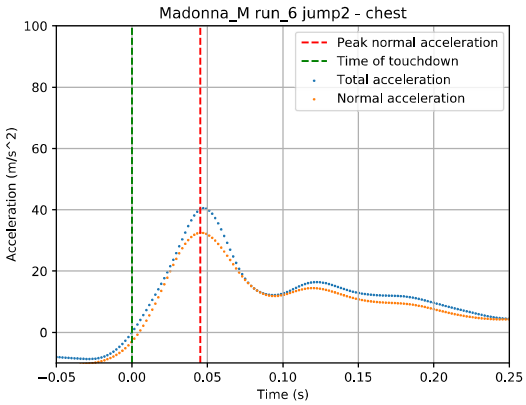
Madonna_M run_6 jump2 - chest
Peak normal acceleration
Time of touchdown
Total acceleration
Normal acceleration
Acceleration (m/s^2)
Time (s)

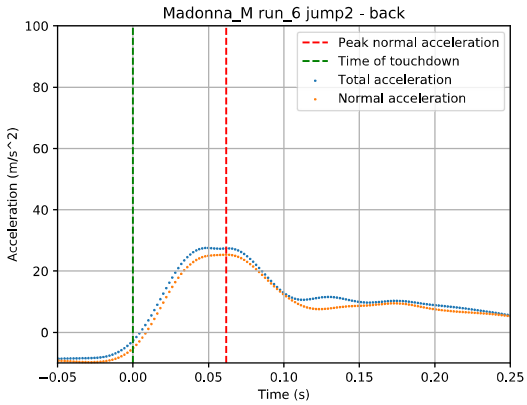
Madonna_M run_6 jump2 - back
Peak normal acceleration
Time of touchdown
Total acceleration
Normal acceleration
Acceleration (m/s^2)
Time (s)

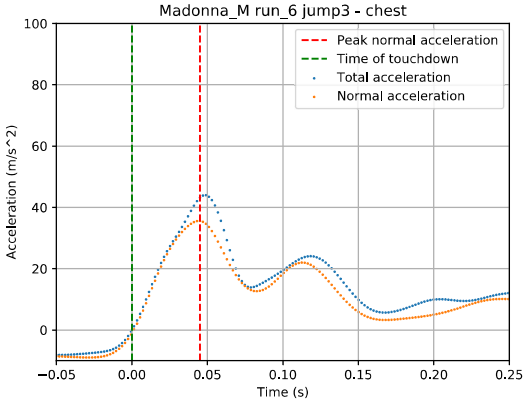
Madonna_M run_6 jump3 - chest
Peak normal acceleration
Time of touchdown
Total acceleration
Normal acceleration
Acceleration (m/s^2)
Time (s)

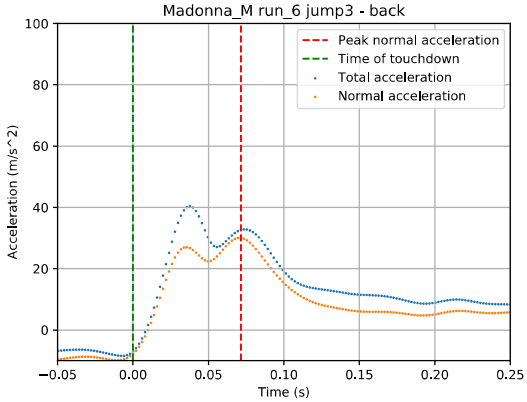
Madonna_M run_6 jump3 - back
Peak normal acceleration
Time of touchdown
Total acceleration
Normal acceleration
Acceleration (m/s^2)
Time (s)

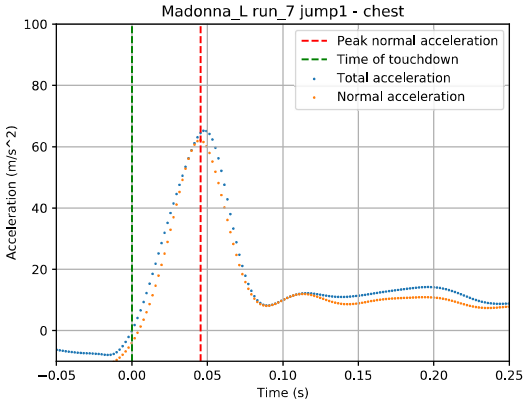
Madonna_L run_7 jump1 - chest
Peak normal acceleration
Time of touchdown
Total acceleration
Normal acceleration
Acceleration (m/s^2)
Time (s)

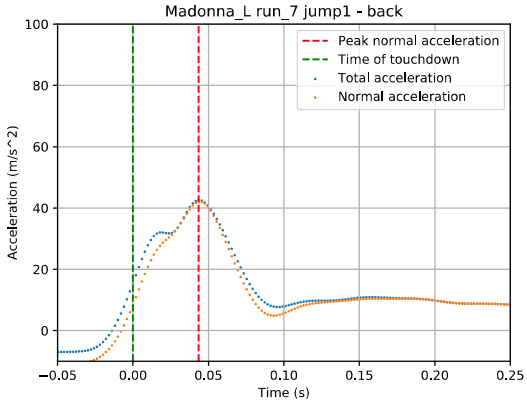
Madonna_L run_7 jump1 - back
Peak normal acceleration
Time of touchdown
Total acceleration
Normal acceleration
Acceleration (m/s^2)
Time (s)

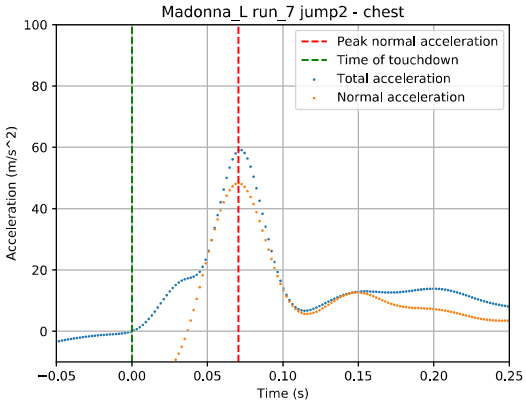
Madonna_L run_7 jump2 - chest
Peak normal acceleration
Time of touchdown
Total acceleration
Normal acceleration
Acceleration (m/s^2)
Time (s)

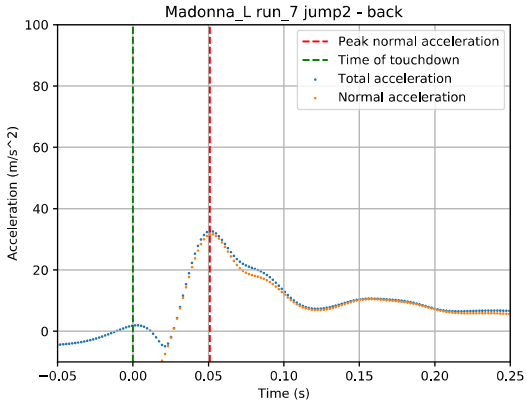
Madonna_L run_7 jump2 - back
Peak normal acceleration
Time of touchdown
Total acceleration
Normal acceleration
Acceleration (m/s^2)
Time (s)

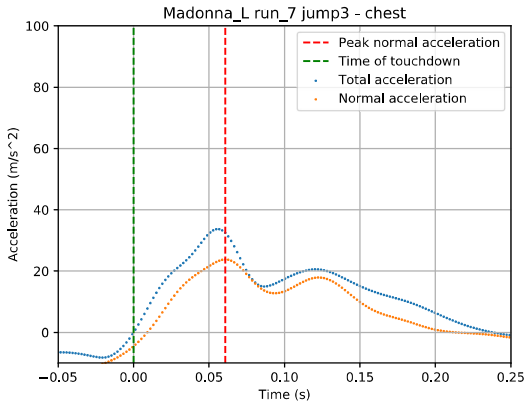
Madonna_L run_7 jump3 - chest
Peak normal acceleration
Time of touchdown
Total acceleration
Normal acceleration
Acceleration (m/s^2)
Time (s)

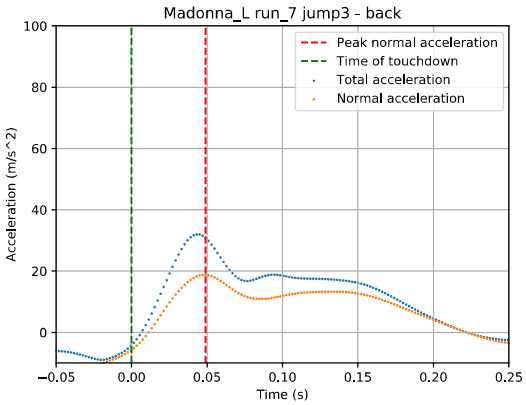
Madonna_L run_7 jump3 - back
Peak normal acceleration
Time of touchdown
Total acceleration
Normal acceleration
Acceleration (m/s^2)
Time (s)

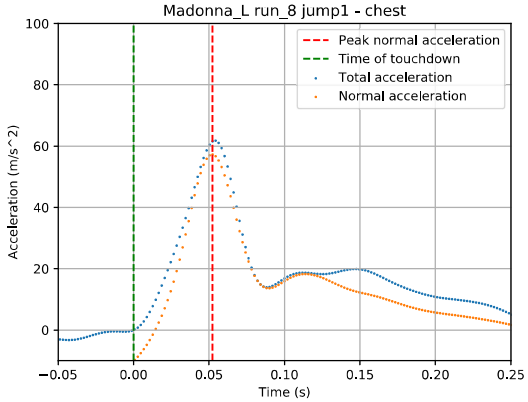
Madonna_L run_8 jump1 - chest
Peak normal acceleration
Time of touchdown
Total acceleration
Normal acceleration
Acceleration (m/s^2)
Time (s)

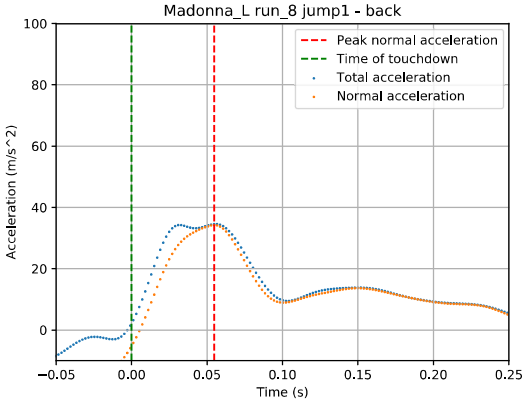
Madonna_L run_8 jump1 - back
Peak normal acceleration
Time of touchdown
Total acceleration
Normal acceleration
Acceleration (m/s^2)
Time (s)

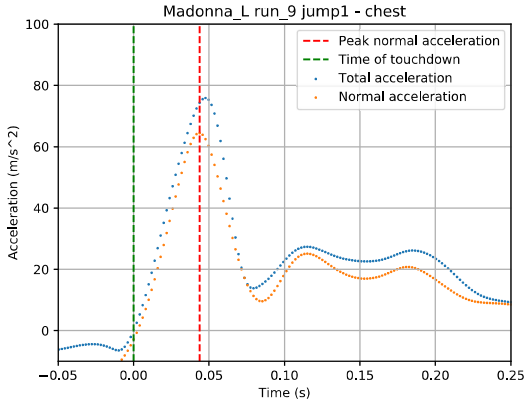
Madonna_L run_9 jump1 - chest
Peak normal acceleration
Time of touchdown
Total acceleration
Normal acceleration
Acceleration (m/s^2)
Time (s)

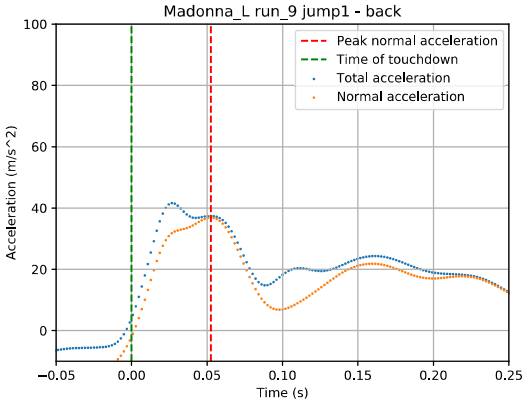
Madonna_L run_9 jump1 - back
Peak normal acceleration
Time of touchdown
Total acceleration
Normal acceleration
Acceleration (m/s^2)
Time (s)

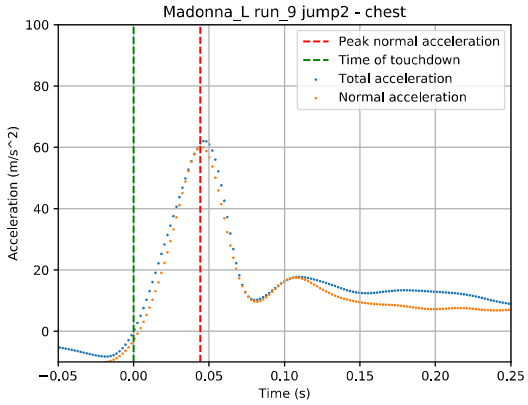
Madonna_L run_9 jump2 - chest
Peak normal acceleration
Time of touchdown
Total acceleration
Normal acceleration
Acceleration (m/s^2)
Time (s)

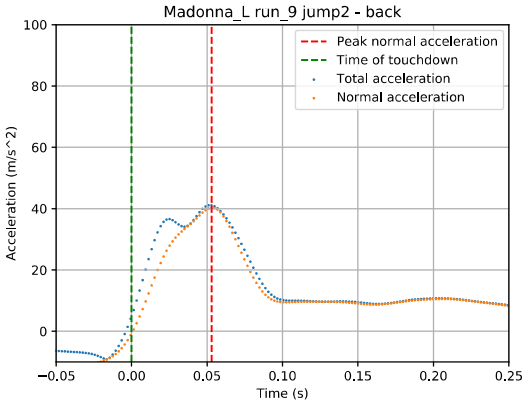
Madonna_L run_9 jump2 - back
Peak normal acceleration
Time of touchdown
Total acceleration
Normal acceleration
Acceleration (m/s^2)
Time (s)

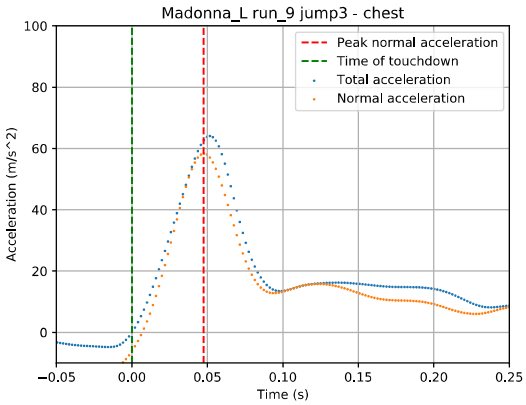
Madonna_L run_9 jump3 - chest
Peak normal acceleration
Time of touchdown
Total acceleration
Normal acceleration
Acceleration (m/s^2)
Time (s)

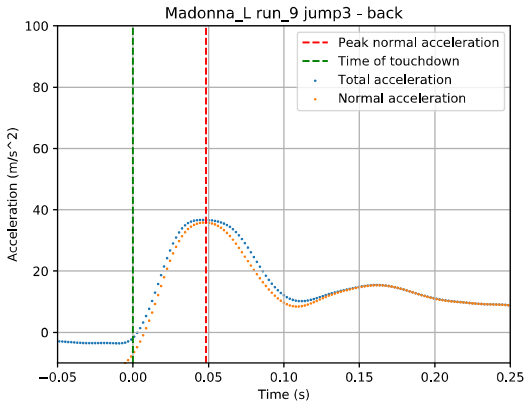
Madonna_L run_9 jump3 - back
Peak normal acceleration
Time of touchdown
Total acceleration
Normal acceleration
Acceleration (m/s^2)
Time (s)

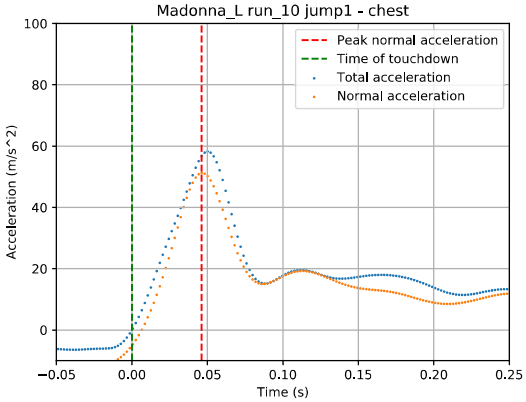
Madonna_L run_10 jump1 - chest
Peak normal acceleration
Time of touchdown
Total acceleration
Normal acceleration
Acceleration (m/s^2)
Time (s)

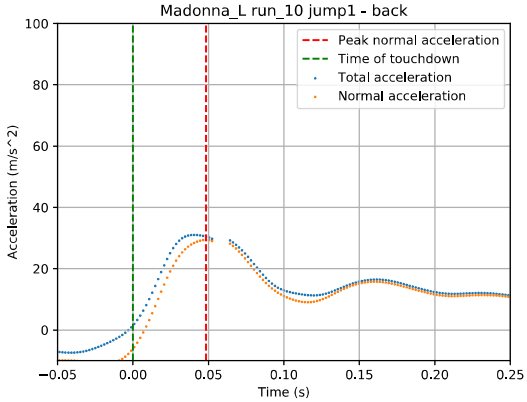
Madonna_L run_10 jump1 - back
Peak normal acceleration
Time of touchdown
Total acceleration
Normal acceleration
Acceleration (m/s^2)
Time (s)

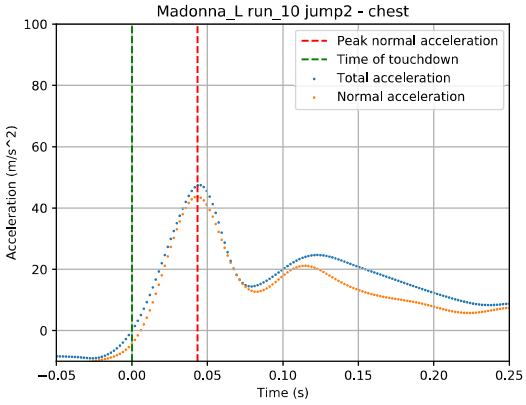
Madonna_L run_10 jump2 - chest
Peak normal acceleration
Time of touchdown
Total acceleration
Normal acceleration
Acceleration (m/s^2)
Time (s)

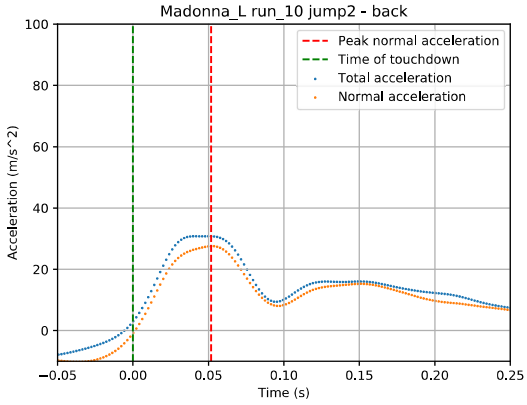
Madonna_L run_10 jump2 - back
Peak normal acceleration
Time of touchdown
Total acceleration
Normal acceleration
Acceleration (m/s^2)
Time (s)

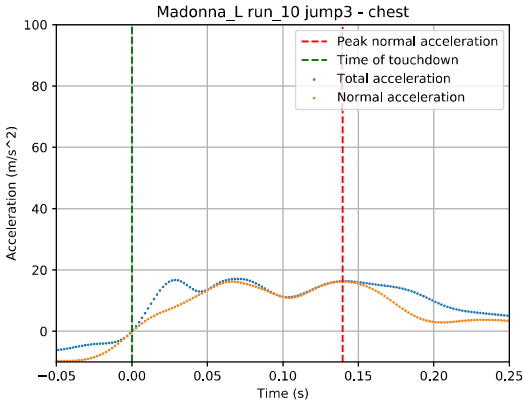
Madonna_L run_10 jump3 - chest
Peak normal acceleration
Time of touchdown
Total acceleration
Normal acceleration
Acceleration (m/s^2)
Time (s)

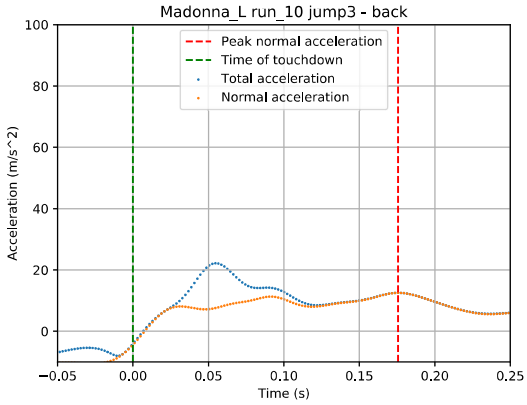
Madonna_L run_10 jump3 - back
Peak normal acceleration
Time of touchdown
Total acceleration
Normal acceleration
Acceleration (m/s^2)
Time (s)

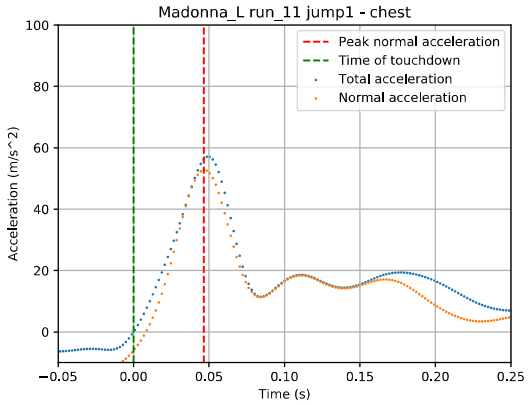
Madonna_L run_11 jump1 - chest
Peak normal acceleration
Time of touchdown
Total acceleration
Normal acceleration
Acceleration (m/s^2)
Time (s)

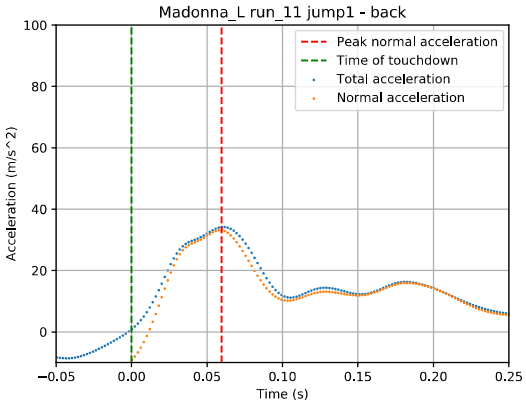
Madonna_L run_11 jump1 - back
Peak normal acceleration
Time of touchdown
Total acceleration
Normal acceleration
Acceleration (m/s^2)
Time (s)

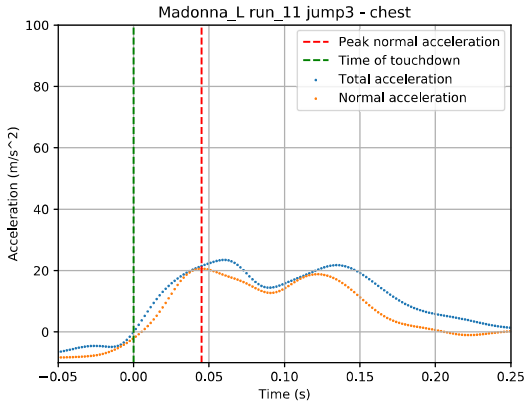
Madonna_L run_11 jump3 - chest
Peak normal acceleration
Time of touchdown
Total acceleration
Normal acceleration
Acceleration (m/s^2)
Time (s)

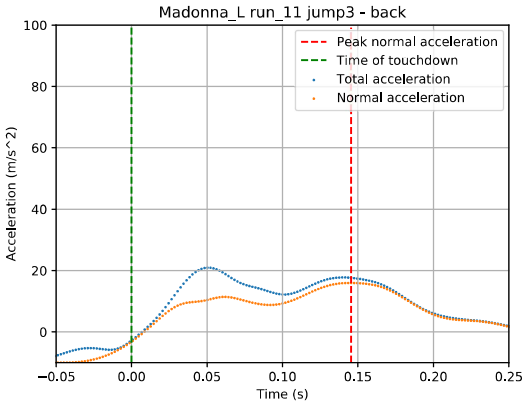
Madonna_L run_11 jump3 - back
Peak normal acceleration
Time of touchdown
Total acceleration
Normal acceleration
Acceleration (m/s^2)
Time (s)